Technische Universität München

TUM School of Engineering and Design

Synthetic Power Grid Development: Optimal Power System Planning-based Approach and Its Application for Singapore Case Study

Andrej Trpovski

Vollständiger Abdruck der von der TUM School of Engineering and Design der Technischen Universität München zur Erlangung des akademischen Grades eines

Doktors der Ingenieurwissenschaften

genehmigten Dissertation.

Vorsitz:

Prof. Dr. Carlo L. Bottasso

Prüfende der Dissertation:

1. Prof. Dr. Thomas Hamacher
2. Asst. Prof. Dr. Xu Yan,
   Nanyang Technological University

Die Dissertation wurde am 31.10.2022 bei der Technischen Universität München eingereicht und durch die TUM School of Engineering and Design am 07.03.2023 angenommen.

Abstract

To cope with the progressive challenges imposed by recent technological advancements in the power and energy sector, it is essential to modernize the power systems into 'smarter' and more resilient grids. Strict environmental and sustainability objectives have accelerated the development of renewable energy (RE), distributed energy resources (DER), battery energy storage systems (BESS), electric vehicles (EVs) and information and communication technologies (ICT).

The loads are defined as flexible and controllable, the consumers become prosumers, the energy mix is changing, new programs such as demand response are continuously explored and introduced, and the energy markets transition to a deregulated market environment. These developments give way for new concepts and opportunities and introduce many new stakeholders that change the grid landscape. Despite the numerous potential benefits offered with such advancements, there is a necessity to analyze the impact on the grid and identify the associated challenges.

The above-mentioned technologies and developments will have an effect on the power system which needs to be analyzed in details. These developments are just adding further pressure on utilities to reach the modern grid objectives, with minimal investment cost, without putting at risk the critical services they currently provide. Considering the importance of the power system as an essential facility, providing an uninterrupted service is the primary concern for a real-life implementation. However, it has been acknowledged that the absence of near-real world research, development and demonstration (RD&D) capabilities are challenges that power industry players need to overcome to enable the development, validation, and help qualify technologies, applications, and solutions as part of the smart grid initiative.

However, detailed real power system models are classified as critical infrastructure of high priority with confidentiality restrictions. Such information is not publicly disclosed and in many instances is accessible by only few employees with a special security clearance. This represents a challenge for both industry and research entities, as they face difficulties to comply with the necessary RD&D capabilities.

To tackle some of the above mentioned challenges, the work in this thesis proposes a framework that will provide a holistic approach to generating a realistic synthetic grid. To ensure a feasible grid operation and realistic system design, various power system planning (PSP) methods, often used by planning engineers, are defined. The approach to sourcing data from various sources is also introduced and summarized.

At first, distribution PSP is discussed and elaborated with the introduction of novel mathematical optimization models for radial, ring and slightly meshed distribution system respectively. The work further discusses and introduces the concepts of transmission PSP. Two different TSP models are defined as a DC power flow TSP approach and a

conic AC power flow relaxation approach for the TSP problem. Furthermore, a detailed comparison and the strengths and differences of each of these models is presented and discussed. As part of the TSP, it is also essential to consider the security requirements imposed by the system regulators for system stability and an uninterrupted power supply. To address the security criteria requirements, a novel N-1 transmission system expansion planning model definition is proposed.

A case study of the application of the proposed framework is defined for the development of a synthetic grid of the Singaporean power system. The available data and sources are discussed and the system structure is explained. The approach to developing the synthetic Singaporean grid is a bottom-up approach which considers the end user demand being allocated to adequate distribution systems. Once the distribution system is defined using the proposed distribution PSP methodology, the framework continues to model the sub-transmission and transmission networks to the highest voltage level.

To demonstrate the usefulness of the proposed framework, the developed grid is used for the study and analysis of the viability and application of a novel distribution network expansion planning with Li-ion BESS. A hybrid optimization approach using a genetic algorithm (GA) and a mixed integer quadratically constrained programming (MIQCP) is defined. The GA determines the selection of new lines combined with the placement of the BESS, which are then used in the MIQCP sub-optimization to provide the optimal BESS sizing and test the power flow feasibility. To demonstrate the key benefits of the proposed method, the model is tested on the Singaporean synthetic grid model. The results are analyzed to conclude the benefits of combining new lines and BESS as an approach for a feasible cost effective distribution system expansion planning solution.

Zusammenfassung

Um die fortschreitenden Herausforderungen, die durch die jüngsten technologischen Fortschritte Im Strom- und Energiesektor auferlegt werden, zu Bewältigen ist es unerlässlich, die Stromversorgungssystemein intelligentere“ und widerstandsfähigere Netze zu modernisieren. Strenge Umwelt- und Nachhaltigkeitsziele haben die Entwicklung von erneuerbaren Energien (RE), dezentralen Energieressourcen beschleunigt (DER), Batterie-En- ergiespeichersysteme (BESS), Elektrofahrzeuge (EVs) und Informations- und Kommunikationstechnologien (IKT).

Die Lasten sind definiert als flexibel und steuerbar, die Konsumenten werden zu Prosumenten, Der Energiemix verändert sich, neue Programme wie Nachfragereaktion werden laufend erforscht und eingeführt, und die Energiemärkte gehen in einer deregulierten Marktumgebung über. Diese Entwicklungen weichen vor neuen Konzepten und Möglichkeiten und stellen viele neue Stakeholder vor, die die Grid-Landschaft verändern. Trotz der zahlreichen potenziellen Vorteile solcher Weiterentwicklungen müssen die Auswirkungen auf das Netz analysiert und die damit verbundenen Herausforderungen identifiziert werden.

Die oben genannten Technologien und Entwicklungen werden sich auf das Kraftsystem auswirken, welches im Detail analysiert werden muss. Diese Entwicklungen üben noch zusätzlichen Druck auf die Versorgungsunternehmen aus, um die Ziele moderner Netze mit minimalen Investitionskosten zu erreichen, ohne die kritischen Dienste, die sie derzeit erbringen, zu gefährden. In Anbetracht der Wichtigkeit des Stromversorgungssystems ist das wichtigste Anliegen bei einer Implementierung der unterbrechungsfreie Betrieb desselben. Es wurde jedoch anerkannt dass das Fehlen realitätsnaher Forschung, Entwicklung und Demonstrationsfähigkeiten (RD&D) Herausforderungen sind, die die Akteure der Energiewirtschaft bewältigen müssen, um die Entwicklung, Validierung und Unterstützung bei der Qualifizierung von Technologien, Anwendungen und Lösungen als Teil der Smart-Grid-Initiative zu ermöglichen.

Detaillierte reale Stromsystemmodelle werden jedoch als kritische Infrastruktur mit hoher Priorität mit Vertraulichkeitsbeschränkungen eingestuft. Solche Informationen werden nicht öffentlich bekannt gegeben und sind in vielen Fällen nur wenigen Mitarbeitern mit einer speziellen Sicherheitsfreigabe zugänglich. Dies stellt sowohl die Industrie als auch die Forschungseinrichtungen vor einer Herausforderung weil sie Schwierigkeiten konfrontieren um die erforderlichen (RD&D)-Kapazitäten einzuhalten. Um einige der oben genannten Herausforderungen anzugehen, schlägt die Arbeit in dieser Dissertation ein s.g. Framework vor welches einen ganzheitlichen Ansatz zur Generierung eines realistischen synthetischen Gitters bietet.

Um einen praktikablen Netzbetrieb und eine realistische Systemauslegung zu gewährleisten, werden verschiedene Netzsystem-Planungsmethoden (PSP), definiert die häufig

von Planungsingenieuren verwendet werden. Die Vorgehensweise zur Datenbeschaffung aus verschiedenen Quellen wird ebenfalls vorgestellt und zusammengefasst. Zunächst wird die Distribution PSP mit der Einführung von Mathematischen Optimierungsmodellen für Radial-, Ring- und leichtmaschige Verteilsysteme diskutiert und ausgearbeitet. Danach werden die die Konzepte der PSP-Übertragung diskutiert und eingeführt.Zwei verschiedene TSP-Modelle sind als Gleichstromfluß mit TSP-Ansatz und ein konischer AC-Stromflußlockerung für das TSP-Problem. Außerdem ist ein ausführlicher Vergleich der Stärken und Unterschiede jedes dieser Modelle vorgestellt und besprochen. Im Rahmen des TSP müssen auch die Sicherheitsanforderungen der Systemregulatoren für die Systemstabilität und eine unterbrechungsfreie Stromversorgung berücksichtigt werden. Um die Anforderungen der Sicherheitskriterien zu erfüllen, wird ein neuartiges N-1-Übertragungssystem des Expansionsplanungsmodells vorgeschlagen.

Für die Entwicklung wird eine Fallstudie zur Anwendung des vorgeschlagenen Frameworks eines synthetischen Netzes des singapurischen Energiesystems definiert. Die verfügbaren Daten und Quellen werden besprochen und der Systemaufbau erläutert. Der Ansatz zur Entwicklung des synthetischen singapurischen Netz ist ein Bottom-up-Ansatz, der den Bedarf des Endbenutzers berücksichtigt und wird angemessenen Verteilungssystemen zugeordnet. Wenn das Vertriebssystem unter Verwendung der vorgeschlagenen Verteilungs-PSP-Methodik definiert ist, wird das Framework die Unterübertragungs- und Übertragungsnetze auf der höchsten Spannungsebene fortsetzen.

Um die Nützlichkeit des vorgeschlagenen Frameworks zu demonstrieren, wird das entwickelte Raster für die Untersuchung und Analyse der Realisierbarkeit und Anwendung eines neuartigen Vertriebsnetzes mit Ausbauplanung mit Li-ion BESS verwendet. Ein hybrider Optimierungsansatz unter Verwendung eines genetischen Algorithmus (GA) und eine gemischte ganzzahlige quadratisch eingeschränkte Programmierung (MIQCP) wird definiert. Der GA bestimmt die Auswahl neuer Linien kombiniert mit der Platzierung von dem BESS, die dann in der MIQCP-Unteroptimierung verwendet werden, um das Optimierte BESS zu dimensionieren und bereitzustellen. Um die wichtigsten Vorteile der vorgeschlagenen Methode zu demonstrieren wird das Modell auf dem synthetischen Gittermodell Singapurs getestet. Die Ergebnisse werden analysiert, um die Vorteile der Kombination von neuen Linien und BESS als einen Ansatz für eine realisierbare, kostengünstige Planungslösung für die Erweiterung des Verteilungssystems zu sehen.

Contents

List of Figures

List of Tables

1 Introduction

1.1 Grid Modernization and the Smart Grid

1.1.1 Recent Developments and Upcoming Trends

Modernizing the power system to evolve into a 'smarter' and more resilient grid has become an inevitable component in coping with the progressive challenges imposed by recent technological advancements [7, 9, 10].

Strict environmental and sustainability objectives have accelerated the development of renewable energy (RE) conversion technologies for predominantly intermittent sources such as solar and wind. The use of RE has seen a continuous growth trend reaching a share of 27.5% of the world electricity generation in early 2020, with a growth of the installed generation capacity of solar photovoltaics (PVs) of more than 14 times in the course of a decade [11, 12]. For instance, the city-state of Singapore has a target to reach a share of PVs integration of up to 43% of the total electric power demand by 2050, which represents an increase of 13 times from the current PVs installed capacity [13].

Such recent developments, together with the phasing out of nuclear and coal power plants, are considerably changing the global power generation mix. This poses a significant planning and operational problem due to the non-controllable variability, partial unpredictability, and the locational dependency of the newly introduced RE generating units [14]. In the case of Singapore, an initial assessment of the grid impact of RE has shown the need for various mitigation measures to be considered [13].

The energy storage systems (ESS) are considered as one of the principal technologies necessary for the energy transition [15, 16, 17]. Battery energy storage systems (BESS) account for most of the market growth, with Li-ion batteries (LIB) leading the way due to their recent price decrease of 88.5% since 2010. The global BESS markets are expected to have an annual growth of three to five times the current installed capacity [18]. Similarly, Singapore has announced a post-2025 target of 200 MW of storage [19].

Consequently, the conventional approach to power system operation is being altered with BESS offering services such as frequency regulation, flexible ramping and black start services, in addition to enhancing RE integration by reducing RE curtailment and capacity firming. Utility-scale BESS can also be used for a cost-optimal grid investment planning through energy shifting and capacity investment deferral, and transmission and distribution congestion relief [20].

The advancement of LIB and their improved affordability also give way to a rapidly growing deployment of electric vehicles (EVs). Combined with a substantially subsidized policy support, EVs has expanded globally with an annual rate of 60% in the last five years to reach a total of 10.4 million vehicles in 2020 [21]. For instance, Singapore

has committed to deploy fully electric and hybrid buses to reach a 100% cleaner energy public bus fleet and an overall transport electrification of 52% by 2050 [22, 23]. These developments are expected to increase the electricity consumption and considerably change the power flows, grid losses and voltage profile patterns along the grid [24]. Additional capabilities of EVs to provide energy to the system or store energy when required, together with smart charging, provide both opportunities and challenges that require further consideration.

Furthermore, the hierarchically and centrally controlled power systems are no longer suitable for the smart grid concept. The proliferation of information and communication technologies (ICT) in the modern grid infrastructure is essential to provide closer monitoring and automation of all voltage levels, with the focus being on the distribution level [25]. Supported by the recent developments in ICT, sensor and metering technologies, advanced distribution management systems (ADMS) and distributed energy resources management systems (DERMS) are being introduced and further developed to enhance the grid's operational efficiency and reliability [26].

The loads are defined as flexible and controllable with the introduction of demand response (DR) programs [27]. The consumers become prosumers in a deregulated market environment, which is an important element of the modern grid [28]. These developments give way for new concepts and opportunities and introduce many new stakeholders that change the grid landscape. Despite the numerous potential benefits offered with such advancements, there is a necessity to analyze the impact on the grid and identify the associated challenges.

1.1.2 The Need for Smart Grid Research and Development

The above-mentioned technologies and developments will have an effect on the power system which needs to be analyzed in details. This will identify the path and the insights to reach a modernized grid with the purpose of improving grid reliability, resiliency, and system efficiency. The objective is to fully utilize the potential benefits and opportunities, while minimizing the risk and overcoming the identified challenges and limitations.

Given the complexity and the economic implications, it is important to understand that the required development toward a modernized grid is set to follow an evolutionary path from the existing system rather than a complete overhaul. The rapid technological developments are just adding further pressure on utilities to reach the modern grid objectives as soon as possible, with minimal investment cost, without putting at risk the critical services they currently provide.

The required transitioning of the aging infrastructure and the change in organization and processes for a more uncertain future are circumstances the players in the electrical power sector are already familiar with. The problem most power companies and regulatory bodies face is not the lack of technology, rather how to seamlessly integrate the plethora of new technologies and concepts in the existing grid and market environment.

Considering the importance of the power system as an essential facility, providing an uninterrupted service is the primary concern for a real-life implementation. Despite the capabilities and the potential benefits of the smart grid, utilities may not embark into

adopting new technologies without exhaustive validation and qualification. Therefore, "one can readily see that one of the major difficulties utilities across the world are facing is the absence of near-real world research, development and demonstration (RD&D) capability to enable them develop, validate, and qualify technologies, applications, and solutions for their smart grid programs", as stated in [29].

1.1.3 The Important Role of Realistic Test Systems

To meet the grid modernization goals, new technologies and concepts are required to be developed, tested and analyzed on real power system models. Doing so will provide the necessary validation and qualification to showcase the potential benefits and help initiate the solution implementation.

However, detailed real power system models are classified as critical infrastructure of high priority with confidentiality restrictions. Such information is not publicly disclosed and in many instances is accessible by only few employees with a special security clearance. This represents a challenge for both industry and research entities, as they face difficulties to comply with the necessary RD&D capabilities.

One viable alternative is the use of standard test systems. Both the Institute of Electrical and Electronics Engineers (IEEE) and the International Council on Large Electric Systems (CIGRE) have made significant contribution by introducing numerous benchmark test systems. For instance, the IEEE 14, 30, 57 and 118 Bus systems are defined as being part of the American Electric Grid since the 1960s. Similarly, the CIGRE B4, Medium Voltage and Nordic 32 are European test systems, with the Medium Voltage test system being a benchmark for both European and American version for the integration of renewable energy resources in the medium voltage distribution systems. The standard IEEE and CIGRE test systems are widely used and have proven to be of great benefit for researchers around the globe, as shown in [30]. However, the authors in [30] also discuss the necessity for further efforts required to make this test systems relevant for the modern power system.

Despite the wide adoption of benchmark test systems in the research community, these models might not be well suited for investigating various real-life implementation studies. The benchmark systems mostly define a simplified section of a power system, limited to a particular voltage level and a specific set of data. Furthermore, each power system is unique in terms of it's overall design and characteristics. For instance, while most power systems and test systems are considering overhead transmission, the power systems of Singapore and Hong Kong are planned and built as completely underground systems with significantly different electrical properties.

The installed generation capacity, type of power stations, voltage levels, grid infrastructure and configuration, power system operation, grid interconnection, energy source availability, consumer's demand and behavior are just some of the components which characterize each power system individually. In addition, the geographical and spatial representation and availability play a critical role on the overall power system planning (PSP) and operation. Therefore, it is of great importance to consider realistic power system models with a high resemblance to the actual grids.

1.2 Motivation

The above mentioned developments and the need for test systems of real grids lead the way for creating a framework which will serve as a guide to generate realistic publicly available test systems with a high resemblance of a particular grid. The main objectives of such framework can be defined as follows:

- to research, gather and process publicly available data from various sources;
- to utilize the obtained data and provide a geographically and spatially correct power system representation of an existing grid;
- to generate synthetic grid data for missing information such that a feasible power system operation is ensured in line with safety regulations;
- to provide a holistic approach for generating a synthetic power system as a whole, including both transmission and distribution systems; and
- validate the generated synthetic grid and perform load flow analysis to confirm the power system feasibility.

To accomplish the objectives of the envisioned framework, an approach used by the planning engineers to design the power system may be required. Power systems are planned and engineered in a cost-effective manner with respect to the overall investment and operational costs [31, 32]. Power system planning is a commonly used approach to determine the placement, sizing and selection of generating units and power stations, transformers and substations, transmission and distribution lines and line configurations, and to define the optimal grid operation. In addition to the cost minimization objectives, an important role of the planning process is to ensure the grid's operational feasibility and continuity of supply in line with the regulatory requirements.

When it comes to utilizing the PSP approach for the purpose of generating a synthetic grid, there exist certain challenges as follows:

1. For the application of PSP models, a specific set of input parameters is required. However, when generating a synthetic grid, publicly available data with a rather limited access to grid details is used. Such circumstances can often make the available data insufficient and the PSP models unusable.
2. Due to the extensive history of the existence and development of the power system, most PSP optimization methods found in the literature propose grid expansion planning as an upgrade to an already existing grid. However, to generate a realistic synthetic grid, a methodological approach for a complete power system reproduction is needed.
3. The power system consists of both transmission and distribution systems. Despite the interdependence of the two systems, there are rather different characteristics and requirements that need to be taken into account for the design, planning and operation of both systems.

1.3 State-of-the-art

Given the requirements for the development of a framework for realistic synthetic grid generation by utilizing power system planning as a suited approach, this section describes the recent literature.

1.3.1 Synthetic Grid Generation

With a main objective of generating a synthetic grid, [33, 34, 35, 36, 37, 38, 39, 40, 41, 42, 43, 44] present some recent work found in the literature. An approach for generating synthetic grids with a focus on distribution grids is proposed in [33, 34, 35, 36], while [37, 38, 39, 40, 41, 42, 43, 44] consider transmission power systems.

1.3.1.1 Distribution Synthetic Grid Generation

In [33], statistical patterns in the form of probability density function (PDF) are identified using a large data set from a distribution system operator (DSO) in the Netherlands. Similarly, the authors in [34] study the topological and electrical properties of distribution systems and point out an evident small-world network resemblance. An algorithm for automated generation of random distribution grids that statistically resemble the real grid is then proposed [33, 34].

The authors in [35] model a synthetic medium voltage urban and rural networks, following the basic radial and ring main unit distribution system concepts. Standardized parameters to define the input parameters such as cables, overhead lines and transformers are used. In order to provide and test a joint simulation environment of the transmission and distribution grid, a synthetic distribution grid model is being considered as an extension to an already existing transmission grid model in [36]. For this purpose, benchmark grids are used as grid modules, which are then combined as modular and scaled to match the installed power of the loads and additional parameters.

1.3.1.2 Transmission Synthetic Grid Generation

In terms of transmission systems, [38] defines the fundamental steps for creating synthetic models as identifying geographically accurate loads and generator substation placement, and the assignment of the electrical parameters for the transmission lines. However, creating a feasible and power flow solvable transmission network topology and synthetic grid cases are identified as key components that require further development. The methodology is further detailed in [39], with comprehensive load and generator clustering algorithms. Furthermore, the grid structural characteristics are being described using the theory of Delaunay triangulation, which has proven to be a better match than using the small-world networks. To address the need for geographically realistic synthetic grids, the authors extend the model for geomagnetic disturbance studies in [42]. The importance of an alternating current (AC) power flow convergence and reactive power planning as a key component in creating synthetic grids is discussed in [40].

The structural properties of the North American grids are also studied in [43], and an algorithm for synthetic grid generation based on the graph theory analysis is proposed. The use of correlated assignment of generation, load and connection buses for an improved synthetic power grid modeling approach is presented in [37]. Similarly, the characterization of the correlation of the bus type assignment is done statistically, based on data obtained from number of different realistic grids. Using voltage-level dependent parameters, the authors in [44] distinguish between transmission lines and transformers to enhance the proposed random-topology synthetic grid modeling.

Although the above-mentioned methods define somewhat realistic grids, random synthetic grids are being generated. A most commonly used approach to generate a realistic synthetic grid is to utilize the statistical characteristics of a real grid. However, the availability of such information is fairly limited to only a few distribution and transmission systems found in the literature, and does not necessarily represent a match to any other system. In addition, another thing in common for both transmission and distribution synthetic grid generation methods is the limited consideration of the power flow convergence when modeling the grid. The primary focus is to generate statistically and structurally correct grids before considering the power flow feasibility and electrical constraints.

1.3.2 Power System Planning

Power system planning methods have been used over the decades to ensure a normal and cost-effective power system operation by determining the optimal network plan with minimal investment cost. Extensive efforts have been made and discussed in the literature, with [45, 46, 47, 48, 49, 50, 51, 52, 53] focusing on distribution system planning (DSP), while [54, 55, 56, 57, 58, 59, 60, 61, 62, 63, 64, 65, 66, 67, 68, 69] are some contributions made with a focus on transmission system planning.

1.3.2.1 Distribution System Planning

With the need to restructure the distribution grids to be more efficient, reliable and cost effective, new and improved DSP models are being frequently developed and introduced [2, 5]. Numerous research efforts have been reported and discussed in the literature over the years [46]. With the improvements in information technology, DSP methods are being advanced to be more accurate, more detailed and more sophisticated to include the recent smart grid concepts [45].

In order to reach an economically viable planning strategy, the DSP approach can incorporate a detailed cost evaluation of all the major planning decisions [49]. In addition to planning the feeders, substations and transformers, new integrated approach that consider distributed generation (DG) as part of the distribution system planning methods are introduced in [48]. Dynamic distribution system planning methods are also enabled with the current state-of-the-art in computer technology, which can further re-

duce the investment costs by determining the best time schedule for realizing the planned investments [47].

The increase of DGs installed in the grid introduces uncertainties such as variable load demand and RE generation, which can be accounted for by introducing probabilistic modeling in the distribution system planning method as proposed in [50]. Furthermore, the grid reliability is introduced as part of the decision making process in the planning approach in [51]. The grid can reach the full potential in its low-carbon sustainable objectives by considering demand response together with RE as part of the planning process, as described in [52]. The DSP approach is further advanced to consider the new and deregulated market structures for the consideration of private DG and independent DSOs [53].

1.3.2.2 Transmission System Planning (TSP)

There are numerous research efforts made in the literature for different transmission expansion planning (TEP) methods with various applications [3, 4]. Due to the complex nature, a static long term TEP as a single stage deterministic cost optimization method is commonly used [54, 55, 56]. Other methods may include stochastic programming or heuristic approaches such as a genetic algorithm or a constructive heuristic algorithm [57, 58, 59]. In addition, various multi-stage methods are proposed to address the increase in complexity of the TEP when different applications are introduced [60, 61, 62, 63].

One of the applications in the TEP optimization is an energy market environment with a pool-based market equilibrium that considers the social welfare and a free trade electricity market [62, 63, 64]. Uncertainties such as load variations, generator rescheduling, market competitions and availability of the system facilities are introduced with probabilistic modeling as part of the TSP method in [57]. Recent work includes the consideration of DGs, such as RE and ESS combined with a TEP approach, as proposed in [57, 65, 66]. Further applications include a TEP with shunt compensation devices, as well as a short-circuit level constrained TEP [56, 67].

However, most TEP methods do not consider the required security criteria of the system. This means that contingencies caused by the outage of a single component such as a transmission line, transformer or a generator, known as the N-1 criteria, are not considered when obtaining the optimal solution. The ability of a power system to preserve the normal state during N-1 outage is a universally accepted fundamental security criteria for the transmission system operation [68]. The significance of including the N-1 security constraint in the TEP methodology is emphasized in [3, 69].

Despite the advanced state of the numerous DSP and TEP methods in the literature, an approach tailored to utilize the publicly available data and generate the required missing part of the grid is needed for the purpose of generating a synthetic grid. To realistically model the power system, the framework needs to include a holistic approach that accounts for the security and reliability criteria of the power system operation. This is defined through enhanced grid configurations such as rings in the DSP optimization problem and the fundamental N-1 security constraints in the TEP optimization problem.

1.4 Thesis Contribution

In this thesis, a framework for generating a realistic synthetic grid based on publicly available data that corresponds to a particular real grid is proposed. The contributions made with this work are as follows:

- One of the most important aspects to defining the framework is the availability of public data. To identify the required data, a rather comprehensive and unconventional approach for sourcing the needed information is presented.
- Instead of generating a random synthetic grid with statistical properties of a real grid, the framework is focused to include as much real data into the generation of the synthetic grid as publicly available. Consequently, the synthetic grid is generated with an aim to geographically and spatially match the existing grid.
- To generate a realistic synthetic power system, a PSP approach used by planning engineers is utilized. To ensure a feasible power system operation, a convex AC power flow is used to define both DSP and TEP optimization methods.
- In addition to the DSP and TEP optimization models, a novel deterministic scenario-based model for ring distribution system expansion planning and a deterministic scenario-based N-1 security constraint transmission expansion planning model are proposed.
- To demonstrate the practicality of the obtained synthetic power system, a novel heuristic distribution system expansion planning optimization considering BESS is defined and tested on a section of the grid.

Although the development of the framework is done with the purpose of universality and the ability to be implemented on any power system for which the required data can be obtained, the proposed work is focused on generating a synthetic grid of the Singaporean power system.

1.5 List of Publications

In the course of this thesis, publications which directly and indirectly helped in identifying the research direction of the presented work were made, as follows:

1. **A. Trpovski**, P. Banerjee, Y. Xu and T. Hamacher, "A Hybrid Optimization Method for Distribution System Expansion Planning with Lithium-ion Battery Energy Storage Systems," *2020 IEEE Sustainable Power and Energy Conference (iSPEC)*, Chengdu, China, 2020, pp. 2015-2021, doi: 10.1109/iSPEC50848.2020.9351208.

2. **A. Trpovski** and T. Hamacher, "Ring Distribution System Expansion Planning using Scenario Based Mixed Integer Programming," *2020 IEEE/PES Transmission and Distribution Conference and Exposition (T&D)*, Chicago, IL, USA, 2020, pp. 1-5, doi: 10.1109/TD39804.2020.9299971.

3. **A. Trpovski** and T. Hamacher, "Scenario Based N-1 Transmission Expansion Planning using DC Mixed Integer Programming," *2019 IEEE Power & Energy Society General Meeting (PESGM)*, Atlanta, GA, USA, 2019, pp. 1-5, doi: 10.1109/PESGM40551.2019.8973506.

4. **A. Trpovski** and T. Hamacher, "A Comparative Analysis of Transmission System Planning for Overhead and Underground Power Systems using AC and DC Power Flow," *2019 IEEE PES Innovative Smart Grid Technologies Europe (ISGT-Europe)*, Bucharest, Romania, 2019, pp. 1-5, doi: 10.1109/ISGTEurope.2019.8905510.

5. **A. Trpovski**, D. Recalde and T. Hamacher, "Synthetic Distribution Grid Generation Using Power System Planning: Case Study of Singapore," *2018 53rd International Universities Power Engineering Conference (UPEC)*, Glasgow, UK, 2018, pp. 1-6, doi: 10.1109/UPEC.2018.8542054.

6. **A. Trpovski**, D. F. R. Melo, T. Hamacher and T. Massier, "Stochastic optimization for distribution grid reconfiguration with high photovoltaic penetration," *2017 IEEE International Conference on Smart Energy Grid Engineering (SEGE)*, Oshawa, ON, Canada, 2017, pp. 67-73, doi: 10.1109/SEGE.2017.8052778.

7. D. Recalde, **A. Trpovski**, S. Troitzsch, K. Zhang, S. Hanif and T. Hamacher, "A Review of Operation Methods and Simulation Requirements for Future Smart Distribution Grids," *2018 IEEE Innovative Smart Grid Technologies - Asia (ISGT Asia)*, Singapore, 2018, pp. 475-480, doi: 10.1109/ISGT-Asia.2018.8467850.

8. S. Troitzsch, S. Hanif, K. Zhang, **A. Trpovski** and T. Hamacher, "Flexible Distribution Grid Demonstrator (FLEDGE): Requirements and Software Architecture," *2019 IEEE Power & Energy Society General Meeting (PESGM)*, Atlanta, GA, USA, 2019, pp. 1-5, doi: 10.1109/PESGM40551.2019.8973567.

1.6 Authorship Attribution Statement

This thesis contains material from 5 papers published in peer-reviewed conference proceedings where I was the first author, as follows

Chapter 3 includes some modified content published in A. Trpovski, D. Recalde and T. Hamacher, "Synthetic Distribution Grid Generation Using Power System Planning: Case Study of Singapore," *2018 53rd International Universities Power Engineering Conference (UPEC)*, Glasgow, UK, 2018, pp. 1-6, doi: 10.1109/UPEC.2018.8542054 [2].

The contributions of the co-authors are as follows:

- The direction and the idea was revised with Dr. D. Recalde and discussed with Prof. T. Hamacher.

- I prepared the manuscript draft, which was then revised by Dr. D. Recalde and discussed with Prof. T. Hamacher.
- I implemented the approach and conducted the simulations. The results were revised with Dr. D. Recalde and discussed with Prof. T. Hamacher.

Chapter 3 includes some modified content published in A. Trpovski and T. Hamacher, "Ring Distribution System Expansion Planning using Scenario Based Mixed Integer Programming," *2020 IEEE/PES Transmission and Distribution Conference and Exposition (T&D)*, Chicago, IL, USA, 2020, pp. 1-5, doi: 10.1109/TD39804.2020.9299971 [5].

The contributions of the co-authors are as follows:

- The direction and the idea was discussed with Prof. T. Hamacher.
- I prepared the manuscript draft, which was then discussed with Prof. T. Hamacher.
- I implemented the approach and conducted the simulations. The results were discussed with Prof. T. Hamacher.

Chapter 4 includes some modified content published in A. Trpovski and T. Hamacher, "Scenario Based N-1 Transmission Expansion Planning using DC Mixed Integer Programming," *2019 IEEE Power & Energy Society General Meeting (PESGM)*, Atlanta, GA, USA, 2019, pp. 1-5, doi: 10.1109/PESGM40551.2019.8973506 [3].

The contributions of the co-authors are as follows:

- The direction and the idea was discussed with Prof. T. Hamacher.
- I prepared the manuscript draft, which was then discussed with Prof. T. Hamacher.
- I implemented the approach and conducted the simulations. The results were discussed with Prof. T. Hamacher.

Chapter 4 includes some modified content published in A. Trpovski and T. Hamacher, "A Comparative Analysis of Transmission System Planning for Overhead and Underground Power Systems using AC and DC Power Flow," *2019 IEEE PES Innovative Smart Grid Technologies Europe (ISGT-Europe)*, Bucharest, Romania, 2019, pp. 1-5, doi: 10.1109/ISGTEurope.2019.8905510 [4].

The contributions of the co-authors are as follows:

- The direction and the idea was discussed with Prof. T. Hamacher.
- I prepared the manuscript draft, which was then discussed with Prof. T. Hamacher.
- I implemented the approach and conducted the simulations. The results were discussed with Prof. T. Hamacher.

Chapter 7 includes content published in A. Trpovski, P. Banerjee, Y. Xu and T. Hamacher, "A Hybrid Optimization Method for Distribution System Expansion Planning with Lithium-ion Battery Energy Storage Systems," *2020 IEEE Sustainable Power and Energy Conference (iSPEC)*, Chengdu, China, 2020, pp. 2015-2021, doi: 10.1109/iSPEC50848.2020.9351208 [6].

The contributions of the co-authors are as follows:

- The direction and the idea was prepared with Mr. P. Banerjee, revised by Prof. Y. Xu and discussed with Prof. T. Hamacher.
- The manuscript draft was prepared together with Mr. P. Banerjee, revised by Prof. Y. Xu and discussed with Prof. T. Hamacher.
- Mr. P. Banerjee implemented the approach and conducted the simulations. The results were discussed with Prof. Y. Xu and Prof. T. Hamacher.

2 Research Framework

To tackle some of the challenges for further development of the necessary RD&D capabilities towards the modernization of the electric power system, the work in this thesis is focused to define a framework that will provide a holistic approach to generating a realistic synthetic grid. To ensure a feasible grid operation and realistic system design, various power system planning methods, often used by planning engineers, are defined. In this chapter, an overview of the proposed framework is presented.

2.1 Publicly Available Grid Data Acquisition

One of the key aspects to enabling the usage of the proposed framework is the ability to identify the input parameters from publicly available sources. However, this is easier said than done due to the confidentiality restrictions and the high priority of the power system as a critical infrastructure. Therefore, an approach to conduct an exhaustive search from various sources is required. With an ever-growing internet accessibility, some of the sources considered for collecting power system data can include, but not limited to:

- Energy market regulator
- Power system operator (PSO)
- DSOs and TSOs
- Energy market participants
- Power engineering companies
- Research articles
- Geographic information system (GIS)
- News media and magazines
- Professional social media
- Import/export trade data
- Data platforms and web articles

2.1.1 Energy Market Regulator, PSO, DSOs, TSOs

Given the public nature of the service provided by the energy market regulator, PSO, DSOs and TSOs, it is very common to have annual reports published to share key statistical energy data and relevant completed or ongoing projects in the power sector. Furthermore, considering the recent market deregulation and the tendency to provide

a fair competition in the energy markets, more data of the energy market participants is made available. This data may provide some insights on the structure of the power system including different voltage levels, electricity prices, consumer demand, generation mix, generating units, substations, typical equipment and components used, etc. Some tender and procurement documentation may also be publicly shared, which can give further insights on the equipment and components used and their prices.

2.1.2 Energy Market Participants

Some of the relevant energy market participants include generation facilities, retailers and wholesale market traders, and interruptible loads. Although very limited information is being shared by these entities, it is often useful to identify all the involved parties in the market. For instance, given a list of generating units by the market regulator, identifying the generating facility can provide an accurate location and further information shared by the company.

2.1.3 Power Engineering Companies

Being the contractors that built the grid, power engineering companies play an important role in the power system environment. Consequently, these companies can be a valuable source of information to obtain relevant data for the existing power system infrastructure. Through professional media channels, promotional materials, or their own web sites, companies often publicly share a reference list of past projects to demonstrate and promote their capabilities. Some of the information that can be obtained includes substation identification, types and sizes of transformers, cross section area and types of cables, location and installed capacity of shunt reactors, etc. Furthermore, manufacturing companies provide catalogs with detailed technical specification of power system components, such as conductors and transformers.

2.1.4 Research Articles

The research community is regularly involved in different power system studies, resulting in numerous publications. It is often of interest to players in the power industry to take part and finance such relevant projects run by local and national institutions. Although very limited and often bound by confidentiality restrictions, some information that gives better understanding of the existing power system can be found.

2.1.5 GIS, Data Platforms and Web Articles

GIS software, such as Google Maps[1], is one of the essential tools needed for generating a realistic and geographically correct power system. Through the use of satellite imagery and street maps, an accurate location of key power system components such as power stations, substations and consumers can be obtained. The use of application programming interfaces (API) also provides realistic line corridors and cable lengths as required.

[1] https://maps.google.com/

Furthermore, there are increasingly more data platforms available, such as Foresquare[2] and in the case of Singapore OneMap[3] and OneMap3D[4], that provide relevant location information of power system facilities and 3D maps useful for consumer demand modeling. Web articles from various sources may also include some insights that support and broaden the understanding of the collected data.

2.1.6 News Media, Magazines and Professional Social Media

Many of the power engineering projects are of public interest and of great significance, hence news media and magazines often feature content and press releases on the recent developments in the grid. With archives being made available online, it is worth looking into such sources for any relevant power system information. Furthermore, recent trends in professional social media, such as LinkedIn[5], are often the preferred place where current and past power system projects and developments are publicized.

2.1.7 Import/export Trade Data

As part of the power system planning approach to define an optimal grid design, one of the required input parameters is the price of the equipment. However, due to the limited offer and competitive nature of the industry, in addition to the constantly changing commodity price of key materials such as copper, steel and aluminum, prices of the power system components are rarely published. To realistically consider the investment costs, a global trade import and export data can be used. For instance, online database providers, such as Zauba[6], can be used to search import and export shipment records of power system equipment such as power cables and transformers. The nett export/import price can then be increased by a factor that corresponds to the import tax of the country and estimated shipping costs.

Given the diverse nature of the above mentioned sources, various power system data can be obtained. Consequently, analyzing and combining all the gathered data will provide a better understanding of the existing power system in greater detail. Based on the obtained information, some of the missing data such as the consumer demand can be modeled [70]. Realistic line corridors, including the line length, type of conductors and technical characteristics can be defined. Power stations and substations location, together with generator and transformer types, sizes and specification can also be found. The price of the equipment can be defined and the use of some additional components such as shunt reactors can be identified.

In Chapter **??**, the above mentioned approach for sourcing publicly available data of a power system is practically demonstrated for determining publicly available information of the power system of Singapore.

[2] https://foursquare.com/
[3] https://www.onemap.gov.sg/
[4] https://www.onemap3d.gov.sg/
[5] https://www.linkedin.com/
[6] https://www.zauba.com/

2.2 A Holistic Power System Planning Approach

Following an exhaustive research, analysis and modeling of the power system data, we presume the following input parameters as **known**:

- Distribution and transmission voltage levels
- Consumer demand and their location
- Power stations and specification of the generating units
- Substations location and transformer characteristics and price
- Cables/conductors type, size and estimated price
- Identified line corridors (high voltage transmission)
- Installed shunt reactors or other equipment (if applicable)

However, due to insufficient data and high confidentiality restrictions, the following power system data is **unknown**:

- Detailed line configuration
- Load allocation and transformer loading

Considering the known power system data as input parameters to a problem definition for determining the unknown information, power system planning optimization is a suitable approach to realistically model and complete a feasible synthetic grid.

2.2.1 Power System Planning Framework

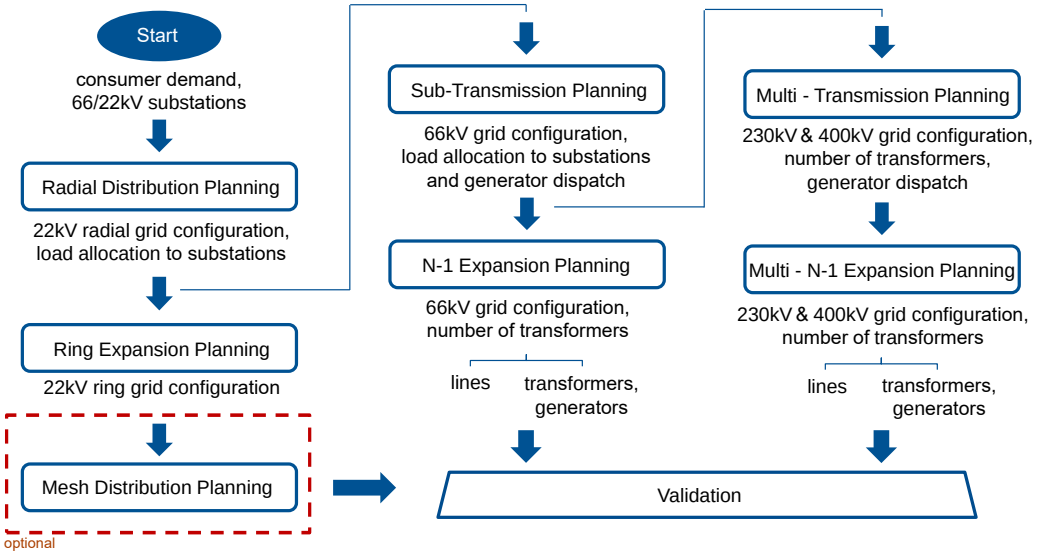

Figure 2.1: A holistic power system planning framework

For the purpose of generating the synthetic grid, a bottom up approach consisting of both distribution and transmission power system planning optimizations is used. The proposed framework is shown in Figure 2.1. The proposed optimization models are defined to consider a power system with distribution, sub-transmission and transmission voltage levels, as in the case of the Singaporean power system.

2.2.1.1 Radial Distribution System Planning

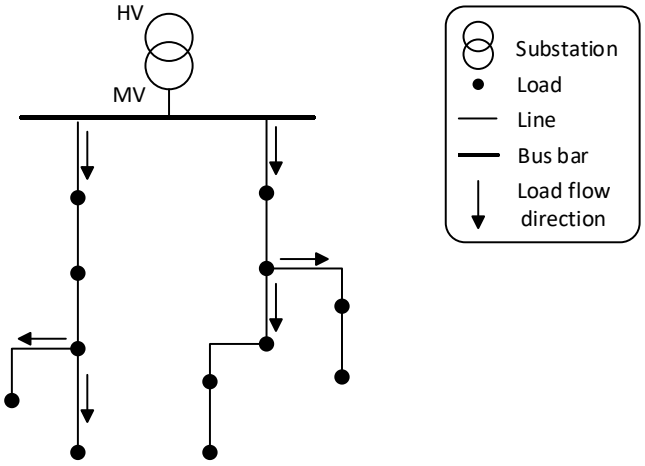

Figure 2.2: Radial distribution grid configuration

Distribution systems are considered to be a vital part of the grid to link the bulk power system and its end users. Traditionally, distribution systems are built and operated in a simple and cost-effective manner by using radial feeders, as shown in Figure 2.2. The configuration is characterized with a source, most commonly a substation with the high voltage (HV) side connected to the sub-transmission or transmission system, and different feeders which radiate from the medium voltage (MV) busbar to supply the loads. The power flow is unidirectional, from the source to the loads along the feeder. This allows for a minimal infrastructure investment and a simple grid operation. The basic reason behind having a rather simplified approach is the overall scale of the distribution system and its economic implications, as well as the fact that outages of a single feeder have a very limited and localized impact compared to an outage in the transmission system which may cause widespread catastrophic economic consequences [71].

Given the widespread adoption of radial grid operation in the distribution systems, the initiation of the framework in Figure 2.1 is defined with a radial DSP optimization. Following a clustering approach, the consumer demand of the end users is assigned to distribution substations [72], which are then considered as input load parameters for the optimization. The sub-transmission substations are considered as sources through the use of step-down transformers, which supply the energy to the distribution level. A set of possible line connections between the MV nodes is defined. Using the cost of the

grid components and the operational losses, a DSP optimization is used to determine a cost-effective radial grid configuration to supply the demand. The radial configuration allocates the loads to an adequate sub-transmission level substation and determines the optimal number of transformers by considering their cost. To ensure feasibility, the grid configuration and load allocation are subjected to constraints defined by load flow and power balance equations, together with the physical constraints of the system. Furthermore, to consider some realistic design parameters, such as the future peak demand growth, additional constraints are introduced.

2.2.1.2 Ring Distribution System Expansion Planning

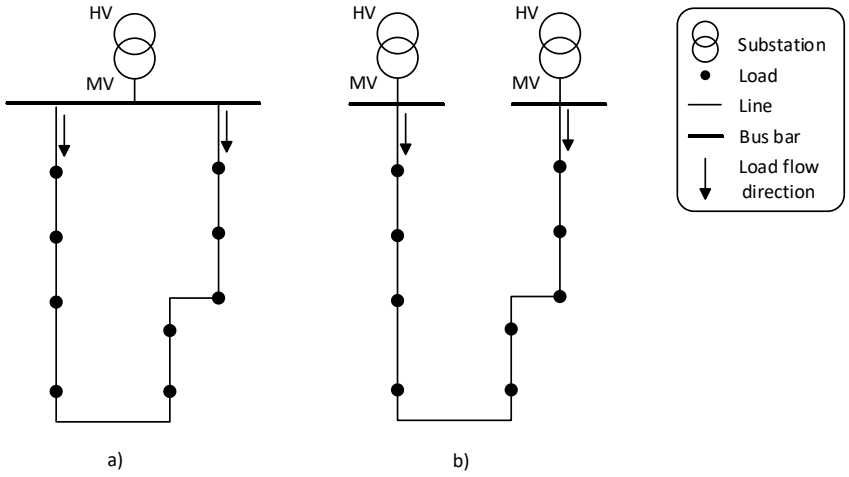

Figure 2.3: Ring distribution grid configuration

Despite the simplicity and the economic consideration of the radial grid configuration, more than 80% of the supply interruptions are reported to happen in the distribution system. Consequently, the distribution grid has been identified as the weakest link between the source of supply and the end users [71]. With the necessity to meet the strict grid regulations, cope with the smart grid trends and improve customer satisfaction, a most common approach for enhancing the reliability of supply is for planning engineers to consider an alternative feed as an addition to the standard radial distribution feeders [5]. To provide a backup supply from the reserve capacity of a transformer or from an adjacent substation, ring configurations are introduced, as shown in Figure 2.3 a) and Figure 2.3 b) respectively. Some of the advantages of the ring configurations is an increased reliability through the ability to isolate the load without disturbing the supply, as well as a potentially improved voltage profile [73].

For the purpose of modeling ring configurations, a ring distribution system expansion planning approach is defined [5]. The method considers the initially obtained radial grid configuration and provides an expansion in the form of rings by connecting the end nodes of the radial feeders. Similarly, the optimization approach is defined through a

cost minimization objective, where the cost of building a new line and upgrading the existing lines are considered. The constraints include an AC power flow model and power balance equations, combined with the physical constraints of the system. Depending on the input parameters, the optimization can provide a solution for both type of ring configurations shown in Figure 2.3.

2.2.1.3 Mesh Distribution System Expansion Planning

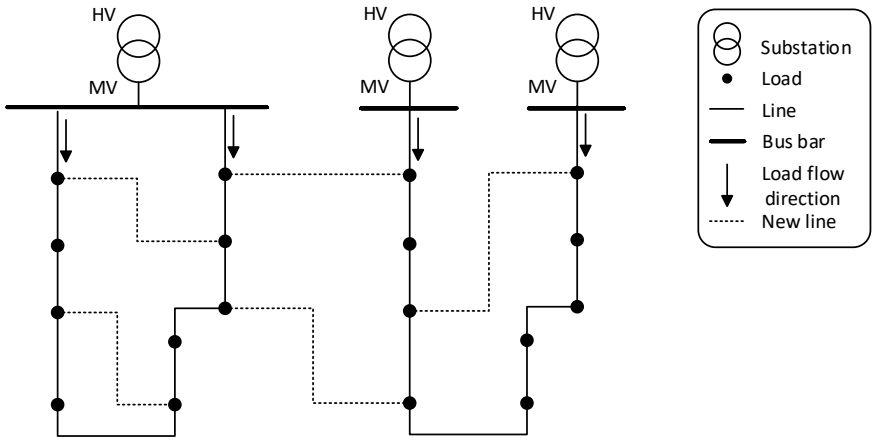

Figure 2.4: Mesh distribution grid configuration

The distribution grid can further be expanded and organized in a mesh structure, as shown in Figure 2.4. However, mesh configurations are mostly used on the high voltage side, rather than the distribution side. It is a significantly more complex structure when compared to radial and ring configurations. To provide a mesh operation of the distribution grid, significant infrastructure updates are required. A more simplified approach to include a mesh configuration is to follow a radial or ring grid structure with redundant lines in addition to the main lines [73]. The additional lines are then used to change the radial configuration and the path of the power flow when required. This represents a significant challenge in terms of operation and protection of the system, and it is not a widely adopted approach. However, the adoption of mesh distribution systems may be one way to deal with the uncertainty and the bi-directional power flow of DG in the grid. Therefore, an approach for mesh distribution system expansion planning is included as an optional step in the proposed framework.

2.2.1.4 Sub-transmission System Planning

Following the first step of the framework for radial distribution system planning, the loads are allocated to the sub-transmission substations. Consequently, the number of HV/MV step-down transformers and their peak demand are defined. Having obtained

the distribution system, it is next required to generate the sub-transmission grid which serves as a link between the generators and the transmission system on one side, and the distribution system and the end users on the other side.

The sub-transmission system is designed with a mesh structure, similarly to the transmission systems. The nominal voltages usually considered for sub-transmission level are between 33kV and 110kV. In addition to the generating units found in the transmission system level, DG and some smaller generators are also present in the sub-transmission system. While it is common to have multiple circuits and bundled conductors in a single corridor of a transmission system, the proposed approach for sub-transmission PSP is defined with an assumption of a single circuit per corridor. Other differences include shorter lines and more substation nodes in the same covered area for the sub-transmission system when compared to the transmission system.

Having defined the HV/MV transformers as loads, the sub-transmission PSP has an objective to generate a cost optimal grid configurations and allocate the loads to the transmission substations by considering both the cost of the lines and the cost of the high voltage transformers. The objective is subjected to constraints that ensure grid feasibility through the use of AC power flow, power balance equations, and the physical constraints of the system. In addition, the structural characteristics of the system can also be considered to provide a more realistic solution with a higher resemblance of a real grid.

2.2.1.5 N-1 Sub-transmission System Expansion Planning

Considering the complex nature of the PSP problem, the initial step of sub-transmission system planning does not account for the security criteria of the system. Although the obtained optimal solution is feasible in terms of the power flow convergence, any contingencies caused by the outage of a relevant power system component such as a line, a transformer or a generator are not considered. The ability of a power system to preserve the normal state during an outage of a single component is a universally accepted fundamental security criteria for the power system operation, known as the N-1 criteria [3, 68]. Therefore, a N-1 sub-transmission system expansion planning optimization is introduced as part of the framework.

The N-1 expansion planning approach takes the previously obtained sub-transmission system as input, and provides a grid reinforcement to comply with the N-1 security criteria. The objective of the optimization is to add lines to the existing system in a cost-effective manner and provide an uninterrupted system operation considering all possible N-1 outages. Although it is common to mostly consider line outages in the expansion planning stage of methods available in the literature, the proposed method is defined with a flexibility to evaluate all N-1 outages including transformers and generators [3]. Similarly to the sub-transmission system planning approach, the constraints include an AC power flow with a power balance equation, the physical constraints of the system and a consideration of the structural characteristics of the grid.

2.2.1.6 Transmission System Planning

Figure 2.5: Multi-circuit transmission line, *source: https://bit.ly/3y1md6a*

The electric power transmission system is designed for a bulk movement of the electrical energy from the power plants to the sub-transmission or distribution systems to reach the consumers. To reduce the energy losses and enable an efficient transmission of large amount of electric power, high voltages from 110kV and above are used. The power at the generation stations is typically generated at voltages ranging between 11kV to 28kV, and then increased to transmission voltage level using step-up transformers. Once the desired location is reached, substations with step-down transformers are used to transfer the power to the sub-transmission or distribution system. The system is highly meshed, with an advanced control and monitoring infrastructure to provide maximum reliability and uninterrupted supply.

Because of the large amount of energy transported, the costly transmission line infrastructure and the environmental challenges, it is common for transmission lines to include bundled conductors and multiple circuits in a single line corridor, as shown in Figure 2.5. This is the major difference when compared to the sub-transmission system planning approach in the previous step of the framework. Consequently, a modified PSP approach for transmission systems with multiple circuits per line corridor is defined.

The load allocation and the loading of the high voltage transformers obtained from the sub-transmission system planning approach is defined as the load demand of the transmission system. The available generating units in the system are defined as the sources of electric power in the transmission system planning optimization as well. The objective is to generate a grid configuration and generation dispatch that will supply the load demand with a minimum investment cost. Similarly, the constraints include an AC

power flow with a power balance equation, the physical constraints of the system, and a consideration of the structural characteristics of the grid.

2.2.1.7 N-1 Transmission System Expansion Planning

Following the first step of the TSP approach, a high voltage transmission system network and generation dispatch are obtained. However, the initial TSP approach does not consider the compulsory security grid regulations, described in section 2.2.1.5. To enhance the transmission network, a N-1 transmission system expansion planning optimization model is defined. Similarly to the N-1 sub-transmission system expansion planning, the optimization model considers all possible N-1 system outages and provides an expansion for the grid configuration and the number of transformers. The model can be used with both AC or DC power flow constraints, together with the physical constraints of the system and the structural characteristics of the grid.

2.2.1.8 Power Flow Analysis and Validation

Following the above-mentioned optimization steps in the proposed framework, a synthetic power system model is obtained. Each of the PSP optimization steps is subjected to constraints to ensure that a feasible grid is generated. However, due to the complexity and non-linearity of the exact power flow calculations, a simplified and relaxed representation is used. Therefore, once the generation of a synthetic grid representation for every voltage level is completed, a power flow analysis is enforced. Consequently, the final solution is tested to ensure that a feasible power system with convergent power flow results is obtained.

Another aspect considered for the validation of the synthetic grid is the resemblance of the synthetic model to a real power system. For this purpose, Complex Network Science (CNS) is used for statistical analysis and validation. CNS is used to describe the generated synthetic grid using statistical parameters such as the average node degree, the hop distance, the normalized characteristic path length, Delaunay triangulation, etc., which are then compared and validated with reference to a real power system [2, 33, 74, 39].

With the solution being tested and validated as mentioned above, the framework methodology described with Sections 2.2.1.1 - 2.2.1.8 provides a realistic synthetic grid model with a high resemblance of the existing power system.

3 Distribution System Planning

This chapter defines the methodology for generating a synthetic power distribution system utilizing publicly available data as input parameters. In this chapter, a slightly modified content of 'Synthetic Distribution Grid Generation Using Power System Planning: Case Study of Singapore' published in the proceedings of 53rd International Universities Power Engineering Conference (UPEC) and of 'Ring Distribution System Expansion Planning using Scenario Based Mixed Integer Programming' published in the proceedings of 2020 IEEE/PES Transmission and Distribution Conference and Exposition (T&D) is reproduced [2, 5].

The approach is defined as a power distribution system planning optimization. DSP models are more frequently introduced as there is a need for restructuring the grid towards a more efficient, reliable and cost effective power systems. Many different distribution system planning techniques and algorithms are being developed and improved over the last four decades [46]. With the rapid advancement in information technologies, more accurate, more detailed and more sophisticated models are defined [45]. However, when generating a synthetic grid, most of the information typically known to the planning engineer is not publicly available, such as the routes and lengths of potential lines. Hence, potential line routes and line lengths can be determined based on the geographical and spatial evaluation such that obstacles like ponds, lakes, rivers and already existing buildings and infrastructure are considered. Having defined a set of potential lines, the proposed DSP approach is used to generate a synthetic distribution grid topology and allocate the loads to adequate substations by utilizing the available system data such as the consumer demand, cable types and sizing, transformer capacity, etc.

3.1 Radial Distribution System Planning

For the initial step of the proposed methodology, a radially operated distribution network is considered. A balanced distribution system is assumed, represented by its single phase equivalent as a steady state of the system. A simplified AC power flow model is introduced based on an electric equivalent radial power flow with eliminated voltage phase angle [75]. The AC definition of the power flow model makes sure that the electrical constraints of the grid such as voltage and current limits are considered and satisfied. Similar definitions are being discussed in [76, 77]. The nonlinear part of the power flow definition in Section 3.1.3 has less binary variables and constraints compared to [76], and it is a simplified version with less continuous variable and constraints compared to [77]. The simplifications made due to the different purpose and different objectives of the models can be beneficial when considering a large scale combinatorial problem.

3.1.1 Cost Minimization Objective Function

Power distribution systems are planned and engineered in a cost efficient manner with respect to the overall investment and operational costs [78]. The synthetic power distribution grid model is generated employing a similar cost efficient planning approach used by the planning engineers. The synthetic grid generation model is defined using power system planning optimization that utilizes the publicly available data of the existing grid, which makes the synthetic grid to have high resemblance to the actual grid.

The cost minimization objective function is defined as follows

$$\min \qquad \Lambda = \lambda_1 + \lambda_2 + \lambda_3 \tag{3.1}$$

subject to

$$\lambda_1 = \sum_{(i,j)\in\Omega_l} L_{ij} \cdot 2 \cdot \Psi_{ij}^{line} \cdot \alpha_{ij} \tag{3.2}$$

$$\lambda_2 = \sum_{(i,j)\in\Omega_l} R_{ij} \cdot I_{ij}^2 \cdot S^{base} \cdot \Psi^{loss} \tag{3.3}$$

$$\lambda_3 = \sum_{i\in\Omega_s} (\Psi_i^{trafo} \cdot \tau_i + \Psi_i^{subs}) \tag{3.4}$$

Equation (3.1) is a multi-objective function with a goal to minimize the total cost of the power distribution system considering the investment cost of lines, operational cost of the system and the investment cost of substations.

Equation (3.2) defines the investment cost of lines λ_1. It is calculated by multiplication of the length of the lines L_{ij} and the cost of the chosen cable Ψ_{ij}^{line}. The cost minimization for λ_1 as a variable is achieved by selecting the most optimal line configuration considering the line investment costs. A binary variable α_{ij} is used to assure that I_{ij} is considered only for lines selected in the solution, and set $I_{ij} = 0$ when a line is not selected as part of the solution. Since the installation cost for underground cable installations can amount to 50 % of the total cost of the line, the cost of the cable is multiplied by a factor of two [79]. This way the optimization model considers both cable and installation costs.

The operational cost of the system λ_2 is defined with equation (3.3). Similarly to (3.2), the cost minimization is achieved by selecting the most optimal line configuration. This parameter is the operational cost of the system and is a direct representation of the cost of losses. The cost of the losses Ψ^{loss} is estimated to equal the cost of the wholesale electricity price.

In (3.4), the investment cost for the substations is calculated. The parameter Ψ_i^{trafo} is the cost of a single transformer. A single type of transformer and sizing is chosen according to reports of the DSO, matching the transformers installed in the power system. An integer variable τ_i is defined to represent the number of transformers at each substation node.

The cost minimization of λ_3 is achieved by optimizing the allocation of each load to an adequate substation by analyzing different line configurations with respect to the

installed transformer capacity. The obtained solution provides a minimum number of transformers τ_i for each substation node $i \in \Omega_s$. In this way the installed transformer capacity will be matched to the total demand of the system in a cost efficient manner. Ψ_i^{subs} is another cost parameter which is fixed and includes the estimated cost of the switchgear equipment per substation. Although Ψ_i^{subs} is a fixed parameter, it is included in the substation investment cost and the overall system cost so that the objective function and all of the objectives are weighted closer to a realistic scenario of the existing distribution system.

3.1.2 Annual Multi-Objective Weighting

The cost minimization objective given in (3.1) is a multi-objective function represented as a sum of three different cost parameters (3.2)-(3.4). When the total sum of the investment costs of the lines and the substations are considered in $S\$$, the ratio between these two parameters and the variable operational cost of the system will be incomparable due to the time span at which the cost in per $S\$$ is calculated. The investment cost of lines and substations is calculated in $S\$$ for a period of 40 and 35 years respectively, while the operational cost of the system is calculated in $S\$$ for a period of one hour. In such case, the cost of the losses would be so small, that it can be easily neglected as irrelevant. For successful implementation of the proposed optimization, a certain methodology to equally weight the three cost parameters is implemented. Annual time period and a mutual cost unit of $S\$/year$ for all cost parameters are introduced. In this way, all three cost parameters will be equally considered when obtaining the grid topology and the loads allocation.

3.1.2.1 Annual Investment Cost of Lines

$$\lambda_1^* = \Xi^{line} \cdot \lambda_1 = \frac{u \cdot (1+u)^{t^{line}}}{(1+u)^{t^{line}} - 1} \cdot \lambda_1 \tag{3.5}$$

The total annual investment cost of lines is calculated using the *annual equivalent-worth criterion* [80]. The investment cost parameter of the lines λ_1 is replaced with the *equivalent uniform annual worth* parameter λ_1^* by using the *capital-recovery factor* Ξ^{line} defined in (3.5).

3.1.2.2 Annual Operational Cost of the System

$$\lambda_2^* = EPLT \cdot \lambda_2 = \frac{\frac{\sum_1^{365}(P_{tot}^d)^2}{365}}{max\{(P_{tot}^d)^2\}} \cdot 8760 \cdot \lambda_2 \tag{3.6}$$

The power distribution system is designed such that it meets the peak demand of the system. However, in normal daily operation of the system, peak loads are seldom reached. The cost of the losses calculated when only peak demand is considered is not an accurate cost consideration. For instance, according to statistics for half-hourly system

demand data in Singapore, the system demand is within an interval of 5% of the peak demand for only 9.22% of the time. For a more accurate definition of the annual cost of the losses, an *equivalent peak loss time* factor (EPLT) is introduced [78]. The cost calculation of the annual variable cost of the distribution system is defined with equation (3.6).

3.1.2.3 Annual Cost of Substations

$$\lambda_3^* = \Xi^{subs} \cdot \lambda_3 = \frac{u \cdot (1+u)^{t^{subs}}}{(1+u)^{t^{subs}} - 1} \cdot \lambda_3 \tag{3.7}$$

Similarly to (3.5), the cost of the substations λ_3 is reformulated to an annual cost of substations λ_3^* using the *capital-recovery factors* Ξ^{subs} in (3.7).

3.1.2.4 Weighted Multi-objective Function

$$\min \qquad \Lambda^* = \lambda_1^* + \lambda_2^* + \lambda_3^* \tag{3.8}$$

Having the multiple objective parameters proportionally weighted, the objective function (3.1) is redefined in $S\$/year$ as shown in equation (3.8).

3.1.3 Constraints

It is necessary that the synthetic grid generated with the proposed model satisfies the electrical constraints of the system. An AC power flow that constrains the node voltage and limits the line carrying capacity is defined.

For simplified and more convenient notation, the following squared variables are introduced:

$$\upsilon_i = V_i^2 \qquad \text{and} \qquad \ell_{ij} = I_{ij}^2.$$

The annually weighted objective function defined with equation (3.8) is subjected to the constraints (3.9) - (3.17) as follows

$$\sum_{(j,i)\in\Omega_l} P_{ji} - \sum_{(i,j)\in\Omega_l} P_{ij} - \sum_{(i,j)\in\Omega_l} [R_{ij} \cdot \ell_{ij}] + P_i^g = P_i^d \qquad \forall i \in \Omega_n \tag{3.9}$$

$$\sum_{(j,i)\in\Omega_l} Q_{ji} - \sum_{(i,j)\in\Omega_l} Q_{ij} - \sum_{(i,j)\in\Omega_l} [X_{ij} \cdot \ell_{ij}] + Q_i^g = Q_i^d \qquad \forall i \in \Omega_n \tag{3.10}$$

Equations (3.9) and (3.10) define the power balance of the active and reactive power flow respectively. These constraints ensure that the power demand of each load node is supplied, and an adequate power input from the generation or substation nodes is required. Furthermore, the active and reactive line losses, defined with $[R_{ij} \cdot \ell_{ij}]$ and $[X_{ij} \cdot \ell_{ij}]$ respectively, are also considered in the power dispatch.

$$\upsilon_i - \upsilon_j = \omega_{ij} + 2 \cdot R_{ij} \cdot P_{ij} + 2 \cdot X_{ij} \cdot Q_{ij} + Z_{ij}^2 \cdot \ell_{ij} \qquad \forall (i,j) \in \Omega_l \tag{3.11}$$

$$|\omega_{ij}| \leq \left((V^{max})^2 - (V^{min})^2\right) \cdot (1 - \alpha_{ij}) \qquad \forall (i,j) \in \Omega_l \text{ (3.12)}$$

Equation (3.11) is a function of the current magnitude and the branch parameters along with the active and reactive power flow, which determine the voltage drop across the connected lines. Since the potential difference $\upsilon_i - \upsilon_j$ between any two nodes i and j will never equal zero, an auxiliary variable ω is introduced to ensure feasibility in the case of a non-existent line between the two nodes i and j.

In equation (3.12), the auxiliary variable ω is constrained and assigned a zero value when the line ij is connected. When line ij is not connected, ω can get any other value within the defined limits, to satisfy (3.11).

$$\ell_{ij} \cdot \upsilon_j = P_{ij}^2 + Q_{ij}^2 \qquad \forall (i,j) \in \Omega_l \text{ (3.13)}$$

Equation (3.13) is a power flow equation defined to calculate the power flow parameters of the lines.

$$|P_{ij}| \leq V^{max} \cdot I_{ij}^{max} \cdot \alpha_{ij} \qquad \forall (i,j) \in \Omega_l \text{ (3.14)}$$

$$|Q_{ij}| \leq V^{max} \cdot I_{ij}^{max} \cdot \alpha_{ij} \qquad \forall (i,j) \in \Omega_l \text{ (3.15)}$$

Constraints (3.14) and (3.15) set the boundaries of the active and reactive power flow. These are considered and calculated only when a line is connected, otherwise the active and reactive power flow parameters are assigned to zero.

$$0 \leq \ell_{ij} \leq (I_{ij}^{max})^2 \cdot \alpha_{ij} \qquad \forall (i,j) \in \Omega_l \text{ (3.16)}$$

$$(V^{min})^2 \leq \upsilon_i \leq (V^{max})^2 \qquad \forall i \in \Omega_n \text{ (3.17)}$$

Similarly, equation (3.16) sets the limits of the current flowing in the connected lines. Constraint (3.17) defines voltage limits for each node respectively.

$$\sum_{(i,j) \in \Omega_l} \alpha_{ij} = n_n - n_s \qquad \text{(3.18)}$$

Equation (3.18) is defined to address the radial operation of the network. However, this condition alone is not enough to guarantee the network's radiality. Together with power flow balance constraints (3.9) and (3.10) both conditions are met and network radiality is guaranteed [81].

$$P_i^{gmin} \leq P_i^g \leq P_i^{gmax} \cdot \tau_i \qquad \forall i \in \Omega_n \text{ (3.19)}$$

$$Q_i^{gmin} \leq Q_i^g \leq Q_i^{gmax} \cdot \tau_i \qquad \forall i \in \Omega_n \text{ (3.20)}$$

$$1 \leq \tau_i \leq N^{Tmax} \qquad \forall i \in \Omega_s \text{ (3.21)}$$

Equations (3.19) - (3.20) define the limit of the power input into the grid with respect to the installed transformer capacity defined by the number of transformers selected in

each substation node $i \in \Omega_s$. Equation (3.21) defines the limits of the integer variable τ_i and sets the maximum possible number of transformers at a single substation node.

3.1.3.1 Second Order Conic Relaxation

The DSP optimization problem defined with (3.8) - (3.17) represents a Mixed-Integer Quadratically Constraint Programming (MIQCP) optimization. The optimization problem can be modeled using a General Algebraic Modeling Language (GAMS) and solved via numerous solvers such as CPLEX and MOSEK [82, 83, 84]. However, (3.13) is a non-convex quadratic equality and the convergence to optimality cannot be guaranteed [85].

To make the optimization problem convex and guarantee its optimality, a conic relaxation technique is introduced. The use of second-order cones is proposed and widely studied approach to relax the non-convex power flow equations. The solution obtained via the conic relaxation has no gap or a very small gap when compared to the original exact power flow equations, as shown in [86, 87].

The quadratic equality of the power flow equation (3.13) can be relaxed by performing a conic relaxation to obtain the following inequality [88]

$$\ell_{ij} \cdot \upsilon_i \geq P_{ij}^2 + Q_{ij}^2, \quad P_{ij} \geq 0 \qquad \forall (i,j) \in \Omega_l \, (3.22)$$

Furthermore, the second order conic relaxation (3.22) can be defined as

$$2\left(P_{ij}\right)^2 + 2\left(Q_{ij}\right)^2 + \left(\ell_{ij} - \upsilon_i\right)^2 \leq \left(\ell_{ij} + \upsilon_i\right)^2 \qquad \forall (i,j) \in \Omega_l \, (3.23)$$

Equation (3.22) is equivalent to (3.23), hence it can be reformulated as a standard second order cone formulation (3.24)

$$\left\| \begin{matrix} 2P_{ij} \\ 2Q_{ij} \\ \ell_{ij} - \upsilon_i \end{matrix} \right\|_2 = \ell_{ij} + \upsilon_i \qquad \forall (i,j) \in \Omega_l \, (3.24)$$

By replacing (3.13) with (3.22) in the optimization formulation, a convex MIQCP optimization problem is defined, which assures that a global optimal solution is reached [77].

The model for DSP optimization used for the radial synthetic distribution grid generation is defined by the objective function (3.8) subjected to the constraints (3.9) - (3.12), (3.14) - (3.21) and (3.22).

3.1.4 Application

For the application of the above-mentioned radial distribution system planning approach, the following input parameters are required

- Cost parameters
  - cost of lines
  - cost of power losses
  - cost of transformers and substations
  - annual rates and life span of equipment
- Technical parameters
  - consumer demand
  - line resistance, reactance and impedance
  - line carrying capacity
  - node voltage limits
  - transformer installed capacity
- Set definition
  - set of potential line connections
  - set of substation nodes

With an objective of investment cost minimization, the decision variables of the optimization problem are defined as the binary variable α_{ij} and the integer variable τ_{ij}. While α_{ij} determines the status of the lines in the line configuration, τ_{ij} represents the number of transformers assigned to the substation nodes. Consequently, the line configuration obtained as a solution is directly dependent on the number of transformers obtained for each substation node, and vice versa. An optimal solution is reached when a cost minimal combination of lines and transformers is obtained, such that all the constraints are met. In addition, a power flow solution based on the new radial line configuration is obtained.

3.2 Ring Distribution System Expansion Planning

In addition to the considerable research efforts, distribution system planning is an essential and commonly used tool in the power engineering sector. With the necessity to meet the strict grid regulations, cope with the smart grid trends and improve customer satisfaction, DSOs are under increased pressure to obtain the required grid expansions and enhancements in a most cost-effective manner. Due to the simplicity and low first cost, the distribution systems are normally designed and operated radially. The unidirectional power flow of a radial path is used to design a straightforward circuit arrangement, which requires a small amount of switching equipment and a simple protective relaying. However, the lack of continuity of supply of the radial system is a major disadvantage that significantly affects the grid reliability.

A most common approach for enhancing the reliability of supply is for planning engineers to consider alternative feed as an addition to the standard radial feed structure. Ring configurations are introduced as alternative feed to provide a backup capacity by a means of a standby transformer or from adjacent substations or by a combination of both [71, Ch.11]. Due to cost restrictions for significantly oversizing the grid infrastructure, the minimum backup capacity is determined as a percentage of the coincident peak

demand of the observed feeder. The percentage is determined with respect to the type of the customers supplied, as well as the size and peak load of the feeder.

The ring configuration grid expansion is typically done by the planning engineers using a deterministic criteria to obtain a cost-effective solution [71]. To the best of authors' knowledge, there is limited literature on proposed optimization models that focus on the ring configuration expansion planning approach.

Furthermore, due to the binary decision making nature of the distribution planning problem and the guaranteed optimality of the solution, mixed integer programming is the most commonly used model in the literature [49, 51, 53, 89]. However, some of the recent applications in the planning methodologies require a heuristic model definition and the use of meta-heuristics. Similarly, the ring distribution system expansion planning problem can be described as an optimization problem with a heuristic nature. Some heuristic models include modified genetic algorithm, constructive heuristic algorithm, particle swarm optimization and ant colony system algorithm [47, 90, 50, 91]. Even though these algorithms may provide a sufficiently good solution, the biggest disadvantage is that there is no information about the optimality of the solution.

To propose a ring distribution system expansion planning optimization approach that will overcome the disadvantages of the heuristic nature of the problem, a scenario based mixed integer programming method is used. The model definition extends to consider multiple cable sizing options for each line corridor. This is particularly useful since some of the existing lines will require a cable upgrade with an overall bigger power carrying capacity. Furthermore, the scenario based approach is introduced by using a predefined set of parameters, giving a flexibility to select multiple ring configuration layouts and individually define the required backup capacity. Similarly to Section 3.1, the power flow constraints are defined using a relaxed conic AC power flow representation.

3.2.1 Model Definition

For simplified and more convenient notation, the following squared variables are introduced

$$\upsilon_i = V_i^2 \qquad \text{and} \qquad \ell_{ij} = I_{ij}^2.$$

3.2.1.1 Multi-Cable Distribution System Planning

Based upon the model defined in Section 3.1, A mixed integer optimization model for distribution system planning that considers multiple cable sizing options for each line corridor is introduced as follows

$$\sum_{(i,j)\in\Omega_l, l\in\Omega_c} L_{ij} \cdot \Psi_{ij,l}^{line} \cdot \alpha_{ij,l} \tag{3.25}$$

The objective function defined with (3.25) is a cost minimization function that provides the most economically viable grid configuration by considering the cost of the lines. The objective function is subjected to the constraints defined with (3.26) - (3.38) as follows

$$\sum_{(j,i)\in\Omega_l, l\in\Omega_c} P_{ji,l} - \sum_{(i,j)\in\Omega_l, l\in\Omega_c} P_{ij,l} - \sum_{(i,j)\in\Omega_l, l\in\Omega_c} [R_{ij,l}\cdot \ell_{ij,l}] + P_i^g = P_i^d \qquad \forall i \in \Omega_n \quad (3.26)$$

$$\sum_{(j,i)\in\Omega_l, l\in\Omega_c} Q_{ji,l} - \sum_{(i,j)\in\Omega_l, l\in\Omega_c} Q_{ij,l} - \sum_{(i,j)\in\Omega_l, l\in\Omega_c} [X_{ij,l}\cdot \ell_{ij,l}] + Q_i^g = Q_i^d \qquad \forall i \in \Omega_n \quad (3.27)$$

Equations (3.26) and (3.27) define the active and reactive power balance equations which ensure that the power demand is adequately supplied.

$$\upsilon_i - \upsilon_j = \omega_{ij,l} + 2\cdot R_{ij,l}\cdot P_{ij,l} + 2\cdot X_{ij,l}\cdot Q_{ij,l} + Z_{ij,l}^2\cdot \ell_{ij,l} \quad \forall (i,j)\in\Omega_l, \forall l\in\Omega_c \quad (3.28)$$

$$|\omega_{ij,l}| \le \left((V^{max})^2 - (V^{min})^2\right)\cdot(1-\alpha_{ij,l}) \qquad \forall (i,j)\in\Omega_l, \forall l\in\Omega_c \quad (3.29)$$

Equation (3.28) determines the voltage drop across the connected lines as a function of the current magnitude and the branch parameters along with the active and reactive power flow, which. The auxiliary variable ω is introduced to ensure feasibility in the case of a non-existent line between i and j, and it is constraint with equation (3.29).

$$\ell_{ij,l}\cdot \upsilon_j \ge P_{ij,l}^2 + Q_{ij,l}^2 \qquad \forall (i,j)\in\Omega_l, \forall l\in\Omega_c \quad (3.30)$$

Equation (3.30) is a conic relaxation of the power flow equation defined to calculate the power flow parameters of the lines.

$$|P_{ij,l}| \le V^{max}\cdot I_{ij,l}^{max}\cdot \alpha_{ij,l} \qquad \forall (i,j)\in\Omega_l, \forall l\in\Omega_c \quad (3.31)$$

$$|Q_{ij,l}| \le V^{max}\cdot I_{ij,l}^{max}\cdot \alpha_{ij,l} \qquad \forall (i,j)\in\Omega_l, \forall l\in\Omega_c \quad (3.32)$$

Constraints (3.31) and (3.32) set the limits of the active and reactive power flow when a line is connected, and set power flow parameters to zero when no line exists.

$$0 \le \ell_{ij,l} \le (I_{ij,l}^{max})^2\cdot \alpha_{ij,l} \qquad \forall (i,j)\in\Omega_l, \forall l\in\Omega_c \quad (3.33)$$

$$(V^{min})^2 \le \upsilon_i \le (V^{max})^2 \qquad \forall i\in\Omega_n \quad (3.34)$$

Similarly, equation (3.33) sets the limits of the current flowing in the connected lines, and (3.34) defines the voltage limits for each node respectively.

$$\sum_{\forall l\in\Omega_c} \alpha_{ij,l} \le 1 \qquad \forall (i,j)\in\Omega_l \quad (3.35)$$

$$\sum_{(i,j)\in\Omega_l, \forall l\in\Omega_c} \alpha_{ij,l} = n_n - n_s \quad (3.36)$$

The constraint (3.35) is introduced to ensure that only one type of cable per line is selected. Equation (3.36) together with power flow balance constraints (3.26) and (3.27)

guarantees the radial operation of the network.

$$P_i^{gmin} \leq P_i^g \leq P_i^{gmax} \cdot \tau_i \qquad \forall i \in \Omega_n \quad (3.37)$$

$$Q_i^{gmin} \leq Q_i^g \leq Q_i^{gmax} \cdot \tau_i \qquad \forall i \in \Omega_n \quad (3.38)$$

Equations (3.37) - (3.38) define the limit of the power input into the grid in each substation node $i \in \Omega_s$.

The model for multi-cable distribution system planning is defined by the objective function (3.25) subjected to the constraints (3.26) - (3.38).

3.2.1.2 Application

With the introduction of the set of cable sizing options $l \in \Omega_c$, the distribution system planning optimization defined with equations (3.25) - (3.38) considers multiple cable sizing options for each line corridor and selects the most cost optimal option. For this purpose, the line parameters such as $\Psi_{ij,l}, R_{ij,l}, X_{ij,l}, Z_{ij,l}, P_{ij,l}^{max}, Q_{ij,l}^{max}$ and $I_{ij,l}^{max}$ need to be defined for every cable option l of each line ij respectively. These line parameters are predefined and input during the initialization stage of the optimization. Furthermore, the constraint (3.35) is added to ensure that a maximum of one cable option per line corridor is selected.

3.2.1.3 Ring Distribution System Expansion Planning

A scenario based ring configuration expansion planning optimization based on the multi-cable distribution system planning model is defined as follows

$$\sum_{(i,j)\in\Omega_l, l\in\Omega_c} L_{ij} \cdot \Psi_{ij,l}^{line} \cdot \alpha_{ij,l} \qquad (3.39)$$

subject to

$$\sum_{(j,i)\in\Omega_l, l\in\Omega_c} P_{ji,l}^{(s)} - \sum_{(i,j)\in\Omega_l, l\in\Omega_c} P_{ij,l}^{(s)} - \sum_{(i,j)\in\Omega_l, l\in\Omega_c} \left[R_{ij,l} \cdot \ell_{ij,l}^{(s)}\right] + P_i^{g(s)} = P_i^{d(s)} \qquad \forall i \in \Omega_n, \forall s \in \Omega_f \quad (3.40)$$

$$\sum_{(j,i)\in\Omega_l, l\in\Omega_c} Q_{ji,l}^{(s)} - \sum_{(i,j)\in\Omega_l, l\in\Omega_c} Q_{ij,l}^{(s)} - \sum_{(i,j)\in\Omega_l, l\in\Omega_c} \left[X_{ij,l} \cdot \ell_{ij,l}^{(s)}\right] + Q_i^{g(s)} = Q_i^{d(s)} \qquad \forall i \in \Omega_n, \forall s \in \Omega_f \quad (3.41)$$

$$v_i^{(s)} - v_j^{(s)} = \omega_{ij,l}^{(s)} + 2 \cdot R_{ij,l} \cdot P_{ij,l}^{(s)} + 2 \cdot X_{ij,l} \cdot Q_{ij,l}^{(s)} + Z_{ij,l}^2 \cdot \ell_{ij,l}^{(s)} \qquad \forall (i,j) \in \Omega_l, \forall l \in \Omega_c, \forall s \in \Omega_f \quad (3.42)$$

$$\left|\omega_{ij,l}^{(s)}\right| \leq \left((V^{max})^2 - (V^{min})^2\right) \cdot (1 - \alpha_{ij,l}) \qquad \forall (i,j) \in \Omega_l, \forall l \in \Omega_c, \forall s \in \Omega_f \quad (3.43)$$

$$\ell_{ij,l}^{(s)} \cdot \upsilon_j^{(s)} \geq P_{ij,l}^{(s)2} + Q_{ij,l}^{(s)2} \qquad \forall (i,j) \in \Omega_l, \forall l \in \Omega_c, \forall s \in \Omega_f \quad (3.44)$$

$$\left| P_{ij,l}^{(s)} \right| \leq P_{ij,l}^{max(s)} \cdot \alpha_{ij,l} \qquad \forall (i,j) \in \Omega_l, \forall l \in \Omega_c, \forall s \in \Omega_f \quad (3.45)$$

$$\left| Q_{ij,l}^{(s)} \right| \leq Q_{ij,l}^{max(s)} \cdot \alpha_{ij,l} \qquad \forall (i,j) \in \Omega_l, \forall l \in \Omega_c, \forall s \in \Omega_f \quad (3.46)$$

$$0 \leq \ell_{ij,l}^{(s)} \leq (I_{ij,l}^{max(s)})^2 \cdot \alpha_{ij,l} \qquad \forall (i,j) \in \Omega_l, \forall l \in \Omega_c, \forall s \in \Omega_f \quad (3.47)$$

$$(V^{min})^2 \leq \upsilon_i^{(s)} \leq (V^{max})^2 \qquad \forall i \in \Omega_n, \forall s \in \Omega_f \quad (3.48)$$

$$\sum_{\forall l \in \Omega_c} \alpha_{ij,l} \leq 1 \qquad \forall (i,j) \in \Omega_l \quad (3.49)$$

$$\sum_{\forall l \in \Omega_c} \alpha_{ij,l} = 1 \qquad \forall (i,j) \in \Omega_{fix} \quad (3.50)$$

$$\sum_{(i,j) \in \Omega_l, \forall l \in \Omega_c} \alpha_{ij,l} = n_n - n_s + n_f \quad (3.51)$$

$$P_i^{gmin} \leq P_i^{g(s)} \leq P_i^{gmax} \cdot \tau_i \qquad \forall i \in \Omega_n, \forall s \in \Omega_f \quad (3.52)$$

$$Q_i^{gmin} \leq Q_i^{g(s)} \leq Q_i^{gmax} \cdot \tau_i \qquad \forall i \in \Omega_n, \forall s \in \Omega_f \quad (3.53)$$

Similarly to the multi-line definition, the objective function defined with (3.39) is a cost minimization function that provides the most economically viable grid configuration. The power balance constraints introduced with equations (3.40) and (3.41) ensure a zero sum of the generated, consumed and transmitted power at each node. The voltage drop at each node is calculated with equation (3.42). With the use of the auxiliary variable $\omega_{ij,l}^{(s)}$, constraint (3.43) makes sure that the voltage drop between two nodes is considered only if a line exist. Equation (3.44) calculates the power flow using the relaxed AC conic power flow model. The line power flow limits are set using constraints (3.45) and (3.46), while the line current limits are defined with constraint (3.47). The node voltage boundaries are set with constraint (3.48). Equation (3.51) limits the total number of lines in the configuration, and together with (3.40) and (3.41) guarantees the network radiality. The selection of a maximum of one cable per line corridor is ensured with (3.49), while (3.50) makes sure that the existing lines are considered and fixed as part of the solution. Equations (3.52) and (3.53) limit the power output according to the maximum installed capacity at the substation nodes.

3.2.1.4 Application

The ring expansion planning approach is defined by introducing a set of scenarios $s \in \Omega_f$ such that the number of scenarios equals the total number of distribution feeders in the radial grid configuration. Each feeder is assigned a scenario in which the power limit $P_{ij,l}^{max(s)}$ of the first line that connects the feeder to the substation is predefined and input

as follows

$$P_{ij,l}^{max(s)} = (1 - \frac{\eta_{ring}}{100}) \cdot P_{peak}^{(s)}$$

where η_{ring} is the required backup capacity in percentage and $P_{peak}^{(s)}$ is the total peak demand of the feeder. The current limit of the first line of the feeder $I_{ij,l}^{max(s)}$ is similarly derived.

Having limited the line capacity that connects the feeder to the substation restrains the power supplied to the feeder and makes the existing radial configuration infeasible. To satisfy the constraints (3.40) - (3.48) and obtain a feasible solution that will supply the required backup capacity for each feeder, an expansion of the existing configuration and the addition of new lines is required.

In order to ensure a ring configuration for all feeders, the constraint (3.51) permits the addition of only one line per feeder. The constraint (3.50) makes sure that the existing configuration is respected, while the constraint (3.49) permits only one cable per line and gives the opportunity to upgrade the existing lines. The cost parameter $\Psi_{ij,l}$ of an existing line is predefined to zero for the first cable option $l = 1$, and is assigned the cost of upgrading to a bigger cable for the other cable options.

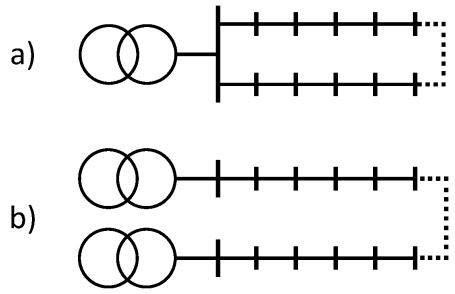

Figure 3.1: Ring configuration layout options

Furthermore, the proposed model can be used to obtain a cost optimal ring expansion plan using specific ring configuration layouts. By controlling the input data set of the lines Ω_l, the configuration layouts detailed in Figure 3.1 can be individually used. When the line data sets are combined, the ring configuration layout is determined based on the overall investment cost subjected to the power flow constraints.

3.3 Mesh Distribution System Expansion Planning

The increasing dissemination of DG facilities has a great impact on distribution systems, mainly transforming them from passive to active networks [92]. As previously discussed, distribution systems have been historically designed and operated adopting radial and ring topologies, exploiting the simplicity of the unidirectional power flow and continuously decreasing voltage profile guaranteed by such configurations.

However, the increase in installed DG capacity has introduced certain challenges such as violations of voltage and current limits, unplanned interaction and triggering of the protection and the control systems, and increased harmonic disturbance. In this context, traditional radial network architectures have shown to be a limiting factor in the reliability improvements that are needed to effectively mitigate disruptions caused by DG [93].

To improve the reliability by increasing the number of paths to each load, advanced network topologies and mesh configurations are investigated. It is also found that mesh topologies help in balancing the voltage profile and improve the system operation in the smart grid environment [94]. However, upgrading the radial and ring distribution systems with any additional connections is a costly undertaking for the DSOs. Thus, the economic viability has to be verified using an cost-minimization optimization approach.

To evaluate the mesh distribution grid topologies obtained using a grid expansion planning optimization, a measure of grid reliability needs to be introduced in the objective function. This allows to consider the impact of novel grid configurations on the cost to customers with respect to the cost of power supply interruptions or the deterioration of power quality. Some model formulations found in the literature consider the reliability in terms of interruptions, either including one or more of the standard aggregate reliability indexes, or evaluating failures that affect individual load points [45, 95, 96].

The cost of reliability can also be introduced in the objective function by considering the outage cost known as the cost of energy not supplied (ENS), which is the cost customers are expected to experience if their load is disconnected for a set amount of time [97]. In this thesis, a distribution system expansion planning model that considers mesh configurations using the energy not supplied (ENS) as a measure of reliability is defined.

3.3.1 Model Definition

The mesh distribution system expansion planning model is defined using a cost minimization multi-objective function as follows

$$\min \qquad \Lambda = \lambda_1 + \lambda_2 + \lambda_3 \tag{3.54}$$

subject to

$$\lambda_1 = \Xi^{line} \cdot \sum_{(i,j)\in\Omega_l} L_{ij} \cdot 2 \cdot \Psi_{ij}^{line} \cdot \alpha_{ij} \qquad \forall (i,j) \in \Omega_l \tag{3.55}$$

$$\lambda_2 = EPLT \cdot \sum_{(i,j)\in\Omega_l} R_{ij} \cdot I_{ij}^2 \cdot S^{base} \cdot \Psi^{loss} \qquad \forall (i,j) \in \Omega_l \tag{3.56}$$

$$\lambda_3 = \sum_{(i,j)\in\Omega_l} \zeta_{ij} \cdot L_{ij} \cdot t_{ij}^R \cdot \Psi^{ENS} \cdot P_{ij}^{LNS} \cdot \alpha_{ij} \tag{3.57}$$

As already shown in section 3.1.2, equation (3.55) defines the annually weighted investment cost of the lines. Similarly, (3.56) calculates the operational cost of the distribution grid in terms of power losses, as shown in section 3.1.2.2.

To account for the lack of reliability in the system, the cost of ENS defined with (3.57) is introduced in the objective function (3.54). By evaluating the total demand that would suffer an interruption in case of an outage on each of the active lines, a measure of the system's reliability can be obtained. Contrary to the increase in investment cost (3.55) and the cost of losses (3.56) when new lines are added, the cost of ENS will expectedly decrease as new supply paths to the loads are introduced.

To economically quantify the significance of an outage in the system, the failure rate and repair time of each line are included in the cost formulation. Since the failure rate is expressed in events per year per kilometer of line, the length of the lines is introduced. To calculate the cost of the ENS, the failure rate, repair time and the length of the lines are multiplied by the amount of load that is expected to be lost during each outage and its economic value. The amount of load lost during an outage is referred to as the load not supplied (LNS). To determine the LNS, an iterative heuristic approach is required.

3.3.1.1 Constraints

The objective function is subjected to the following constraints

- Active and reactive power balance to supply all loads
- Power flow calculation
- Line current carrying capacity limits
- Node voltage limits
- Maximum installed generator/transformer capacity at source nodes
- Fixed existing lines in line configuration

The application of the solution methodology and the model implementation is detailed in section 3.3.1.3.

3.3.1.2 Load Not Supplied Algorithm

To define the LNS, it should be noted that a load is considered as 'disconnected' following a line outage to characterize the set of nodes which would fall out of the feasible operating conditions defined with the model constraints. This does not refer to any security procedure such as load curtailment, load shedding, grid reconfiguration, etc.

The general flow chart for the LNS algorithm is detailed in Figure 3.2. Each iteration of the algorithm computes the value P_{ij}^{LNS}, which is the LNS following an outage of a specific branch (i, j). If all lines are ordered and labeled from one to n and all buses are numbered from one to m, a LNS matrix P^{LNS} can be initialized as follows

$$P^{LNS} = \begin{bmatrix} P_{11}^{LNS} & \cdots & P_{1n}^{LNS} \\ \vdots & \ddots & \vdots \\ P_{m1}^{LNS} & \cdots & P_{mn}^{LNS} \end{bmatrix} \tag{3.58}$$

Initially, an active branch is disconnected and the power flow computations for the modified system are performed. This is defined as an iterative process that works column by column and disconnects all the respective lines to evaluate how the network is affected. If any node falls out of the operating conditions, the corresponding element in the LNS matrix is updated with the value of its active power demand. Once the iterations are completed, the sum of each column gives the LNS of each line, whereas the sum of the whole matrix determines the total LNS for the distribution system configuration.

The loads can be disconnected either because they are physically detached from the power supply or because of their electrical parameters are outside of the operating limits. The algorithm performs two checks, a connection check and a voltage and current check, in order to determine which nodes fall into either of the two categories, as shown in Figure 3.2.

Connection check If the algorithm detects an isolated part of the network which is not supplied after the disconnection of a line in a feeder, it will directly include all the nodes within the island. If there are no remaining nodes supplied by the feeder, the rest of the steps are skipped and the algorithm continues with the next feeder. If any part of the feeder still has a power supply, the current and voltage check is initiated.

Current and voltage check A power flow is computed for the grid section that is still connected to the power supply. If a voltage violation is detected, the node with the lowest voltage is disconnected and its load is added to the LNS matrix. This is repeated until all the voltage violations have been eliminated. Similarly, if a current overload of a line is detected, the power transfer distribution factor (PTDF) matrix is considered in order to determine which buses are the greatest contributors to the current flowing in that particular line [98]. Among these, the node at lowest voltage is then disconnected. This is iterated until all violations have been eliminated.

The final values for the LNS for each disconnected line are then used in (3.57) to obtain the total cost of the ENS for the system configuration. The inclusion of the line's failure rate and its repair time allow to characterize the contribution of each line to the total cost based on its relative importance. If a line has a high failure rate or a high repair time, it will be penalized during the optimization.

The economic cost Ψ^{ENS} in (3.57) represents a value lost by the customers during an outages, which can be difficult to quantify, and typically requires the use of a customer damage functions (CDF) [95]. In this formulation, Ψ^{ENS} is assumed equal to the value of lost load (VoLL), which in the context of energy markets is the maximum price customers are willing to pay in order not to have their load disconnected.

3.3.1.3 Solution Algorithm

As the optimization approach required to solve the proposed model is of heuristic nature, a genetic algorithm (GA) is used [99]. The GA heuristic nature allows for a straightforward implementation of the conditional statements and the iterative sub-algorithms

required to calculate the cost of the ENS. The GA works by evolving the population of candidate solutions until an optimal solution is reached. Each of the candidate solutions is defined as a chromosome, which is a string of genes defined as binaries to represent the status of the potential lines. The genes and chromosomes are then mutated and altered based on the cost evaluation defined by a fitness function, i.e. the objective function. The iterative evaluation is done by repetitive application of the operators such as reproduction, mutation, crossover, inversion and selection until the fittest individuals in the chromosome are obtained [100, 101]. The candidate solution that will provide a most cost-optimal solution subjected to the constraints is the final optimal solution.

Initially, the cost minimization objective function is defined as the GA fitness function. Starting with the network data and GA configuration parameters, the candidate solutions are initialized as binary strings, chromosomes, spanning the set of possible new lines. The chromosomes are considered as the base decision variables of the fitness function, which considers the binary value as the status of the lines in the network configuration. The network configuration optimization together with the network parameters are then used for the power flow computation. To solve the power flow of the newly obtained system configuration, a suitable AC power flow solver following the Newton-Raphson method is used [102].

Once a convergent power flow solution is reached, the investment and operational cost of the newly obtained grid configuration are calculated, in addition to the cost of ENS computed using the sub-algorithm described in section 3.3.1.2. Having determined the fitness value for each candidate solution in the population, the GA can now applies the operators in an iterative process until a satisfying solution is reached. The flowchart of the solution algorithm is detailed in Figure 3.3.

The algorithm can be modeled in MATLAB, using MATPOWER [102] as the engine for power flow computations and the program's own Global Optimization Toolbox for the genetic algorithm implementation. Furthermore, the Parallel Computing Toolbox has proven to be useful to distribute the computational load and make the model definition more computationally efficient to solve. This brings out the advantages of the adoption of a genetic algorithm, as the possibility of implementing parallel computing is an additional advantage in the model efficiency.

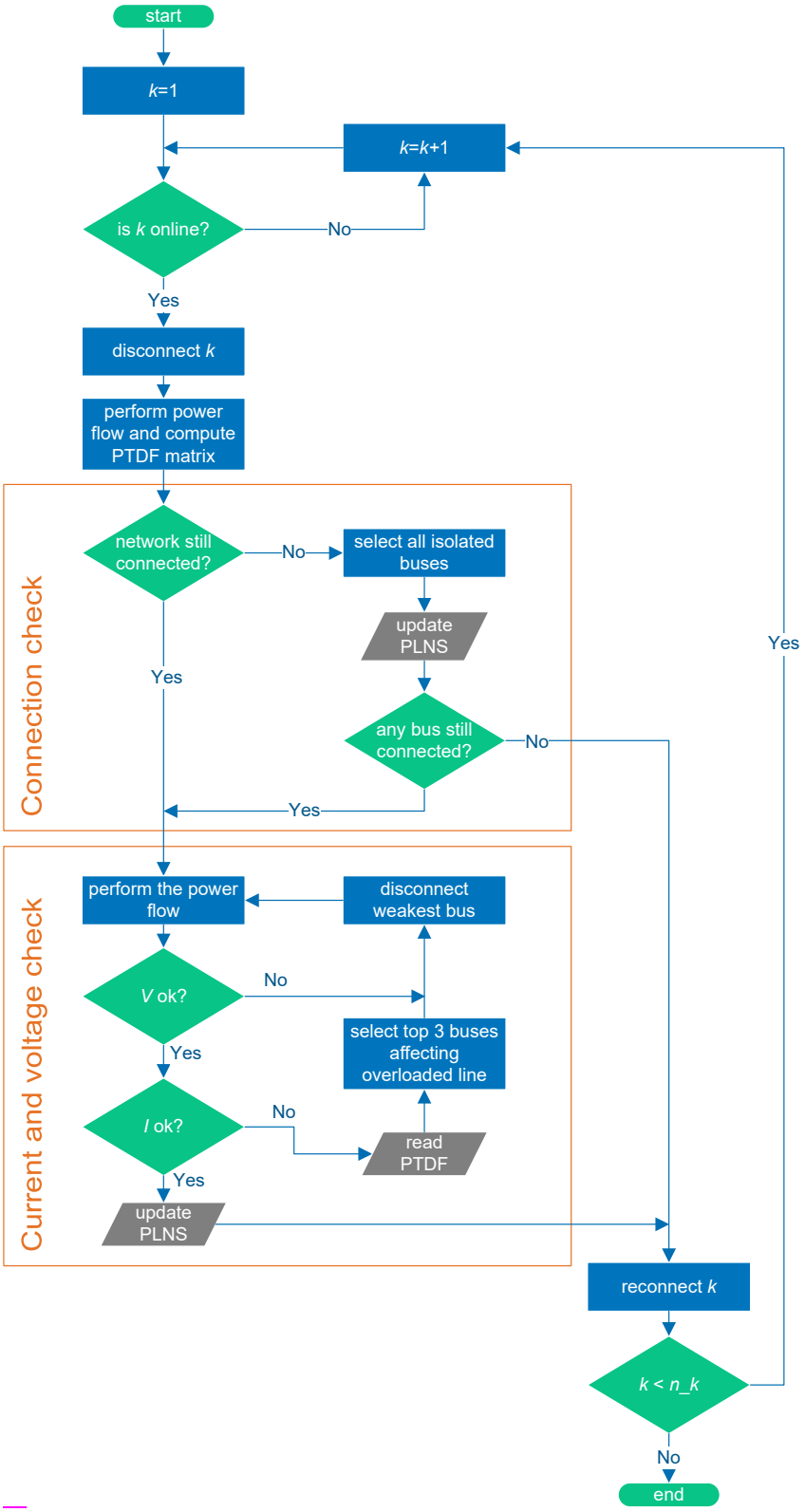

Figure 3.2: Algorithm for determining the load not supplied (LNS)

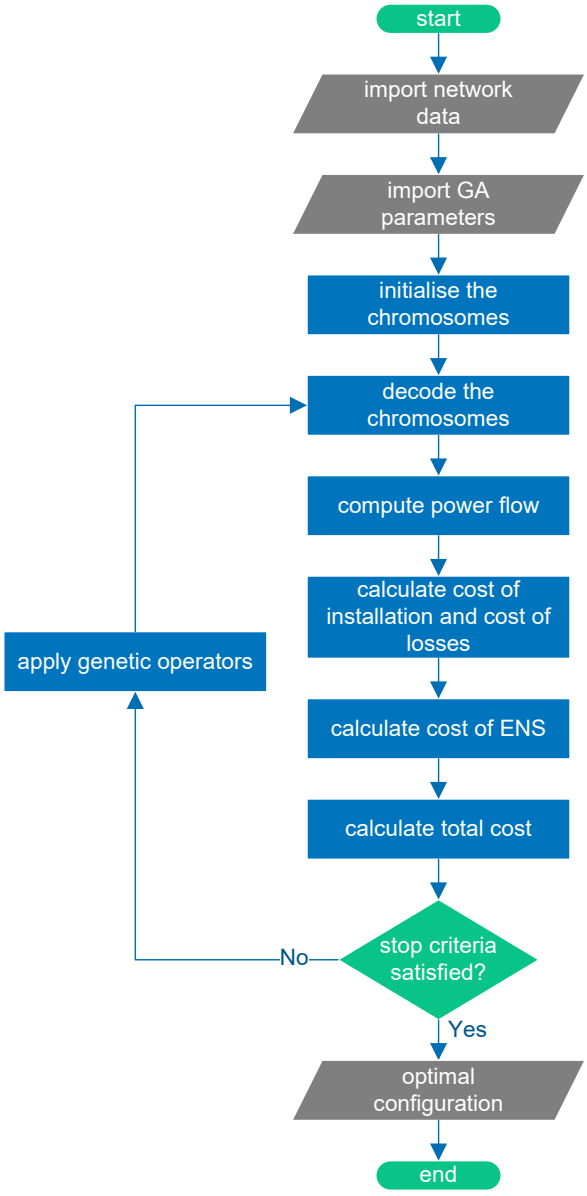

Figure 3.3: Flowchart of the solution algorithm

4 Transmission System Planning

In this chapter, a holistic approach for using power transmission system planning for synthetic grid generation is proposed. The results obtained from the distribution system planning approach are used as input parameters in a bottom up approach in modeling the power system. In this chapter, a slightly modified content of 'Scenario Based N-1 Transmission Expansion Planning using DC Mixed Integer Programming' published in the proceedings of 2019 IEEE Power & Energy Society General Meeting (PESGM) and of 'A Comparative Analysis of Transmission System Planning for Overhead and Underground Power Systems using AC and DC Power Flow' published in the proceedings of 2019 IEEE PES Innovative Smart Grid Technologies Europe (ISGT-Europe) is reproduced [3, 4].

The approach is defined as a transmission system planning optimization. As the power system landscape is constantly changing, the use of TSP is widely accepted as essential to providing a cost optimal transmission system upgrades and economical power system operation. Due to the complexity of the problem and the difficulty to accurately identify the future demand, a static approach for a single point in time in the future is a most commonly accepted TSP approach [55, 69]. The TSP problem can be defined using an AC or a DC power flow model. Due to the simplicity and the linearity of the model, a DC power flow is a commonly accepted model [66]. However, using the DC model often proves to obtain solutions that are infeasible and problematic in an AC system [55]. Therefore, there is an ongoing effort in exploring multiple linearized and relaxed convex AC models, such as a relaxed second order conic model which is compared to a DC model in [103]. This research interest is highly backed by the recent IT development and new optimization software, with a significant increase in computing power.

4.1 DC TSP Model Definition

The objective of the transmission system planning problem is defined as a mixed integer problem as follows

$$\min \qquad \Lambda = \lambda_1 + \lambda_2 \tag{4.1}$$

subject to

$$\lambda_1 = \Xi^{line} \cdot \sum_{(i,j)\in\Omega_l} L_{ij} \cdot 2 \cdot \Psi_{ij}^{line} \cdot \alpha_{ij} \tag{4.2}$$

$$\lambda_2 = \Xi^{trafo} \cdot \sum_{i\in\Omega_s} (\Psi_i^{trafo} \cdot \tau_i + \Psi_i^{subs}) \tag{4.3}$$

The objective function (4.1) is a cost function that minimizes the investment cost of the transmission lines and the installed transformer capacity. A binary and an integer decision variables determine the optimal grid configuration and the minimal number of transformers required to supply the grid. As already discussed in section 3.1, Ξ^{line} and Ξ^{trafo} are used to equally weight the objective function and represent it as the annual investment costs of both lines and transformers.

The objective function is subjected to the constraints (4.4) - (4.9) as follows

$$\sum_{(j,i)\in\Omega_l} P_{ji} - \sum_{(i,j)\in\Omega_l} P_{ij} + P_i^g = P_i^d \qquad \forall i \in \Omega_n \,(4.4)$$

$$P_{ij} = \frac{1}{X_{ij}} \cdot (\theta_j - \theta_i) \qquad \forall (i,j) \in \Omega_l \,(4.5)$$

$$0 \leq |P_{ij}| \leq P_{ij}^{max} \cdot \alpha_{ij} \qquad \forall (i,j) \in \Omega_l \,(4.6)$$

$$0 \leq |P_i^g| \leq P_i^{gmax} \cdot \tau_i \qquad \forall i \in \Omega_g \,(4.7)$$

$$-\frac{\pi}{2} \leq |\theta_j - \theta_i| \leq \frac{\pi}{2} \qquad \forall (i,j) \in \Omega_l \,(4.8)$$

$$\theta_{ref} = 0 \qquad (4.9)$$

$$\alpha_{ij} = 1 \qquad \forall (i,j) \in \Omega_{fix} \,(4.10)$$

A zero sum of the generated, consumed and transmitted power at each node is introduced with constraint (4.4), which maintains the power balance of the system. Equation (4.5) defines the DC power flow calculation, while (4.6) sets the power flow limits of each branch ij. Each generator node has a maximum generating capacity defined with (4.7). Equation (4.8) maintains the grid's operating stability by limiting the phase angle difference. A reference node is chosen and the phase angle at this node is set to zero using constraint (4.9). Setting a reference node is necessary to bound the phase angle in the optimization problem, and it is a common practice for the biggest generator to be selected as a reference node. Lines that already exist in the transmission system are fixed with (4.10).

The phase angle θ_i is defined as a continuous variable which exists for each node of the set Ω_n. Consequently, the phase angle difference $(\theta_j - \theta_i)$ will be calculated even when no line in branch ij exist. This state does not allow the power flow of branch ij in (4.5) to be set to zero, which makes the problem infeasible. To solve the infeasibility, an auxiliary variable $\beta_{i,j}$ is introduced and (4.5) is replaced with (4.11) as follows

$$P_{ij} = \frac{1}{X_{ij}} \cdot (\theta_j - \theta_i) + \beta_{ij} \qquad \forall (i,j) \in \Omega_l \,(4.11)$$

$$0 \leq |\beta_{ij}| \leq P_{ij}^{max} \cdot (1 - \alpha_{ij}) \qquad \forall (i,j) \in \Omega_l \quad (4.12)$$

The auxiliary variable is assigned the value of the angle difference between two nodes i and j whenever the line in ij is not selected and $\alpha_{ij} = 0$. When a line exist and $\alpha_{ij} = 1$, the auxiliary variable is not considered and it is set to zero using constraint (4.12).

However, the above TSP model is limited to consider only one line for each corridor ij. When multiple parallel lines in a branch ij are considered, the resultant reactance X_{ij} in the power flow calculation changes accordingly as follows

$$X_{ij}^{*} = \frac{X_{ij}{}^{\tau_{ij}^{line}}}{\tau_{ij}^{line} \cdot X_{ij}{}^{(\tau_{ij}^{line}-1)}} \quad (4.13)$$

where τ_{ij}^{line} is an integer variable that represents the total number of parallel lines in the branch ij. Then, the DC power flow equation (4.5) becomes

$$P_{ij} = \frac{1}{X_{ij}^{*}} \cdot (\theta_j - \theta_i) \qquad \forall (i,j) \in \Omega_l \quad (4.14)$$

The DC power flow definition in (4.14) becomes very complex and non-linear, which makes it very difficult to solve. To avoid such non-linearity when considering multiple lines in the TSP model, a new multi-line approach is introduced.

The multi-line DC transmission expansion planning is defined as follows

$$\min \qquad \Lambda = \lambda_1 + \lambda_2 \quad (4.15)$$

subject to

$$\lambda_1 = \Xi^{line} \cdot \sum_{(i,j)\in\Omega_l, s\in\Omega_{sc}} L_{ij} \cdot 2 \cdot \Psi_{ij,s}^{line} \cdot \alpha_{ij,s} \quad (4.16)$$

$$\lambda_2 = \Xi^{trafo} \cdot \sum_{i\in\Omega_s} (\Psi_i^{trafo} \cdot \tau_i + \Psi_i^{subs}) \quad (4.17)$$

subject to

$$\sum_{(j,i)\in\Omega_l, s\in\Omega_{sc}} P_{ji,s} - \sum_{(i,j)\in\Omega_l, s\in\Omega_{sc}} P_{ij,s} + P_i^g = P_i^d \qquad \forall i \in \Omega_n \quad (4.18)$$

$$P_{ij,s} = \frac{1}{X_{ij,s}} \cdot (\theta_j - \theta_i) + \beta_{ij,s} \qquad \forall (i,j) \in \Omega_l, \forall s \in \Omega_{sc} \quad (4.19)$$

$$0 \leq |\beta_{ij,s}| \leq P_{ij,s}^{max} \cdot (1 - \alpha_{ij,s}) \qquad \forall (i,j) \in \Omega_l, \forall s \in \Omega_{sc} \quad (4.20)$$

$$0 \leq |P_{ij,s}| \leq P_{ij,s}^{max} \cdot \alpha_{ij,s} \qquad \forall (i,j) \in \Omega_l, \forall s \in \Omega_{sc} \quad (4.21)$$

$$\sum_{s \in \Omega_{sc}} \alpha_{ij,s} \leq 1 \qquad \forall (i,j) \in \Omega_l \quad (4.22)$$

$$\sum_{s \in \Omega_{sc}} \alpha_{ij,s} = 1 \qquad \forall (i,j) \in \Omega_{fix} \quad (4.23)$$

A new set of line scenarios Ω_{sc} is defined. The number of line scenarios corresponds to the maximum allowed number of lines in a corridor. The reactance $X_{ij,s}$ and the cost of the lines $\Psi_{ij,s}$ are pre-calculated for each line scenario s accordingly. Similarly, the maximum power carrying capacity $P_{ij,s}^{max}$ is predefined for each line scenario s. For lines that already exist in a branch, the cost is not considered in the objective function and set to zero. The cost is considered only for additional and non-existing lines. A binary variable for each line scenario s in corridor ij is then assigned. The power flow is computed for each of the selected scenarios based on the binary decision variable $\alpha_{ij,s}$.

To ensure that each corridor ij has a maximum of one scenario selected, an additional constraint (4.22) is defined. Constraints (4.7)-(4.9) are included, but not subjected to the newly defined scenarios. The DC TSP defined with (4.15)-(4.23), (4.7)-(4.9) is a mixed integer programming optimization that can be efficiently solved with most conventional solvers that guarantee the optimality.

4.2 Conic AC TSP Model Definition

In order to consider a convergent and feasible solution when an AC power system operation is considered, a relaxed conic AC power flow model is introduced. Although a conic relaxation of a power flow definition was detailed in 3.1.3.1, the proposed model does not include an accurate representation of the reactive power and is not suitable for a highly meshed transmission system operation. Therefore, a new second-order conic relaxation of an AC power flow model is defined. Furthermore, the model definition is extended to consider multiple lines per corridor, as this is a common practice when planning the transmission systems. The AC conic relaxation of the power flow used for the proposed TSP is detailed in [104].

4.2.1 Transmission Line Loss AC Optimal Power Flow (OPF)

An minimum transmission line loss AC OPF problem is defined as follows [104]

$$\min \qquad \sum_{i \in \Omega_n} P_i^g \quad (4.24)$$

subject to

$$\sum_{(i,j) \in \Omega_l} P_{ij} - \sum_{(j,i) \in \Omega_l} P_{ji} = P_i^g - P_i^d \qquad \forall i \in \Omega_n \quad (4.25)$$

$$\sum_{(i,j)\in\Omega_l} Q_{ij} - \sum_{(j,i)\in\Omega_l} Q_{ji} = Q_i^g - Q_i^d \qquad \forall i \in \Omega_n \,(4.26)$$

$$P_{ij} = n_{ij}^l \cdot p_{ij} \qquad \forall (i,j) \in \Omega_l \,(4.27)$$

$$Q_{ij} = n_{ij}^l \cdot q_{ij} \qquad \forall (i,j) \in \Omega_l \,(4.28)$$

$$\sqrt{p_{ij}^2 + q_{ij}^2} \leq S_{ij}^{max} \qquad \forall (i,j) \in \Omega_l \,(4.29)$$

$$p_{ij} + iq_{ij} = |V_i|^2 \left(g_{ij} - i\left(b_{ij} + \frac{1}{2} b_{\mathrm{sh}ij} \right) \right) - V_i V_j^* (g_{ij} - ib_{ij}) \qquad \forall (i,j) \in \Omega_l \,(4.30)$$

$$P_i^{gmin} \leq P_i^g \leq P_i^{gmax} \qquad \forall i \in \Omega_n \,(4.31)$$

$$Q_i^{gmin} \leq Q_i^g \leq Q_i^{gmax} \qquad \forall i \in \Omega_n \,(4.32)$$

$$V_i^{min} \leq |V_i| \leq V_i^{max} \qquad \forall i \in \Omega_n \,(4.33)$$

The OPF problem is defined with an objective to minimize the transmission line losses through finding the minimal total power generated in the system, as defined with the objective function (4.24). The constraints (4.25) and (4.26) ensure for the active and reactive power balance in the nodes. The constraints (4.27) and (4.28) are introduced to extend the formulation to include multiple circuits in a corridor, with n_{ij}^l being the number of identical parallel circuits in corridor ij. Equations (4.29) and (4.30) define an AC power flow calculation, with (4.29) limiting the apparent power in a circuit. The constraints (4.31) and (4.32) limit the power generation with respect to the installed generating capacity, while (4.33) defines the node voltage limits.

4.2.2 Conic Relaxation of the AC OPF model

For the purpose of modeling the conic relaxation of the AC power flow, let's define an nxn Hermitian matrix ($H = H^*$) with H_{ij} representing an element in the ith role and jth column, where n is the number of nodes in the system [104], as follows

$$H = \begin{bmatrix} |V_1|^2 & \dots & V_1 V_i^* & \dots & V_1 V_n^* \\ \vdots & \ddots & \vdots & & \vdots \\ V_i V_1^* & \dots & |V_i|^2 & \dots & V_i V_n|^* \\ \vdots & & \vdots & \ddots & \vdots \\ V_n V_1^* & \dots & V_n V_i^* & \dots & |V_n|^2 \end{bmatrix} \qquad (4.34)$$

Having defined the matrix H, equations (4.33) and (4.30) can be replaced with

$$p_{ij} + iq_{ij} = H_{ii}\left(g_{ij} - i\left(b_{ij} + \frac{1}{2}b_{\text{sh}ij}\right)\right) - H_{ij}(g_{ij} - ib_{ij}) \qquad \forall(i,j) \in \Omega_l \,(4.35)$$

$$(V_i^{min})^2 \leq H_{ii} \leq (V_i^{max})^2 \qquad \forall i \in \Omega_n \,(4.36)$$

Furthermore, equation (4.35) can be split into the active and reactive power flow component, defined with (4.37) and (4.38). Equations (4.37) and (4.38) give both the real and imaginary parts of H_{ij} respectively.

$$p_{ij} = g_{ij}H_{ii} - g_{ij}\text{Re}\{H_{ij}\} - b_{ij}\text{Im}\{H_{ij}\} \tag{4.37}$$

$$q_{ij} = -\left(b_{ij} + \frac{1}{2}b_{\text{sh}ij}\right)H_{ii} + b_{ij}\text{Re}\{H_{ij}\} - g_{ij}\text{Im}\{H_{ij}\} \tag{4.38}$$

Equation (4.34) can be replaced if H is defined as both semi-definite and rank one [105] as follows

$$H = H^* \succcurlyeq 0 \tag{4.39}$$

$$rank(H) = 1 \tag{4.40}$$

With this, a semidefinite programming (SDP) problem is defined. However, solving a SDP is very computationally demanding and not scalable for TSP mixed-integer problems. On the other side, conic programming has already been introduced as part of commercial solvers, in combination with mixed integer programming. The power flow model can be further relaxed by defining a conic problem by replacing equation (4.39) with (4.41) as follows

$$H_{ii}H_{jj} \geq \text{Re}\{H_{ij}\}^2 + \text{Im}\{H_{ij}\}^2 \qquad \forall(i,j) \in \Omega_{ls} \,(4.41)$$

where

$$\text{Re}\{H_{ij}\} = \text{Re}\{H_{ji}\} \quad \text{and} \quad \text{Im}\{H_{ij}\} = -\text{Im}\{H_{ji}\}.$$

Furthermore, the correlation between the voltage angles is accounted for in the conic model using the following constraints

$$\varepsilon_\theta \leq \theta_i - \theta_j - \text{Im}\{H_{ij}\} \leq \varepsilon_\theta \qquad \forall(i,j) \in \Omega_{ls} \,(4.42)$$

$$-\pi/2 \leq \theta_i \leq \pi/2 \qquad \forall i \in \Omega_n \,(4.43)$$

Though experience with the conic model, Jabr [104] shows that it is best to use values between 0.25 and 0.5 degrees for ε_θ such that a solution that satisfies the AC network model is obtained.

4.2.3 TSP Model Definition

The objective of the transmission system planning problem, when considering a relaxed conic AC power flow representation, is defined as a mixed integer problem as follows

$$\min \qquad \Lambda = \lambda_1 + \lambda_2 + \lambda_3 \tag{4.44}$$

subject to

$$\lambda_1 = \Xi^{line} \cdot \sum_{(i,j)\in\Omega_l} L_{ij} \cdot 2 \cdot \Psi_{ij}^{line} \cdot \alpha_{ij,l} \tag{4.45}$$

$$\lambda_2 = \Xi^{trafo} \cdot \sum_{i\in\Omega_s} (\Psi_i^{trafo} \cdot \tau_i + \Psi_i^{subs}) \tag{4.46}$$

$$\lambda_3 = \chi \cdot EPLT \cdot \sum_{i\in\Omega_n} P_i^g \cdot S^{base} \cdot \Psi^{el} \tag{4.47}$$

The objective function is similarly defined as the TSP in section 4.1, with λ_1 and λ_2 being the annually weighted investment cost of the lines and the transformers respectively. The decision variables are similarly defined with the binary variable $\alpha_{ij,l}$ determining the transmission system line configuration and the integer variable τ_i determining the number of transformers in each substation node. However, a cost minimization function defined only with the cost components λ_1 and λ_2 does not necessarily drive the rotated quadratic constraint (4.41) to be binding at optimality, which is necessary for a feasible power flow solution [104]. Consequently, λ_3 is added to consider a cost minimization of the network losses and define a feasible OPF model similarly to (4.24), with the addition of a penalty coefficient χ to adjust the weighting in the objective function. Furthermore, with the addition of the annual peak demand factor $EPLT$, it is often sufficient to set the penalty coefficient $\chi = 1$.

The objective function (4.44) is subjected to the following constraints

$$\alpha_{ij,l} \in \{0,1\} \qquad \forall(i,j) \in \Omega_{ls}, \quad l = 1, ..., n_{ij}^{l\max} \tag{4.48}$$

$$n_{ij}^{l\min} \leq \sum_{l=1}^{n_{ij}^{l\max}} \alpha_{ij,l} \leq n_{ij}^{l\max} \qquad \forall(i,j) \in \Omega_{ls} \tag{4.49}$$

$$\alpha_{ij,l} \leq \alpha_{ij,(l-1)} \qquad \forall(i,j) \in \Omega_{ls}, \quad l = 2, ..., n_{ij}^{l\max} \tag{4.50}$$

In (4.48), $\alpha_{ij,l}$ is defined as the binary variable with the maximum number of possible lines $n_{ij}^{l\max}$ in a corridor ij. Using constraint (4.49), the existing lines can be fixed by defining a minimum number $n_{ij}^{l\min}$ for the total sum of lines in a corridor ij. Similarly, the maximum number of lines in corridor ij is constrained by $n_{ij}^{l\max}$. Furthermore, the minimum and the maximum number of lines $n_{ij}^{l\max}$ can be individually defined for each

corridor ij. To ensure a sequential installation of the lines, the constraint (4.50) is defined.

$$\sum_{(i,j)\in\Omega_l} P_{ij} - \sum_{(j,i)\in\Omega_l} P_{ji} = P_i^g - P_i^d \qquad \forall i \in \Omega_n \,(4.51)$$

$$\sum_{(i,j)\in\Omega_l} Q_{ij} - \sum_{(j,i)\in\Omega_l} Q_{ji} = Q_i^g - Q_i^d \qquad \forall i \in \Omega_n \,(4.52)$$

$$P_i^{gmin} \leq P_i^g \leq P_i^{gmax} \qquad \forall i \in \Omega_n \,(4.53)$$

$$Q_i^{gmin} \leq Q_i^g \leq Q_i^{gmax} \qquad \forall i \in \Omega_n \,(4.54)$$

Constraints (4.51) and (4.52) represent the power balance equations, while (4.53) and (4.54) limit the installed generator capacity in the generating nodes, as seen in section 4.2.1.

$$P_{ij} = \sum_{l=1}^{n_{ij}^{l\max}} P_{ij,l} \qquad \forall (i,j) \in \Omega_l \,(4.55)$$

$$P_{ij,l} = g_{ij} H_{i(ij),l} - g_{ij}\mathrm{Re}\{H_{ij,l}\} - b_{ij}\mathrm{Im}\{H_{ij,l}\} \quad \forall (i,j) \in \Omega_l, l = 1, ..., n_{ij}^{l\max} \,(4.56)$$

$$Q_{ij} = \sum_{l=1}^{n_{ij}^{l\max}} Q_{ij,l} \qquad \forall (i,j) \in \Omega_l \,(4.57)$$

$$Q_{ij,l} = -\left(b_{ij} + \frac{1}{2} b_{\mathrm{sh}ij}\right) H_{i(ij),l} + b_{ij}\mathrm{Re}\{H_{ij,l}\} - g_{ij}\mathrm{Im}\{H_{ij,l}\}$$
$$\forall (i,j) \in \Omega_l, l = 1, ..., n_{ij}^{l\max} \,(4.58)$$

In (4.55), the total active power flow in corridor ij is defined as the sum of all the active power flowing in each line l. Equation (4.56) models the active power flow calculation of line l in corridor ij. Similarly the sum of the reactive power flow in corridor ij and the reactive power flow model of line l in corridor ij are defined with (4.57) and (4.58) respectively. However, when a line l in corridor ij is not installed and $\alpha_{ij,l} = 0$, the active and reactive power flows are set to zero using the following constraints

$$(V_i^{min})^2 \alpha_{ij,l} \leq H_{i(ij),l} \leq (V_i^{max})^2 \alpha_{ij,l} \qquad \forall (i,j) \in \Omega_l, l = 1, ..., n_{ij}^{l\max} \,(4.59)$$

$$0 \leq \mathrm{Re}\{H_{ij,l}\} \leq V_i^{max} V_j^{max} \alpha_{ij,l} \qquad \forall (i,j) \in \Omega_{ls}, l = 1, ..., n_{ij}^{l\max} \,(4.60)$$

$$-V_i^{max} V_j^{max} \alpha_{ij,l} \leq \mathrm{Im}\{H_{ij,l}\} \leq V_i^{max} V_j^{max} \alpha_{ij,l} \quad \forall (i,j) \in \Omega_{ls}, l = 1, ..., n_{ij}^{l\max} \,(4.61)$$

When a line l is installed such that $\alpha_{ij,l} = 1$, $H_{i(ij)}$ equals the square of the voltage magnitude at the ending node i as follows

$$(V_i^{min})^2 (1 - \alpha_{ij,l}) \leq |V_i|^2 - H_{i(ij),l} \leq (V_i^{max})^2 (1 - \alpha_{ij,l}) \quad \forall (i,j) \in \Omega_{ls}, l = 1, ..., n_{ij}^{l\max} \quad (4.62)$$

In summary, the constraints (4.59) - (4.62) assure that $P_{ij,l}$ and $Q_{ij,l}$ equal zeros by setting $H_{i(ij)}$ with its real and imaginary parts to equal zero. When a line is installed, $H_{i(ij)}$ is forced to equal the square of the voltage magnitude $|V_i|^2$. Furthermore, the bounds of $\mathrm{Re}\{H_{i(ij)}\}$ and $\mathrm{Im}\{H_{i(ij)}\}$ are set.

$$0 \leq \mathrm{Re}\{H_{ij,1}\} - \mathrm{Re}\{H_{ij,l}\} \leq V_i^{max} V_j^{max} (1 - \alpha_{ij,l}) \quad \forall (i,j) \in \Omega_{ls}, l = 2, ..., n_{ij}^{l\max} \quad (4.63)$$

$$-V_i^{max} V_j^{max} (1 - \alpha_{ij,l}) \leq \mathrm{Im}\{H_{ij,1}\} - \mathrm{Im}\{H_{ij,l}\} \leq V_i^{max} V_j^{max} (1 - \alpha_{ij,l}) \quad \forall (i,j) \in \Omega_{ls}, l = 2, ..., n_{ij}^{l\max} \quad (4.64)$$

Considering that all lines installed in parallel in a single corridor have the same power flow, the constraints (4.63) and (4.64) ensure that the values of $H_{i(ij),l}$ and $H_{ij,l}$ for all additional lines equal $H_{i(ij),1}$ and $H_{ij,1}$ respectively.

$$\sqrt{(P_{ij,1})^2 + (Q_{ij,1})^2} \leq S_{ij}^{max} \alpha_{ij,1} \quad \forall (i,j) \in \Omega_l \quad (4.65)$$

$$H_{i(ij),1} H_{j(ji),1} \geq \mathrm{Re}\{H_{ij,1}\}^2 + \mathrm{Im}\{H_{ij,1}\}^2 \quad \forall (i,j) \in \Omega_{ls} \quad (4.66)$$

$$-\varepsilon_\theta - \pi (1 - \alpha_{ij,1}) \leq \theta_i - \theta_j - \mathrm{Im}\{H_{ij,1}\} \leq \pi (1 - \alpha_{ij,1}) + \varepsilon_\theta \quad \forall (i,j) \in \Omega_{ls} \quad (4.67)$$

$$-\pi/2 \leq \theta_i \leq \pi/2 \quad \forall i \in \Omega_n \quad (4.68)$$

The quadratic equation (4.65) sets the apparent power limits of the line l in corridor ij, while (4.66) defines the rotated quadratic constraint detailed in section 4.2.2. The voltage angle spread constraints and the voltage angle boundaries are represented with (4.67) and (4.68) respectively. Since the value of $H_{i(ij),l}$ and $H_{ij,l}$ equals $H_{i(ij),1}$ and $H_{ij,1}$, it is sufficient to only ensure the constraints (4.65) - (4.67) for the first line only [104].

The MIQCP transmission system planning definition when considering an AC conic relaxation for the power flow model consists of (4.44) - (4.68). The optimization problem is solved using commercial software for mixed-integer conic programming , and it is shown to provide feasible and convergent TSP solution without the need of reinforcements commonly required when a DC power flow model is used [104]. The proposed TSP model is suitable to be used for both transmission network planning and transmission network expansion planning (TNEP) problems.

4.3 N-1 Transmission System Expansion Planning (TSEP)

The ability of a power system to preserve the normal operation state during contingencies caused by the outage of a transmission line, a generator, a transformer, or any single component in the system is known as the N-1 security criteria [3]. Due to the nature of the power system as an essential service and also its economical significance, the N-1 security criteria is universally accepted as fundamental security criteria for the system operation [68].

However, most of the expansion planning research work found in the literature does not consider the security criteria of the system. Some contribution in expansion planning that considers the N-1 security criteria can be found in [106, 107, 69, 108]. A common approach to account for the security constraint in the expansion planning is to use a two-stage optimization process [106, 107]. The 1st stage is defined as a mixed integer programming (MIP) to obtain a basic feasible expansion planning of the network. With the use of a similar methodology, the 2nd stage accounts for the line outages and extends the solution to a N-1 satisfactory network. The two stage approach proves to be computationally efficient and reliable. However, the 1st stage is directly influencing the final solution, often resulting in a non optimal solution.

Given the heuristic nature of the problem, metaheuristic methods are often used as an alternative to multi-stage MIP optimization. An improved genetic algorithm that gives a better optimal solution when compared to a two-stage optimization is introduced by the authors in [108]. Other heuristic methods may include taboo search, simulated annealing and particle swarm optimization. However, such heuristic methods have a main disadvantage of the need for a relatively large computational effort.

This work proposes a scenario based mixed integer programming method for TSEP with security constraints. The scenarios are introduced as a predefined set of parameters, which provides an adaptability to extend the model for different applications. To account for the security criteria, the presented mathematical model considers the N-1 line outage. However, the method can also be extended to consider the outage of generators and transformers. A lossless DC power flow model is used as a simplified approach to represent the electrical system for the purpose of demonstrating the methodology. Additionally, the proposed approach can be used with more accurate models like the conic relaxation of the AC model defined in section 4.2.2. The proposed method can be solved to optimality by using commercial MIP solvers such as CPLEX [83].

4.3.1 Scenario Based N-1 DC TSEP

To demonstrate the scenario based N-1 TSEP methodology, the model is defined as an extension to the DC TSP approach detailed in section 4.1 as follows

$$\min \sum_{(i,j)\in\Omega^l, s\in\Omega_{sc}} \Psi_{ij,s} \cdot \alpha_{ij,s} \tag{4.69}$$

subject to

$$\sum_{(j,i)\in\Omega_l, s\in\Omega_{sc}} P_{ji,s}^{(k)} - \sum_{(i,j)\in\Omega_l, s\in\Omega_{sc}} P_{ij,s}^{(k)} + P_i^g = P_i^d \qquad \forall i \in \Omega_n, \forall k \in \Omega_o \,(4.70)$$

$$P_{ij,s}^{(k)} = \frac{1}{X_{ij,s}^{(k)}} \cdot \left(\theta_j^{(k)} - \theta_i^{(k)}\right) + \beta_{ij,s}^{(k)} \qquad \forall (i,j) \in \Omega_l, \forall s \in \Omega_{sc}, \forall k \in \Omega_o \,(4.71)$$

$$0 \leq \left|\beta_{ij,s}^{(k)}\right| \leq P_{ij,s}^{(k)max} \cdot (1 - \alpha_{ij,s}) \qquad \forall (i,j) \in \Omega_l, \forall s \in \Omega_{sc}, \forall k \in \Omega_o (4.72)$$

$$0 \leq \left|P_{ij,s}^{(k)}\right| \leq P_{ij,s}^{(k)max} \cdot \alpha_{ij,s} \qquad \forall (i,j) \in \Omega_l, \forall s \in \Omega_{sc}, \forall k \in \Omega_o (4.73)$$

$$\sum_{s\in\Omega_{sc}} \alpha_{ij,s} \leq 1 \qquad \forall (i,j) \in \Omega_l \,(4.74)$$

$$\sum_{s\in\Omega_{sc}} \alpha_{ij,s} = 1 \qquad \forall (i,j) \in \Omega_{fix} \,(4.75)$$

$$0 \leq |P_i^g| \leq P_i^{gmax} \qquad \forall i \in \Omega_g \,(4.76)$$

$$-\frac{\pi}{2} \leq \left|\theta_j^{(k)} - \theta_i^{(k)}\right| \leq \frac{\pi}{2} \qquad \forall (i,j) \in \Omega_l, \forall k \in \Omega_o \,(4.77)$$

$$\theta_{ref}^{(k)} = 0 \qquad \forall k \in \Omega_o (4.78)$$

Following the N-1 security criterion, the grid is required to continue to normally operate without rescheduling the generation dispatch following the loss of a transmission line. To meet this requirement, a new scenario set Ω_o is introduced. A different line is switched off in each of the scenarios defined by the set Ω_o. This achieved by having constrained the power flow of corridor ij for line scenario s to correspond to a loss of a single line for each of the N-1 scenarios k. The input parameter $P_{ij,s}^{(k)max}$ in (4.73) is predefined accordingly. The reactance $X_{ij,s}^{(k)}$ in (4.71) is pre-calculated to account for the newly occurred situation in the corridor ij for line scenario s, in which a line from the N-1 scenario k is switched off. If there exist only one line in a corridor, the reactance is set to a very high value that will represent infiniteness which sets the power flow calculation of the corridor in (4.71) to zero in addition to the already defined constraint $P_{ij,s}^{(l)max} = 0$ in (4.73).

As it is expected for the outage to be instantaneous, the grid is required to continue to normally operate without a generation re-dispatch. Therefore, the node generation

variable P_i^g is not going to change in any of the scenarios. Since the scenarios are set by the line limit parameter and the reactance parameter instead of the binary variable, $\alpha_{ij,s}$ is not considered in the N-1 scenarios and the binary decision variable does not increase in complexity. However, the power flow calculation needs to be considered for each of the N-1 scenarios in order to prove a feasible and optimal N-1 solution. The binary variable as a decision variable gives a solution that will be feasible for each of the line outages defined with set Ω_o.

4.3.2 Application

By introducing the scenario based N-1 TSEP problem, a single stage deterministic optimization approach is defined. Therefore, solving the proposed method guarantees the optimality of the solution. The optimization model defined with (4.69) - (4.78) is primarily focused to demonstrate the approach for the N-1 line outages of the system. However, the transformers of a transmission system with multiple voltage levels can also be represented as lines and decided upon using the binary decision variable $\alpha_(ij)$. Transformers are represented as a line between nodes i and j, given that i and j are both nodes on different voltage level representing the high and low voltage side of the transformer. Consequently, the N-1 outage of the transformers is included in the current model definition.

Furthermore, the model can be extended to consider the N-1 outages of the generating units as well. This is done by introducing a predefined set of scenarios of generating units outages in addition to the N-1 transmission lines and transformers outages. For that purpose P_i^g and P_i^{gmax} are redefined as $P_i^{g(k)}$ and $P_i^{gmax(k)}$, such that different scenarios for the power dispatch and the generating units are considered. Initially, the scenario based N-1 TSEP is defined using the DC TSP model detailed in section 4.1 as a more simplistic representation to demonstrate the proposed methodology. However, the scenario based approach can also be used with the AC TSP model detailed in 4.2, as well as any other power flow model definition within a TSP approach.

4.4 AC vs DC TSP for Overhead and Underground Power Systems

The constant emergence and development of modern metropolitan cities introduce a necessity to reconsider how the power system is designed and operated. The very densely populated urban environment represents a big challenge to the traditionally accepted overhead transmission systems. The challenging and excessively expensive land acquisition and common public opposition make the underground transmission lines a safe and reliable alternative with lessened environmental impact. Recently established metropolis with limited land availability such as Singapore and Hong Kong are pioneering examples of a transition to completely underground power systems, including voltage levels of up to $400kV$. The steady population growth and the continued economic growth set the course for many more metropolis to follow.

To account for the inevitable growth in energy demand and determine an optimal grid transition plan, it is important that a power system planning approach is used. The research on TSP problem reported in the literature and previously discussed in this thesis has in common that only overhead transmission systems are considered and tested [55, 69]. To the author's knowledge, there is no work investigating and testing an underground transmission system [4]. It is expected that the results of the TEP optimization differ due to the very different electrical characteristics of the underground conductors. Due to the need for high insulation properties, the underground conductors have a significantly higher capacitance and lower reactance and resistance.

Since the focus of this thesis is the generation of synthetic grids of realistic models, including underground power systems such as the Singaporean power system, both AC and DC transmission system planning approaches are investigated and compared for the design of both overhead and underground power systems. Instead of considering an expansion planning of an existing grid, in this work a two-stage approach to design a completely new power system for the purpose of comparing an underground to an overhead TSP. This approach goes in line with the methodology for generating a synthetic grid as part of the framework described in chapter 2. Both, a relaxed conic AC and a DC power flow models are used and compared. The AC and DC TSP model definitions used for the purpose of the comparison are detailed in [4], and are similarly defined as in sections 4.1 and 4.2.3 respectively.

4.4.1 Comparative analysis

The comparative analysis of power system planning for the overhead and underground power systems is performed using a case study of generating a synthetic transmission power system. It consists of three voltage levels such as $66kV$ sub-transmission level and $230kV$ and $400kV$ transmission level. The load data is obtained from a realistic synthetic grid generation study of the Singaporean power system, detailed in [2].

The electrical parameters of the lines are calculated and used as two different data sets. The line parameters of one set are calculated using an aluminium conductor steel-reinforced (ACSR) overhead conductor, and the other set is calculated using a cross-linked polyethylene (XLPE) underground conductor. Three different conductor sizings are selected, one for each of the voltage levels.

In order to be able to validate the comparison of the results between the overhead and the underground power systems, the selection of the conductors is made such that both ACSR and XLPE conductors have an equal current carrying capacity. The parameters of the selected conductors are given in Table 4.1.

The conductors XLPE 800 and Cardinal 954 are considered for the underground and the overhead $66kV$ voltage level respectively. Similarly, the XLPE 1000 and Bunting 1192 and the XLPE 1200 and the Dipper 1351.5 are used in the $230kV$ and the $400kV$ voltage levels. Since the current carrying capacity of the two conductors in a single voltage level does not exactly match, the minimum of the two values is used as a current limit for both overhead and underground line parameters.

Table 4.1: Conductor Data

Type	R (Ω/km)	X (Ω/km)	Bsh ($\mu S/km$)	Imax (A)
XLPE 800	0.0284	0.1234	94.20	997
Cardinal 954	0.0728	0.2418	6.990	990
XLPE 1000	0.0226	0.1376	62.80	1131
Bunting 1192	0.0597	0.2375	7.195	1139
XLPE 1200	0.0194	0.1455	56.52	1208
Dipper 1351.5	0.05315	0.2326	7.349	1229

A significant difference in the conductor parameters is noticed when the overhead and the underground conductors given in Table 4.1 are compared. The resistance R of an ACSR overhead conductor is in average 2.7 times bigger than a XLPE undergound conductor with an equal current carrying capacity at the same voltage level. Similarly, the reactance X of an ACSR overhead conductor is 1.8 times bigger then a XLPE undergound conductor, while the shunt susceptance is up to 13.5 times smaller than the one from an equivalent XLPE conductor. Such differences in the electrical parameters are the primary reason to investigate and compare the outcome of using power system planning for two different types of transmission power systems.

Even though the conductors and installation costs of an underground power system exceeds the cost of an overhead power system by multiple times, the difference in investment cost of both type of systems is reduced when the challenges of land acquisition in metropolitan areas are considered. This work assumes that the cost of both XLPE and ACSR conductors in a single voltage level is equal. This simplification is done in order to make a valid comparison of the two different type of systems solely based on the difference in the electrical parameters of the grid.

Considering the purpose to compare overhead and underground power systems using both AC and DC power flows, four different cases are defined as follows

1. Underground XLPE using DC power flow
2. Overhead ACSR using DC power flow
3. Underground XLPE using AC power flow
4. Overhead ACSR using AC power flow

The results are analyzed and elaborated to illustrate the difference in the resultant grid designs when a power transmission system planning optimization is used in the two different types of systems. In addition, it is investigated how the grid design and the grid operation changes when an AC versus a DC power flow model is used as part of the optimization problem.

4.4.2 Results & Analysis

To analyze the difference between AC and DC TSP for both overhead and underground transmission systems, the optimization problem is solved in two steps. At the initial step, the power system used as a case study does not have any existing lines and the power system planning is considered as an optimal design of a new grid. This grid configuration is then used as an input for the N-1 expansion planning optimization. Once the optimization is concluded and the grid design is obtained, a MATPOWER power flow analysis is run for each test case.

4.4.2.1 Objective Function

The results of the objective function in the power system planning optimization, that represent the investment cost of the lines, are given in Table 4.2. In addition, the final binary count of the total number of lines for each test case is given in Table 4.3. For a better understanding of the obtained grid design, the results are shown per voltage level.

Table 4.2: Investment Cost of Lines per Case Study

	Investment Cost of Lines			
	66 kV	230 kV	400 kV	Total
XLPE_DC	2.2215E+09	2.0441E+09	2.3786E+09	6.6441E+09
ACSR_DC	2.2483E+09	2.1646E+09	3.4764E+09	7.8893E+09
XLPE_AC	1.7738E+09	1.7658E+09	2.6141E+09	6.1536E+09
ACSR_AC	1.9794E+09	1.9402E+09	2.8556E+09	6.7752E+09

Table 4.3: Number of Lines per Case Study

	Number of Lines			
	66 kV	230 kV	400 kV	Total
XLPE_DC	210	32	13	255
ACSR_DC	214	35	16	265
XLPE_AC	186	30	14	230
ACSR_AC	199	31	14	244

When the overhead power system and the underground power system are compared, it is observed that the cost of the objective of the overhead power system is higher by up to 19% for both AC and DC models. Consequently, when the 4.3 is analyzed, the results show that the overhead power system requires more lines to be installed in order to meet the constraints and provide a feasible solution. In addition, if the XLPE underground test case is used to compare the AC and the DC power system planning, it is observed

that using an AC power flow model significantly reduces the cost and the total number of lines required for a feasible grid solution.

Even though the investment cost is directly proportional to the total length of the lines, the same does not always apply to the number of lines. In the two test cases where the AC power flow model is used, both the $400kV$ systems have the same number of lines but a different investment cost since different lines are chosen. Having different electrical parameters or different power flow models often results in selecting distinctive lines in each of the grid configurations. The distinctive lines do not overlap when the two power systems are compared. When the overhead and the underground power systems are compared, there are up to 18% or 47 distinctive lines in the grid configurations when the DC model is used. Similarly, there are up to 17% or 42 distinctive lines when the AC model is used. When the AC and the DC power system planning is compared based on the XLPE underground test case, there are up to 23% or 59 distinctive lines in the resultant grid configurations.

4.4.2.2 Power Flow

A power system with significantly different line electrical parameters and line configuration may result with relatively different power flow results. In addition, the solution obtained using a DC power flow can often be infeasible when tested with an AC power flow. To evaluate the power system planning solutions of each test case, a power flow study is done and the results are shown in Table 4.4.

Table 4.4: Power Flow Results per Case Study

	Min. Voltage [p.u.]	Losses [MW] / [MVar]	Voltage Angle [deg]	Branch Charging [MVar]
XLPE_DC	0.975	82.4 / 445.4	-14.71	5833
ACSR_DC	0.932	224.6 / 811.4	-33.46	918
XLPE_AC	0.985	76.4 / 407.9	-1.91	6035
ACSR_AC	0.951	208.2 / 767.9	-0.96	782

One of the differences between the underground and the overhead power systems is the voltage drop, which is more evident in the DC power system planning. The overhead ACSR power system has a significantly higher voltage drop of 6.8%, which exceeds the 5% limit and makes the power system infeasible [109]. On the contrary, the underground XLPE power system has a voltage drop of 2.5% which is well within the limits. The smaller voltage drop in the underground system is related to the capacitive effect of the underground conductors which results in a high branch charging as observed in Table 4.4. If the branch charging in the DC underground test case is excluded and set to zero, the voltage becomes 0.928 p.u. and the voltage drop is 7.2%.

When the AC power system planning results are considered, it is observed that the voltage drop is within the proposed limits for both cases. Similarly, the underground power system has a smaller voltage drop due to the capacitive nature of the XLPE conductors.

A noticeable difference is also observed when comparing the power losses. Since the losses are proportional to the resistance R and the reactance X, the ratio between the losses in the overhead and the underground power systems directly corresponds to the difference in the electrical parameters of the both types of conductors. According to Table 4.4, using the AC power system planning provides a better solution when the losses of the system are considered. The smaller amount of losses in the test cases with AC planning compared to DC planning corresponds to different generation profiles and shorter overall line length observed in Table 4.2.

4.4.3 Summary

In summary, results show that optimal planning of an underground power system ideally requires less number of lines with up to 19% lower investment cost. When transmission planning using AC and DC models is compared, the results obtained with the relaxed AC model show a better cost optimal solution and lower number of lines. The results obtained for the two types of power systems show that up to 18% of the lines are unique when the two configurations are compared. Similarly, there are up to 23% distinctive lines when the AC and the DC models are compared.

Due to the significant difference in the line electrical parameters and the line configurations, the obtained solutions show different power flow results when analyzed with MATPOWER. The overhead power system proves to be infeasible when it is planned using the DC model. On the contrary, the underground power system is feasible with voltages well within the limits due to the high capacitance of the lines. However, in addition to the better cost optimal solution, the AC model gives a feasible power flow and an improved power flow profile in both type of power systems. The comparative analysis presented with this work also shows that there can be a significant difference in the transmission planning approach when underground conductors are used.

5 The Singaporean Synthetic Power System Model: Data & Inputs

In this chapter, a practical application for generating a synthetic grid model is presented. The framework proposed in this thesis is used with an objective of generating a synthetic grid model of the power system of Singapore. Having obtained and defined the required inputs for using the power system planning models, a bottom up approach of the proposed framework for generating both a distribution and a transmission system model is employed. The method and the input data used are elaborated in a step by step approach, and the results are presented.

5.1 Introduction

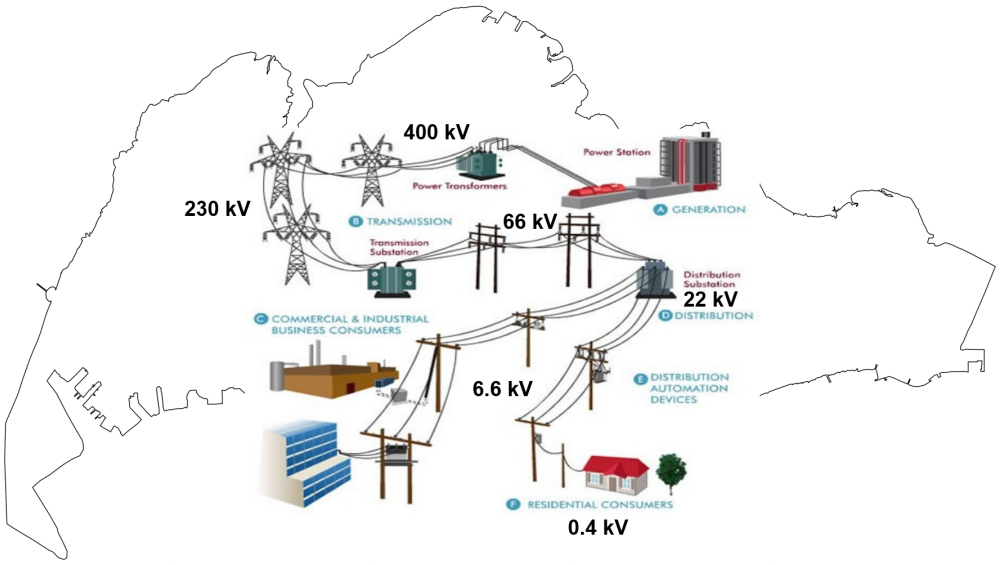

Figure 5.1: The power system of Singapore with different voltage levels

The power system of Singapore is characterized as one of the best and most reliable power system worldwide when indices such as SAIDI and SAIFI are considered. The grid includes multiple voltage levels, such as 0.4kV low distribution voltage, 22kV medium distribution voltage, 66kV sub-transmission voltage and 230kV and 400kV transmission voltage levels as shown in Figure 5.1. The medium voltage distribution system includes a 6.6kV voltage level as well, which is already being phased out and considered not relevant

for the model. The focus of this work is to model the distribution, sub-transmission and transmission voltage levels.

According to the Energy Market Authority of Singapore [110], 'as of end March 2020, CCGT, Co-Generation and/or Tri-Generation plants, Steam Turbines and Open Cycle Gas Turbines accounted for 83.4% (or 10,491.4 MW), 10.8% (or 1,363.6 MW) and 1.4% (or 180.0 MW) of total electricity generation capacity respectively. Waste-To-Energy and Solar PVs contributed to the remaining 2.0% (or 256.8 MW) and 2.3% (or 290.2 MW) of total electricity capacity respectively.' The fuel mix for electricity generation in 2019 included 95.6% of natural gas, 2.8% of other energy products such as municipal waste, biomass and solar, and the rest were contributed by Coal (1.2%) and petroleum products, mainly in the form of diesel and fuel oil (0.4%). The overall electricity consumption in 2019 was 51.7TWh, with a peak demand of 7.4GW.

Due to the geographically constrained and hence very expensive land on the island of Singapore, all voltage levels are designed and engineered using underground power cable installations. In addition, high-voltage gas insulated substations (GIS) that significantly reduce the size are used throughout the island. Due to the very high capacitive nature of an underground power system, especially at higher voltage levels, the installation of numerous shunt reactors is inevitable for a feasible system operation. Having a completely underground power system and using GIS components give the grid significantly increased reliability and stability. However, this needs to be taken into consideration when modeling the grid using different power system planning models, as discussed in section 4.4.

5.2 Modeling assumptions

Given the complexity and the importance of the power system as a key infrastructure component, some information might not be easily accessible for the purpose of modeling the grid. In this chapter, the methodology and the sources for acquiring the relevant data are discussed.

For the purpose of modeling the Singaporean power system, it is required to define the system's load points. As the methodology focuses on a bottom-up approach, the load points are to be identified at the lowest voltage level as the end consumers. However, the exact data is privacy protected and not directly accessible. For this purpose, Ciechanowicz et al. in [111, 72] have used a modeling approach with assumptions on the type of the buildings, size and typical consumptions per household or building that provide the entry load point data for the synthetic grid generation as detailed in section 5.3.

It is known that the Singaporean system is underground system using underground cable installations for all voltage levels. However, the exact model configuration is unknown and represents an output in the methodology proposed in this work. Nevertheless, assumptions can still be made around the way the Singaporean grid is built. For example, the assumptions for synthetic grid include that the system has a ring distribution

grid infrastructure in place with a radial operation. The selection of line paths, cable sizes, technical characteristics and prices are detailed in section 5.5.

As part of the grid modeling, substations at different voltage levels are included. Substations in the sub-transmission and transmission voltage level have been geographically accurately identified together with the prices and technical characteristics of their transformers, as detailed in section 5.4. However, the number of transformers is unknown, and this is another of the outputs defined in the mathematical optimization approach.

Since the Energy Market Authority of Singapore (EMA) has shared all the generators participating in the market, an accurate representation of the generating units is used for the synthetic grid generation, as detailed in 5.4. The challenge and the assumptions made are to specify the voltage levels at which these generators are connected.

The electricity prices, costs and coefficients are defined from various reports and publicly available data sheets, as detailed in section 5.6.

5.3 Load Demand

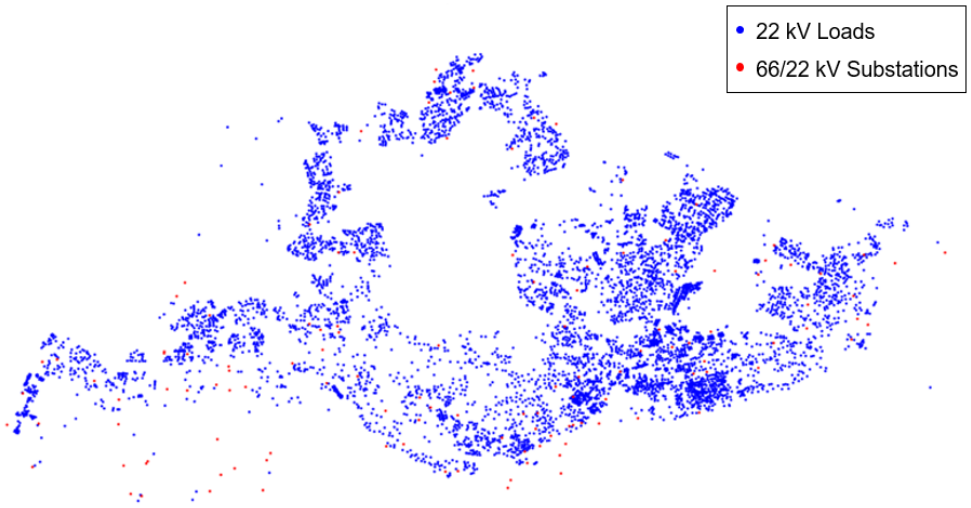

Figure 5.2: Load demand shown at 22kV voltage level as distribution substations

When it comes to modeling the consumer load, the only available data of electricity consumption statistics for consumers in Singapore is for the end users at low voltage level, published by the Energy Market Authority of Singapore [110]. This data is given per zip code with some information about the size of the households. In Singapore, each zip code corresponds to a single building with a particular location, therefore giving the opportunity to accurately identify the location of the loads.

After having modeled the peak demand of the loads based on the available data, a bottom up approach is then used to do clustering of the loads to 22kV/0.4kV substations. The 22kV substations are considered as load nodes for modeling the distribution system. This data is provided and the clustering method is explained in details by Ciechanowicz

et al. in [111, 72]. In total 6161 substations are identified at 22 kV level with a total peak demand of 6.15 GW. As some information from industrial consumers is not fully accounted for, the data is then extended to include more industrial loads at Jurong Island, which sums up to 7.04 GW. Due to the fairly large the number of 22/0.4 kV distribution substations, the loads and substations are segmented into one of the 42 planning areas of Singapore for further study as detailed in section 5.3.1. A plot of the 22kV distribution substations shown as loads and the 66/22 kV substations is shown in Figure 5.2.

5.3.1 Distribution Load Data Split in Zones

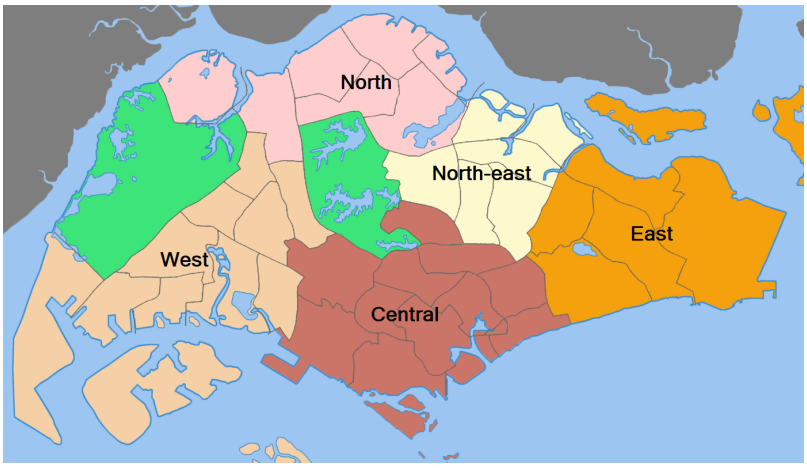

Figure 5.3: Functional zones in Singapore

Considering to solve the power system planning optimization problem for all possible combinations of the 6161 nodes results in an excessive number of binary variables and requires extensive computational power rarely available and possibly very long solving time. To address this issue, an approach to segment the data in functional regions may be required. In the case of Singapore, the island is divided in five operational zones shown in Figure 5.3. In order to reduce the number of binaries and possible scenarios, the data presented in Figure 5.2 is segmented into each zone respectively. The segmented data for four different zones is presented in Figure 5.4. An overview of the number for load and substation nodes for all zones is shown in Table 5.1. Furthermore, each zone consists of planning areas, which I are often considered as separate when it comes to infrastructure planning and investments. There are total of 42 planning areas in Singapore, as outlined in Figure 5.3. However, the loads are segmented into 36 planning areas as the rest are water catchments or nature reserves without serving loads.

By analyzing Table 5.1, it can be noticed a significant reduction in the binary variables that need to be considered within a single optimization. However, the number of possible combinations of different scenarios that the solver needs to consider is still causing

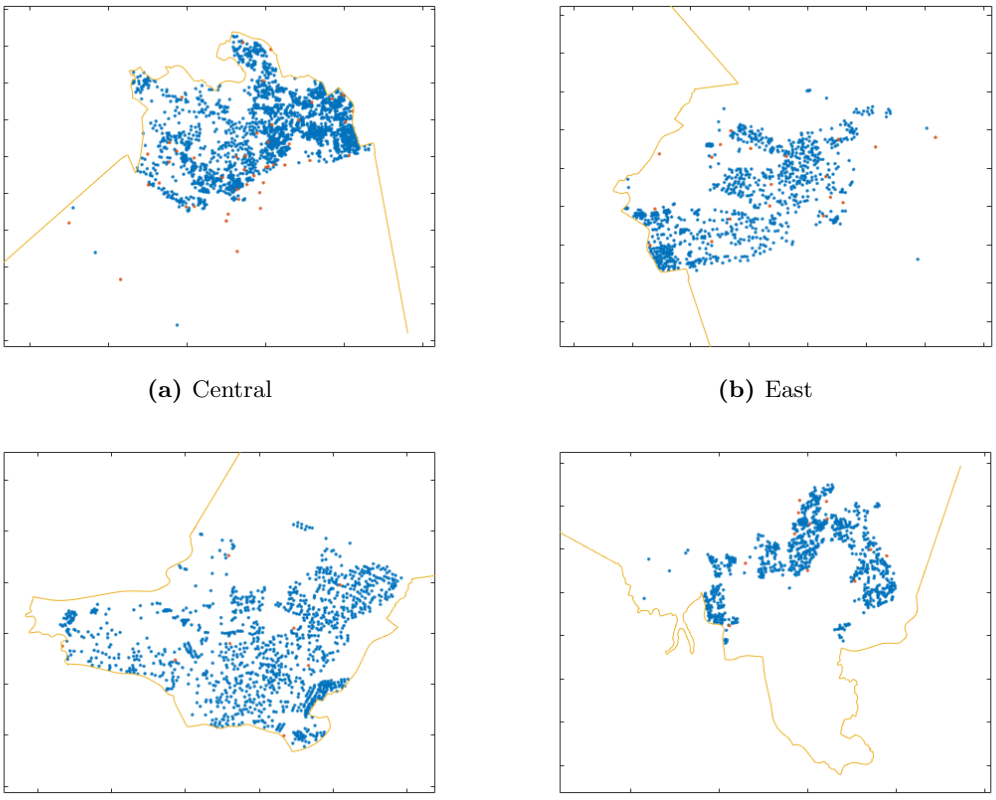

(a) Central **(b)** East

(c) North-east **(d)** North

Figure 5.4: Singapore load and substation nodes split in zones

	Load nodes	Substation nodes	Total	Binary variables
Central	1887	45	1932	1 841 280
East	912	19	931	421 361
North-east	1218	8	1226	512 071
North	842	13	855	353 640
West	1302	45	1347	889 777

Table 5.1: Number of nodes and binary variables per zone

the optimization to run "Out of memory". Since the optimization is a combinatorial problem with an exponential growth, the branch-and-cut algorithm used by the solvers tends to grow big in size, requiring a much greater memory with every binary added to the problem.

The load nodes segmenting is only applicable for the distribution system. When the transmission system is considered, such approach should not be considered due to the

more complex mesh structure of the grid. Furthermore, transmission systems generally consist of comparably fewer nodes than distribution system which makes their solving more tractable.

5.3.2 Selecting Nearest Neighbors for the Distribution Line Set

Furthermore, another practical simplification is done for the attempt to obtain a relevant solution. Normally, when distribution planning is considered, not all possible connections are taken into account. Due to economic and technical reasons, it is most common that lines with the shortest distances are being considered as a possible line connection for an observed node [78]. Therefore, the closest neighboring nodes of the observed node are considered for a possible line connection. Consequently, the nodes that are the furthest from the observed node can be eliminated in a pre-selection process, and only the nearest neighbors are to be considered. A procedure is explained trough a small segment of the data bellow.

In Table 5.2, a small segment of the length matrix is defined.

	node1	node2	node3	node4	node5	node6	node7	node8
node 1	0	1.482	5.473	10.424	5.188	5.741	2.873	7.638
node 2	0	0	4.392	9.122	4.013	4.389	2.911	6.190
node 3	0	0	0	5.160	0.570	1.646	7.146	3.676
node 4	0	0	0	0	5.288	4.744	11.422	3.683
node 5	0	0	0	0	0	1.213	6.692	3.376
node 6	0	0	0	0	0	0	6.746	2.215
node 7	0	0	0	0	0	0	0	8.046
node 8	0	0	0	0	0	0	0	0

Table 5.2: Length matrix of possible line connections

In order to eliminate the lines that are the furthest and select only the nearest neighbors, data is sorted with ascending property for each node accordingly, as shown in Table 5.3.

	node 1	node 2	node 7	node 5	node 3	node 6	node 8	node 4
node 1	0	1.482	2.873	5.188	5.473	5.741	7.638	10.424

Table 5.3: Length matrix in ascending order for node 1

Possible line connections are then selected and considered only from the N nearest nodes, where N is a predefined parameter representing the total number of line connections for each node individually. The bigger the number of possible line connections for each node N, the bigger the number of binary variables considered for the optimization. Consequently, more computational power is required to solve the problem. However, there is also a limit on how small the number N can be, due to possible infeasibility of the problem if not enough lines are considered. A small number of N might

also affect the optimality of the solution. For an optimal solution, it is recommended to perform a sensitivity analysis for the number N for the case study that's being analyzed.

When distribution systems are modeled, fewer N nearest nodes can be considered. However, when transmission systems are modeled only lines connecting very distant nodes are to be excluded from the line set.

5.4 Identification of Substations and Power Stations

Once the end users demand, the low voltage network and the location of the 22kV substations is obtained, the next required step is to identify the substations and the generating units at the sub-transmission and transmission voltage levels. A representation of the 66, 230 and 400 kV substations and power stations in the Singaporean system is shown in 5.5

Figure 5.5: 66, 230 and 400 kV substations and power stations in the Singaporean system

5.4.1 Substations

In order to generate a grid design that is an accurate representation of a real power system, an input of the total number and the geographical location of substations is needed. Publicly available reports and documents containing information of sub-transmission and transmission substations and power stations can be obtained from different sources and reports from EMA, Singapore Power and some other relevant institutions. By the use of Google Maps satellite imagery, coordinates of sub-transmission and transmission substations are identified. Geographical coordinates are taken approximately at the middle

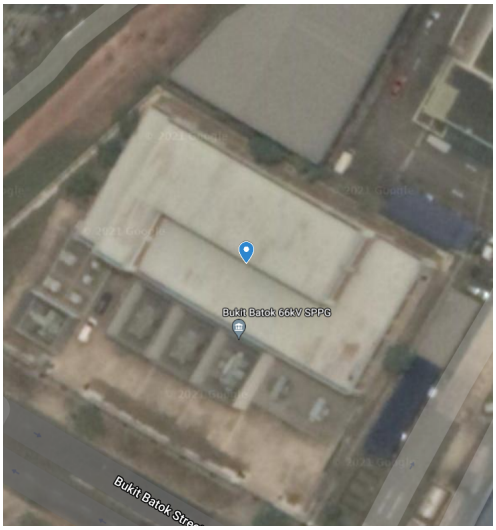

Figure 5.6: Example of a 66kV/22kV substation (source: Google Maps)

of the objects. An example of a satellite image of a 66/22 kV substation is shown on Figure 5.6.

However, even though the number and the coordinates of the substations have been accurately identified, there is no information whatsoever regarding the sizing or the load profiles of these substations. Therefore, an initial modeling of the distribution system is of crucial importance for the allocation of loads to the adequate substations at the higher voltage levels.

The number of substations in the sub-transmission and transmission voltage level is as follows:

- 118 substations 66kV level
- 27 substations 230kV level and 1 substation 230kV/22kV
- 7 substations at 400kV level

5.4.2 Generators

Similarly to the substations, an input of the total number, geographical location and installed capacity of generating units is necessary for an accurate grid representation. Publicly available data sheets containing information on all generating units in Singapore are published by EMA of Singapore. The data sheets provide information such as market participant's name, type of generator, maximum installed capacity, minimum stable load, regulation capacity, primary reserve, frequency responsive status, etc. A sample of this data is shown on 5.7.a). However, the location of these generating units is unknown. The location is determined by using relevant information published by the market participants and Google Maps satellite imagery as shown on 5.7.b). Geographical coordinates are taken approximately at the middle of the objects.

MARKET PARTICIPANT	FACILITY NAME	FACILITY GENERATION TYPE	MAX GENERATION CAPACITY
TUAS POWER GENERATION PTE LTD	TUASPOW	ST	600
SENOKO ENERGY PTE LTD	POWSNKO	CCGT/COGEN/TRIGEN	431
KEPPEL MERLIMAU COGEN	AGCKMCG	CCGT/COGEN/TRIGEN	410
SEMBCORP COGEN	AGCSMBG	CCGT/COGEN/TRIGEN	403.8
PACIFICLIGHT POWER PTE LTD	AGCPACL	CCGT/COGEN/TRIGEN	400
TUASPRING PTE LTD	AGCTSPG	CCGT/COGEN/TRIGEN	395.7
SEMBCORP COGEN	AGCSKCG	CCGT/COGEN/TRIGEN	392.5
YTL POWERSERAYA PTE LIMITED	POWSERY	CCGT/COGEN/TRIGEN	370

a)

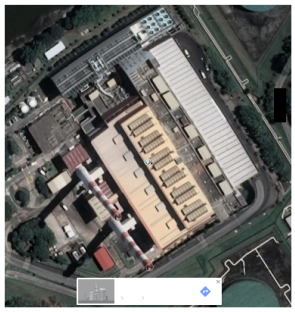

b)

Figure 5.7: a) Generator details (source: EMA) b)Power station (source: Google Maps)

There are total of 46 generators with individual installed capacity bigger than 25MW. The total installed capacity is 13.26GW when all sub-transmission and transmission voltage levels are considered.

5.5 Line Set

Having obtained the geographical coordinates of the load, substation and generator nodes, the line set of both distribution and transmission system models are defined as line connections between the nodes, as detailed in sections 5.3.1 and 5.3.2. However, considering a direct air distance between two nodes may provide inaccurate assumptions due to multiple obstacles such as private properties, lakes, ponds, canals, rivers, etc. An example of a comparison between the air distance and a realistic road distance between two substations is shown in Figure 5.8. The air distance is just 4.8km, however not feasible due to a canal between the two nodes. It can be observed that a realistic road distance between the two substations is 16.8km, which might not be selected during the optimization process compared to a rather short air distance of 4.8km.

As previously discussed, in the case of the power system of Singapore both distribution and transmission lines are built with underground cables. The cables are laid in underground tunnels, ducts and cable conduits, depending on the voltage level and location. The underground cables are placed along road corridors and sidewalks, as shown in Figure 5.9. On the figure, power cable laying works on a road corridor and 230kV cable ducts on a sidewalk are shown.

Consequently, the line sets of possible line connections for the distribution and transmission systems are defined using the road distances between the selected nodes. For this purpose, the Application Programming Interface (API) services provided by Google are used and all road distances are calculated.

Furthermore, articles and publications of some existing line corridors in the transmission system of Singapore are found in [112] and shown in Figure 5.10. The existing line corridors shown in Figure 5.10 are input in the transmission planning optimization as

Figure 5.8: Comparison between air distance and a realistic road distance

fixed, having their road distance and electrical parameters calculated accordingly. However, the grid has significantly expanded with new transmission level substations present in the system. In addition to the existing lines and nodes shown in Figure 5.10, there are additional nodes and lines present in the system.

5.6 Data for the Synthetic Power System Model of Singapore

In addition to the information obtained for the loads, substations, power stations and line lengths in Singapore, described in sections 5.3, 5.4 and 5.5, modeling of the synthetic power system requires some additional input parameters such as various cable data, transformer data and cost parameters.

5.6.1 Costs and Technical Data of Underground Cables

As previously discussed, all voltage levels of the Singaporean power system, starting from 0.4kV and up to 400kV, are completely designed and built underground using power cables. Therefore, power cable and installation costs for underground lines need to be obtained to calculate the fixed investment costs for the lines as part of the power system planning optimization approach. Additionally, the technical data of specific cables within all voltage levels is necessary for the power flow analysis, which is an essential part of the power system modeling. The technical data is required for the optimization methods used to generate the synthetic grid models, since a feasible power system operation including the calculation of power losses and ensuring a power balance are a mandatory requirement.

Figure 5.9: Singapore distribution and transmission underground line corridors

5.6.1.1 Cost of Cables

Power systems are usually planned and built in a cost efficient manner with regards to the overall investment and operational costs. The investment costs of a line include the sum of the cost of the power cables and the installation costs. Unlike the overhead

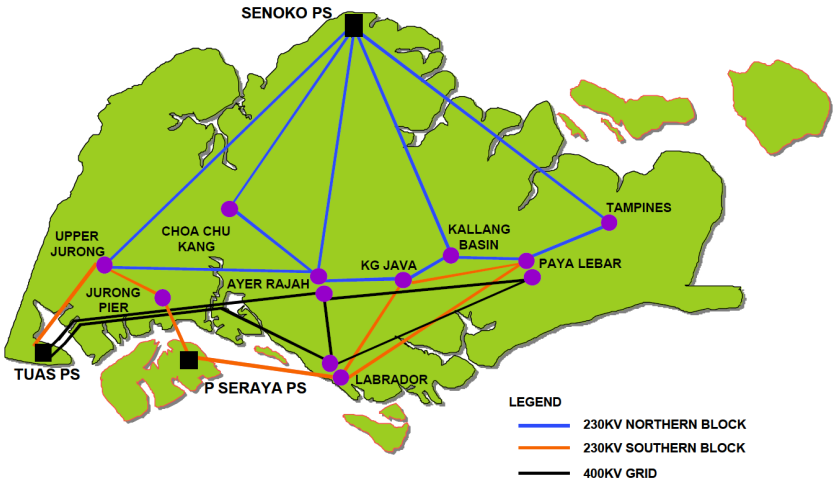

Figure 5.10: Existing 400/230kV underground transmission network. Source: S. T. Chang, K. Y. Chua, C. C. Slew and T. L. Tan, "Power quality initiatives in Singapore," 16th International Conference and Exhibition on Electricity Distribution, 2001. Part 1: Contributions. CIRED. (IEE Conf. Publ No. 482), 2001, pp. 4 pp. vol.2-, doi: 10.1049/cp:20010747.

lines, it is estimated that the power cable installation costs equal the cost of the cables and amount to nearly 50 % of the total cost of the line [79]. Therefore, it is of great importance to accurately determine the cable costs for various cables at different voltage levels.

Price lists of cables for the distribution level are found published on the web by some of the producers such as [113]. The price list used to obtain the costs of 22/12.7 kV cables contains loco prices given in Indian Rupee (Rs). To account for prevailing tax, transportation and additional remaining fees, a 35% price increase to the factory procurement price is calculated.

However, price lists on the cost of sub-transmission and transmission underground cables has proven to be inaccessible from the cable producers. However, alternative ways to obtain this data were found. Some recent global trade platforms provide an option to show customs report on import and export goods within a country. Using this platforms, export costs of the required cables at different voltage levels are obtained. A 35% increase on the export price is calculated in order to account for the prevailing tax, transportation and remaining fees.

5.6.1.2 Cable Sizing

The sizing of cables considered for the line modeling are given as follows:

- $300mm^2$ copper and $300mm^2$ aluminum cables for 22kV level
- $1000mm^2$ copper cables for 66kV level

- $1200mm^2$ copper cables for 230kV level
- $2000mm^2$ copper cables for 400kV level

5.6.1.3 Technical Data Calculation for Power Cables

Initial technical data and specification of cables such as the DC resistance at 20°C $R_{DC\ 20}$, capacitance C and maximum current rating I_{max} can be found in [114] for the 22kV cables, and [115] for the 66 - 400 kV cables. Other parameters are calculated based on the specific cable construction and other given information. For the calculation of cable's parameters, an assumption is made that three single core cables are used. The current rating is determined with an assumption that the cables are put in a pipe duct in a flat formation.

However, the resistance given in the technical specification refers to a DC operation at 20°C. The operating temperature for AC operation is considered to be 90°C. Therefore, first step is to calculate R_{DC20} as follows [116]

$$R_{DCt} = R_{DC20} \cdot 1 + \alpha_{20} \cdot (t - 20)$$

where α_{20} is the temperature coefficient of resistance for the specific conductor material at 20°C; $\alpha_{20\ Copper} = 0.00404$; t is the temperature at which the resistance is calculated, $t = 90$°C.

When AC operation of the cable is considered, the resistance changes when compared to DC due to the skin effect and proximity effect in the conductor. Therefore, skin effect factor y and proximity effect factor y_1 are introduced.

The skin effect factor y is calculated as follows [117]

$$y = \frac{x_s^4}{192 + 0.8 \cdot x_s^4}$$

$$x_s^2 = \frac{8 \cdot \pi \cdot f}{R_{DC90}} \cdot 10^{-7} \cdot k_s$$

where $k_s = 1$ for compact round stranded conductor.

The proximity effect factor y_1 for three single core cables is calculated as follows [117]

$$y_1 = \frac{x_p^4}{192 + 0.8 \cdot x_p^4} \cdot \left(\frac{d_c}{s}\right)^2 \cdot \left[0.312 \cdot \left(\frac{d_c}{s}\right)^2 + \frac{1.18}{\frac{x_p^4}{192+0.8 \cdot x_p^4} + 0.27}\right]$$

$$x_p^2 = \frac{8 \cdot \pi \cdot f}{R_{DC90}} \cdot 10^{-7} \cdot k_p$$

where d_c is the diameter of the conductor; s is the distance between conductor axes; $k_p = 0.8$ for compact round stranded conductor.

The resistance R_{AC90} for AC operation of the cable is calculated as follows [118]

$$R_{AC90} = R_{DC90} \cdot (1 + y + y_1) \quad [\Omega/km]$$

The inductive impedance of the cables X_L is considered as the total impedance X of the cable [119]. Initially the inductance L is calculated as follows

$$L = 0.05 + 0.2 \cdot ln(\frac{K \cdot s}{r}) \quad [mH/km]$$

where $K = 1.26$ for flat formation, s is the distance between cable axes, r is the radius of the conductor [120].

The impedance $X = X_L$ is then calculated as follows

$$X = X_L = \omega \cdot L = 2 \cdot \pi \cdot f \cdot L \quad [\Omega/km]$$

where f is the frequency in $[Hz]$ [119].

Having calculated the resistance and the reactance of the conductor, the impedance Z is calculated as follows

$$Z = \sqrt{R^2 + X^2}$$

The admittance is then calculated as

$$Y = 1/Z$$

The maximum power carrying capacity of a cable is

$$S_{max} = \sqrt{3} \cdot I_{max} \cdot U_n$$

The capacitive susceptance B_C is considered as the shunt susceptance of the cable B_{sh} and is calculated using the capacitive reactance X_C as follows [119]

$$B_{sh} = B_C = 1/X_C = \omega \cdot C = 2 \cdot \pi \cdot f \cdot C$$

The conductance and susceptance of the cable are both represented in $[S/km]$ are calculated as

$$G = \frac{R}{Z^2}$$

$$B = \frac{X}{Z^2}$$

following

$$Y = \sqrt{G^2 + B^2}$$

22 kV	Cross Section Area (mm^2)	Price	
	150	24.23	SGD/m
	185	28.67	SGD/m
	240	32.98	SGD/m
	300	37.13	SGD/m
	400	43.93	SGD/m
	500	54.24	SGD/m
	630	64.35	SGD/m
	800	75.16	SGD/m
	1000	96.71	SGD/m

Table 5.4: XLPE underground cable cost for 22kV

66 kV	Cross Section Area (mm^2)	Price	
	240	37.67	SGD/m
	300	52.03	SGD/m
	400	76.66	SGD/m
	500	105.88	SGD/m
	630	147.42	SGD/m
	800	206.86	SGD/m
	1000	285.72	SGD/m
	1200	378.86	SGD/m
	1600	558.19	SGD/m

Table 5.5: XLPE underground cable cost for 66kV

5.6.1.4 Cable Parameters and Cost

The cost derived for both the 22kV and 66kV cables is shown in Table 5.4 and 5.5. The technical characteristics for the underground cables used in this study are detailed in 5.6, 5.7, 5.8, 5.9 and 5.10 for 22kV, 66kV, 230kV and 400kV respectively.

5.6.2 Electricity Price for Losses

The price of the losses is set to match the cost of the electricity price. In the last report for Singaporean Energy Statistics [121], an average price of each quarter in 2015 is known. As price for the losses, an average annual price is calculated as

$$\Psi_{i,j}^{loss} = \frac{23.3 + 20.9 + 22.4 + 20.4}{4} = 21.7 \quad [Cents/kWh]$$

5.6.3 Cost of substations - Transformer Size and Price

There are two main parameters considered for the substations of the system, which are the cost and the installed capacity. The installed capacity refers to the number of trans-

Copper							
Section	R	X	Bsh	Smax	G	B	Imax
mm^2	Ω/km	Ω/km	S/km	kVA	S/km	S/km	A
35	0.668	0.139	0.000046	2095.5	1.435	0.298	165
50	0.493	0.132	0.000050	2476.5	1.891	0.507	195
70	0.342	0.124	0.000057	2984.5	2.584	0.940	235
95	0.246	0.118	0.000063	3619.5	3.303	1.585	285
120	0.195	0.114	0.000069	4191.0	3.827	2.230	330
150	0.158	0.111	0.000074	4762.5	4.241	2.973	375
185	0.126	0.107	0.000081	5461.0	4.595	3.905	430
240	0.096	0.104	0.000089	6477.0	4.812	5.186	510
300	0.077	0.108	0.000098	7429.5	4.352	6.152	585

Table 5.6: 22kV XLPE underground cable technical parameters

Aluminium							
Section	R	X	Bsh	Smax	G	B	Imax
mm^2	Ω/km	Ω/km	S/km	kVA	S/km	S/km	A
35	1.130	0.139	0.000046	1587.5	0.872	0.107	125
50	0.834	0.132	0.000050	1905.0	1.169	0.185	150
70	0.577	0.124	0.000057	2349.5	1.657	0.357	185
95	0.416	0.118	0.000063	2857.5	2.222	0.630	225
120	0.329	0.114	0.000069	3302.0	2.713	0.937	260
150	0.268	0.111	0.000074	3746.5	3.185	1.317	295
185	0.213	0.107	0.000081	4254.5	3.739	1.881	335
240	0.163	0.104	0.000089	5080.0	4.373	2.785	400
300	0.130	0.108	0.000098	5778.5	4.539	3.778	455

Table 5.7: 22kV XLPE underground cable technical parameters

Section	R	X	Bsh	Smax	G	B	Imax
mm^2	Ω/km	Ω/km	S/km	kVA	S/km	S/km	A
240	0.0967	0.1469	0.00006280	55	3.1274	4.7488	483
300	0.0771	0.1415	0.00006594	62	2.9694	5.4494	544
400	0.0603	0.1365	0.00007222	70	2.7084	6.1306	616
500	0.0470	0.1315	0.00007850	83	2.4074	6.7437	729
630	0.0363	0.1274	0.00008792	95	2.0680	7.2584	828
800	0.0284	0.1234	0.00009420	106	1.7678	7.6959	929
1000	0.0226	0.1193	0.00010362	124	1.5304	8.0893	1087
1200	0.0194	0.1183	0.00011304	134	1.3477	8.2313	1173
1600	0.0145	0.1138	0.00012560	157	1.1018	8.6483	1375
2000	0.0115	0.1102	0.00013816	175	0.9408	8.9775	1530

Table 5.8: 66kV XLPE underground cable technical parameters

Section	R	X	Bsh	Smax	G	B	Imax
mm^2	Ω/km	Ω/km	S/km	kVA	S/km	S/km	A
400	0.0603	0.1596	0.00004396	253	2.0721	5.4838	634
500	0.0470	0.1537	0.00004710	286	1.8172	5.9498	719
630	0.0363	0.1477	0.00005338	335	1.5701	6.3860	842
800	0.0284	0.1427	0.00005652	376	1.3388	6.7400	944
1000	0.0226	0.1376	0.00006280	438	1.1611	7.0764	1100
1200	0.0194	0.1345	0.00006594	472	1.0489	7.2835	1185
1600	0.0145	0.1290	0.00007222	539	0.8599	7.6537	1354
2000	0.0115	0.1251	0.00007536	593	0.7316	7.9266	1489
2500	0.0092	0.1202	0.00008478	624	0.6356	8.2710	1566

Table 5.9: 230kV XLPE Copper Wire Shield underground cable technical parameters

Section	R	X	Bsh	Smax	G	B	Imax
mm^2	Ω/km	Ω/km	S/km	kVA	S/km	S/km	A
630	0.0363	0.1593	0.00004396	567	1.3595	5.9665	819
800	0.0284	0.1540	0.00004710	641	1.1565	6.2814	925
1000	0.0226	0.1484	0.00005338	757	1.0024	6.5873	1093
1200	0.0194	0.1455	0.00005652	816	0.8993	6.7540	1178
1600	0.0145	0.1408	0.00005966	953	0.7232	7.0260	1375
2000	0.0115	0.1359	0.00006280	1048	0.6211	7.3079	1513
2500	0.0092	0.1295	0.00007222	1100	0.5483	7.6849	1588
3000	0.0077	0.1318	0.00007536	1166	0.4414	7.5597	1683

Table 5.10: 400kV XLPE Lead Sheath underground cable technical parameters

formers that a substation has.

It is common in one power system to have typical ratings and types of transformers for different levels. This is common practice due to economical and practical reasons for maintenance and operation of the transformers. Therefore, the rating of a single transformer is chosen according to publicly available data in Singapore Power Reports [122] of procurement and installation of certain transformer ratings in different voltage level. For 66 kV nominal voltage, 75 MVA transformers are being installed island-wide. For 230 kV, 200 MVA transformers are considered, and for 400 kV, 500 MVA transformers are considered.

Since publicly available data for cost of substations in Singapore is not available, data from the System Operator of California [123] is used to derive the cost of the substations. There are two cost parameters defined. One is the fixed cost per substation of a certain voltage level, and the other one is the flexible cost of each substation depending on the number of transformers. In California, there are four independent TSOs with different cost evaluation of same substations and transformer ratings. Therefore, an average of all four TSO is used as the final price for the substations and the transformers.

5.6.4 Calculation of the Equivalent Peak Loss Factor (EPLT)

The calculation of the Equivalent Peak Loss Factor (EPLT) for Singapore is detailed in Figure 5.11

Monthly Electricity Consumption by Sector												
	2016											
	Jan	Feb	Mar	Apr	May	Jun	Jul	Aug	Sep	Oct	Nov	Dec
Overall	**3,875.3**	**3,926.5**	**3,722.7**	**4,042.3**	**4,065.9**	**4,237.7**	**4,049.4**	**4,224.4**	**4,085.3**	**4,165.9**	**4,188.7**	**3,992.7**
Industrial-related	1,630.1	1,642.9	1,515.7	1,629.5	1,626.5	1,727.2	1,705.7	1,782.1	1,721.7	1,765.5	1,769.6	1,695.5
Commerce and Service-related	1,437.1	1,465.8	1,396.7	1,519.4	1,507.2	1,550.9	1,462.3	1,545.9	1,476.1	1,507.5	1,518.6	1,484.2
Transport-related	213.5	214.1	202.8	221.0	219.3	227.1	216.3	224.7	217.1	218.9	232.4	215.7
Households	570.0	580.1	585.0	648.3	688.8	708.2	641.9	646.7	647.4	650.1	644.4	574.8
Others	24.6	23.6	22.5	24.1	24.1	24.4	23.2	25.0	23.0	23.9	23.7	22.5

Source: Energy Market Authority (EMA)

Total hours per month:	744	696	744	720	744	720	744	744	720	744	720	744
Average Power Demand:	**5.209**	**5.642**	**5.004**	**5.614**	**5.465**	**5.886**	**5.443**	**5.678**	**5.674**	**5.599**	**5.818**	**5.367**
Square of Avg Power Demand:	**27.131**	**31.827**	**25.036**	**31.520**	**29.865**	**34.641**	**29.623**	**32.239**	**32.195**	**31.352**	**33.845**	**28.800**
Annual Avg Power Demand:	**5.533**											
Annual Avg of Square Power Demand:	**30.673**											
Peak System Demand:	**6.978**											
Squared Peak System Demand:	**48.692**											
Equivalent Peak Loss Time:	**5518.2**	**hours**										

Figure 5.11: Calculation of the Equivalent Peak Loss Factor (EPLT)

6 The Singaporean Synthetic Power System Model: Results & Analysis

The methodology proposed with this work has been applied to a case study of the Singaporean power system, detailed in chapter 5. The available data and information used for the synthetic grid generation of the Singaporean grid includes:

- load points
- potential line routes and corridors
- technical and economic parameters of cables
- location and voltage level of substations
- technical and economic parameters of transformers
- electricity prices and equivalent peak loss factor

Given the inputs listed above, the methodology is applied as a bottom up approach starting from the 22kV distribution level. The loads are aggregated as 22/0.4 kV distribution substations, with substations and transformers at the 66/22 kV sub-transmission level serving as source nodes. Using the distribution system planning approach, the loads are assigned to a substation and the connecting lines are defined. Furthermore, the optimization approach is considering the sizing of the substations, using an integer variable that determines the number of transformers in each of the substations.

The outputs of the distribution system planning provide the load allocation on the higher voltage substations. These outputs are then used for the sub-transmission and transmission system planning. The results define the system's load allocation and line configuration while considering a pre-defined validation metrics of a real power system.

The outputs of the proposed methodology include:

- line configuration
- load allocation
- number of transformers per substation
- loading of transformers

In addition to the already available, known and modeled data, these outputs are the missing elements for the completion of the synthetic grid model of the Singaporean power system. The completed synthetic grid is further analyzed using MATPOWER to validate the technical constraints of a feasible power flow study.

6.1 The 22kV Distribution System

The Singaporean distribution system is modeled in 36 planning areas as follows:

1. Tuas
2. Boon Lay
3. Pioneer
4. Western Islands
5. Jurong East
6. Clementi
7. Jurong West
8. Choa Chu Kang
9. Bukit Batok
10. Bukit Timah
11. Bukit Panjang
12. Sungei Kandut
13. Queenstown
14. Southern Islands
15. Bukit Merah
16. Tanglin
17. Novena
18. Kallang
19. Central Area
20. Bishan
21. Toa Payoh
22. Geylang
23. Marine Parade
24. Bedok
25. Ang Mo Kio
26. Serangoon
27. Hougang
28. Sengkang
29. Woodlands
30. Sembawang
31. Yishun
32. Seletar
33. Punggol
34. Pasir Ris
35. Changi
36. Tampines

A visual plot of the resultant line configuration of the distribution system on a city-state level is shown in Figure 6.1 below.

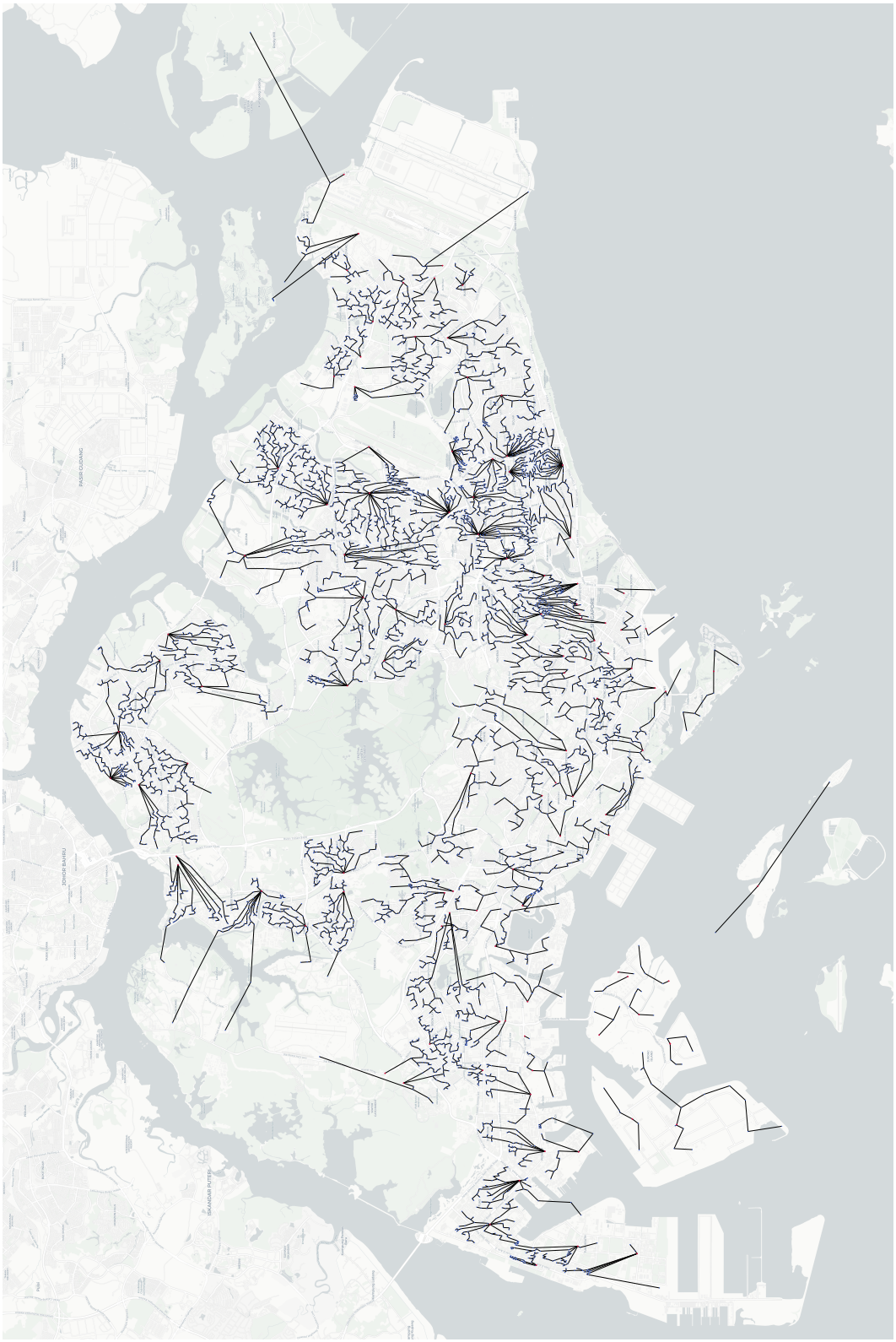

Figure 6.1: A synthetic 22 kV distribution system of Singapore

To better illustrate the results, an example of the solution of a planning area is shown in Figure 6.2. The details of the solution are given in Table 6.1, Table 6.2 and Table 6.3. The results of all planning areas can be found in the Appendix.

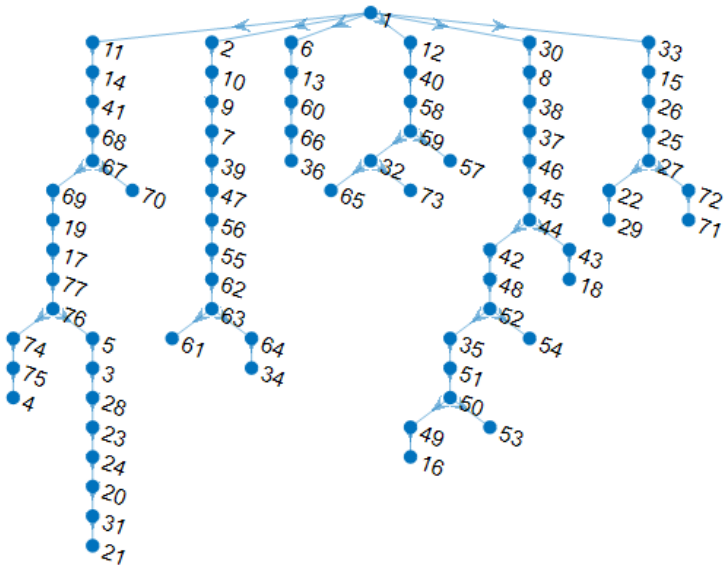

Figure 6.2: Distribution grid configuration results of the Novena planning area

The Novena planning area has a single 66/22 kV substation and 76 load nodes. Considering the line lengths and costs, load size and the technical limits of the conductor, the distribution system planning approach has allocated the loads to the source substation using six different feeders. When there are more than one substation, the optimization approach will also consider to which substation should a load be allocated given the size and the cost of the transformers. The output of the proposed methodology will provide a realistic load allocation, line configuration,substation sizing, and transformer loading based on the input parameters.

The loads of the planning area presented in figure 6.2 are given in Table 6.1. The active and reactive power demand is given in per-units, while the apparent power is represented in kVA. If the apparent power S is analyzed for all the nodes, it can be noticed that there are various different types of consumers being represented at different peak loading levels. The $node1$ is the substation node with no demand.

In Table 6.2, the results of the line configuration are shown. This includes the line resistance, reactance, shunt susceptance, and line carrying capacity in kVA. The type of the cable and a power flow calculation is shown in Table 6.2. The line type is define from 1 to 4 as follows

1. 300 m^2 copper cable
2. 300 m^2 aluminum cable
3. 2 x 300 m^2 copper cables
4. 2 x 300 m^2 aluminum cables

Node ID	P (p.u.)	Q (p.u.)	S (kVA)
node1	0	0	0
node2	0.00096	0.00032	304.6
node3	0.00069	0.00023	217.7
node4	0.00138	0.00045	434.77
node5	0.00137	0.00045	434.18
node6	0.00189	0.00062	597.05
node7	0.00133	0.00044	418.44
node8	0.00055	0.00018	173.84
node9	0.00199	0.00065	629.15
node10	0.00101	0.00033	319.56
node11	0.0022	0.00072	694.55
node12	0.00101	0.00033	319.18
node13	0.00164	0.00054	518.56
node14	0.00134	0.00044	422.82
node15	0.00079	0.00026	247.95
node16	0.00106	0.00035	335.22
node17	0.00055	0.00018	174.5
node18	0.00055	0.00018	172.8
node19	0.00061	0.0002	191.19
node20	0.001	0.00033	316.65
node21	0.00069	0.00023	217.48
node22	0.00069	0.00023	218.86
node23	0.00069	0.00023	217.92
node24	0.00069	0.00023	217.33
node25	0.00077	0.00025	243.47
node26	0.00069	0.00023	216.96
node27	0.00103	0.00034	324.32
node28	0.00101	0.00033	317.42
node29	0.0008	0.00026	252.71
node30	0.00117	0.00038	368.96
node31	0.00067	0.00022	212.23
node32	0.0425	0.01397	13421.05
node33	0.03647	0.01199	11517.88
node34	0.01512	0.00497	4773.26
node35	0.02236	0.00735	7062
node36	0.05479	0.01801	17301.68
node37	0.00073	0.00024	230.09
node38	0.00072	0.00024	227.55
node39	0.00076	0.00025	240.6
node40	0.00072	0.00024	227.88

node41	0.00313	0.00103	987.79
node42	0.00093	0.00031	293.89
node43	0.00079	0.00026	247.92
node44	0.00078	0.00026	247.42
node45	0.00058	0.00019	183.27
node46	0.00091	0.0003	285.9
node47	0.00075	0.00024	235.32
node48	0.00373	0.00123	1179.07
node49	0.00182	0.0006	574.99
node50	0.00072	0.00024	226.4
node51	0.00094	0.00031	297.61
node52	0.00159	0.00052	501.99
node53	0.00056	0.00018	175.99
node54	0.00187	0.00062	591.26
node55	0.00184	0.00061	582.26
node56	0.00191	0.00063	604.39
node57	0.00153	0.0005	482.58
node58	0.00066	0.00022	208.64
node59	0.00181	0.00059	571.4
node60	0.00225	0.00074	710.16
node61	0.00119	0.00039	377.13
node62	0.002	0.00066	630.38
node63	0.00129	0.00042	406.78
node64	0.00102	0.00034	323.64
node65	0.00095	0.00031	299.14
node66	0.00215	0.00071	677.88
node67	0.00206	0.00068	651.58
node68	0.00212	0.0007	669.49
node69	0.00237	0.00078	749.09
node70	0.00178	0.00059	562.83
node71	0.00076	0.00025	239.4
node72	0.00064	0.00021	203.68
node73	0.00118	0.00039	373.58
node74	0.00115	0.00038	361.84
node75	0.00115	0.00038	364.02
node76	0.0016	0.00053	506.79
node77	0.00076	0.00025	241.21

Table 6.1: Load data for Novena planning aread

From	To	R (p.u.)	X (p.u.)	Bsh (p.u.)	Smax (p.u.)
1	2	0.0183	0.0153	3.58998E-05	0.0578
2	10	0.0261	0.0369	8.66974E-05	0.0743
10	9	0.0077	0.0109	2.56139E-05	0.0743
9	7	0.0043	0.0061	1.44476E-05	0.0743
7	39	0.0151	0.0213	5.02001E-05	0.0743
39	47	0.0248	0.0351	8.24966E-05	0.0743
47	56	0.0297	0.042	9.88854E-05	0.0743
56	55	0.0196	0.0163	3.84434E-05	0.0578
55	62	0.0102	0.0085	1.99451E-05	0.0578
62	63	0.0189	0.0157	3.6975E-05	0.0578
63	64	0.0204	0.017	3.98816E-05	0.0578
64	34	0.0123	0.0102	2.40086E-05	0.0578
63	61	0.0219	0.0182	4.27918E-05	0.0578
1	6	0.0256	0.0362	8.51565E-05	0.0743
6	13	0.0222	0.0314	7.39243E-05	0.0743
13	60	0.0501	0.0709	0.000166713	0.0743
60	66	0.0063	0.0089	2.09833E-05	0.0743
66	36	0.0033	0.0047	1.10725E-05	0.0743
1	11	0.0872	0.0726	0.000170774	0.0578
11	14	0.0116	0.0164	3.85905E-05	0.0743
14	41	0.0355	0.0502	0.000118139	0.0743
41	68	0.0157	0.0131	3.07671E-05	0.0578
68	67	0.0124	0.0103	2.421E-05	0.0578
67	69	0.0132	0.011	2.58949E-05	0.0578
69	19	0.0164	0.0136	3.21066E-05	0.0578
19	17	0.0064	0.0053	1.25831E-05	0.0578
17	77	0.0227	0.0189	4.44008E-05	0.0578
77	76	0.0104	0.0087	2.04456E-05	0.0578
76	5	0.009	0.0075	1.75313E-05	0.0578
5	3	0.0114	0.0095	2.23262E-05	0.0578
3	28	0.0118	0.0098	2.30195E-05	0.0578
28	23	0.0187	0.0156	3.66254E-05	0.0578
76	74	0.0108	0.009	2.10687E-05	0.0578
23	24	0.012	0.01	2.34389E-05	0.0578
74	75	0.0113	0.0094	2.21951E-05	0.0578
24	20	0.0162	0.0135	3.17754E-05	0.0578
67	70	0.0069	0.0058	1.3594E-05	0.0578
75	4	0.0096	0.008	1.88011E-05	0.0578
20	31	0.0078	0.0065	1.5192E-05	0.0578
31	21	0.0201	0.0167	3.93895E-05	0.0578

1	12	0.0471	0.0666	0.000156636	0.0743
12	40	0.0151	0.0213	5.01238E-05	0.0743
40	58	0.034	0.048	0.000112916	0.0743
58	59	0.0128	0.0181	4.25728E-05	0.0743
59	32	0.0139	0.0197	4.63312E-05	0.0743
59	57	0.0129	0.0107	2.51893E-05	0.0578
32	73	0.0119	0.0099	2.32939E-05	0.0578
32	65	0.005	0.0041	9.73912E-06	0.0578
1	30	0.0407	0.0338	7.96134E-05	0.0578
30	8	0.0257	0.0364	8.56364E-05	0.0743
8	38	0.0184	0.026	6.11275E-05	0.0743
38	37	0.011	0.0156	3.66836E-05	0.0743
37	46	0.0066	0.0094	2.20662E-05	0.0743
46	45	0.0047	0.0066	1.55389E-05	0.0743
45	44	0.0073	0.0103	2.42731E-05	0.0743
44	42	0.0112	0.0158	3.72733E-05	0.0743
42	48	0.0134	0.019	4.46084E-05	0.0743
48	52	0.0187	0.0156	3.66558E-05	0.0578
52	35	0.0088	0.0073	1.72913E-05	0.0578
35	51	0.0021	0.0018	4.17594E-06	0.0578
51	50	0.0123	0.0103	2.417E-05	0.0578
50	49	0.0112	0.0094	2.19971E-05	0.0578
52	54	0.0116	0.0097	2.28033E-05	0.0578
44	43	0.0218	0.0181	4.26044E-05	0.0578
49	16	0.0187	0.0156	3.66511E-05	0.0578
50	53	0.0146	0.0122	2.86463E-05	0.0578
43	18	0.0254	0.0212	4.98311E-05	0.0578
1	33	0.1316	0.1095	0.000257636	0.0578
33	15	0.0264	0.022	5.17314E-05	0.0578
15	26	0.0303	0.0252	5.93881E-05	0.0578
26	25	0.0136	0.0113	2.66434E-05	0.0578
25	27	0.0125	0.0104	2.44002E-05	0.0578
27	22	0.0149	0.0124	2.9257E-05	0.0578
27	72	0.0139	0.0116	2.72641E-05	0.0578
22	29	0.0184	0.0153	3.59465E-05	0.0578
72	71	0.0108	0.009	2.11434E-05	0.0578

Table 6.2: Novena planning area results - line configuration & technical parameters

From	To	Cable Type	MVA	MW	MVar
1	2	3	0.0329	0.0313	0.0104
2	10	1	0.0319	0.0303	0.01
10	9	1	0.0308	0.0293	0.0097
9	7	1	0.0287	0.0273	0.009
7	39	1	0.0273	0.0259	0.0086
39	47	1	0.0265	0.0252	0.0083
47	56	1	0.0257	0.0244	0.008
56	55	3	0.0237	0.0225	0.0074
55	62	3	0.0217	0.0206	0.0068
62	63	3	0.0196	0.0186	0.0061
63	64	3	0.017	0.0161	0.0053
64	34	3	0.0159	0.0151	0.005
63	61	3	0.0013	0.0012	0.0004
1	6	1	0.0664	0.063	0.021
6	13	1	0.0643	0.061	0.0203
13	60	1	0.0623	0.0592	0.0195
60	66	1	0.0599	0.0569	0.0187
66	36	1	0.0577	0.0548	0.018
1	11	3	0.0306	0.0291	0.0096
11	14	1	0.0283	0.0269	0.0089
14	41	1	0.0268	0.0255	0.0084
41	68	3	0.0235	0.0224	0.0074
68	67	3	0.0213	0.0202	0.0067
67	69	3	0.0173	0.0164	0.0054
69	19	3	0.0148	0.014	0.0046
19	17	3	0.0141	0.0134	0.0044
17	77	3	0.0135	0.0129	0.0042
77	76	3	0.0127	0.0121	0.004
76	5	3	0.0072	0.0068	0.0022
5	3	3	0.0057	0.0054	0.0018
3	28	3	0.005	0.0047	0.0016
28	23	3	0.0039	0.0037	0.0012
76	74	3	0.0039	0.0037	0.0012
23	24	3	0.0032	0.0031	0.001
74	75	3	0.0027	0.0025	0.0008
24	20	3	0.0025	0.0024	0.0008
67	70	3	0.0019	0.0018	0.0006
75	4	3	0.0014	0.0014	0.0005
20	31	3	0.0014	0.0014	0.0004
31	21	3	0.0007	0.0007	0.0002

1	12	1	0.0533	0.0505	0.0168
12	40	1	0.0521	0.0495	0.0164
40	58	1	0.0513	0.0487	0.0161
58	59	1	0.0505	0.048	0.0158
59	32	1	0.047	0.0447	0.0147
59	57	3	0.0016	0.0015	0.0005
32	73	3	0.0012	0.0012	0.0004
32	65	3	0.001	0.0009	0.0003
1	30	3	0.0448	0.0425	0.0142
30	8	1	0.0436	0.0414	0.0138
8	38	1	0.0429	0.0407	0.0135
38	37	1	0.0421	0.04	0.0132
37	46	1	0.0413	0.0393	0.013
46	45	1	0.0404	0.0383	0.0127
45	44	1	0.0398	0.0378	0.0125
44	42	1	0.0375	0.0356	0.0118
42	48	1	0.0365	0.0347	0.0114
48	52	3	0.0326	0.0309	0.0102
52	35	3	0.0289	0.0275	0.009
35	51	3	0.0054	0.0051	0.0017
51	50	3	0.0044	0.0042	0.0014
50	49	3	0.003	0.0029	0.0009
52	54	3	0.002	0.0019	0.0006
44	43	3	0.0014	0.0013	0.0004
49	16	3	0.0011	0.0011	0.0003
50	53	3	0.0006	0.0006	0.0002
43	18	3	0.0006	0.0005	0.0002
1	33	3	0.0449	0.0426	0.014
33	15	3	0.0065	0.0062	0.002
15	26	3	0.0057	0.0054	0.0018
26	25	3	0.0049	0.0047	0.0015
25	27	3	0.0041	0.0039	0.0013
27	22	3	0.0016	0.0015	0.0005
27	72	3	0.0015	0.0014	0.0005
22	29	3	0.0008	0.0008	0.0003
72	71	3	0.0008	0.0008	0.0002

Table 6.3: Novena planning area - line type & power flow solution

Given that Singapore is a densely populated island, the distances between nodes are relatively short. In addition, the grid is completely built with underground cables. Consequently, there is no significant voltage drop in the feeders. However, it is worth

mentioning that the proposed distribution system planning approach is a relaxed AC conic power flow that does account for the voltage drops when the build decisions are made.

6.1.1 Validation of the synthetic distribution grid

To validate the distribution system grid developed, a Complex Network Theory metrics of real power systems are used. The metrics applied for the validation of the synthetic Singaporean distribution system are as follows

- Average Node Degree - is defined using the number of nodes N (order) and the number of edges M (size) for a specific sample. The average node degree is defined as
$$\frac{2M}{N}$$
- Characteristic Path Length - is the median of the length between any two nodes in the system.
- Normalized Characteristic Path Length - is defined as
$$\frac{CharactericPathLength}{AverageLineLength}$$
- Hop distance - is the number of edges along a path between two nodes.

The validation metrics and the expected values and characteristics are detailed in [33, 74], derived from real-world distribution systems.

The average node degree has been calculated for all the feeders in the system. Results are shown in Table **??**, which correspond to a radial topology.

Area	Feeder ID	No of Nodes	No of Lines	Average Node Degree
Tuas	1	65	64	1.969231
	2	58	57	1.965517
	3	26	25	1.923077
	4	33	32	1.939394
	5	48	47	1.958333
Bukit Panjang	6	113	112	1.982307
Tanglin	7	45	44	1.955556
Novena	8	77	76	1.974026
Toa Payoh	9	101	100	1.980198
Serangoon	10	120	119	1.983333
Sengkang	11	171	170	1.988304
Seletar	12	114	113	1.982456

Table 6.4: Average node degree of different feeders

The normalized characteristic path length of different planning areas is detailed in Table 6.5. The results are comparable to the real-world distribution grids detailed in [33, 74].

Area	Charac. Path Length (CPL)	Average Length	Normalized CPL
Bukit Panjang	3.6293	0.2216	16.3777
Tanglin	7.0154	0.5303	13.22912
Novena	4.5044	0.2872	15.68384
Toa Payoh	3.399	0.2514	13.52029
Serangoon	5.8148	0.303	19.19076
Sengkang	4.2997	0.1981	21.70469
Seletar	6.8349	0.3584	19.070592
Punggol	3.3516	0.1912	17.529289

Table 6.5: Normalized characteristic path length of selected planning areas

To validate the generated distribution synthetic grid based on the hop distance, the hop distances are represented using a histogram and fitted with a cumulative density function typical for similar real distribution systems. Examples of the fitted negative binomial cumulative density function on different planning areas are shown in Figures 6.3-6.7.

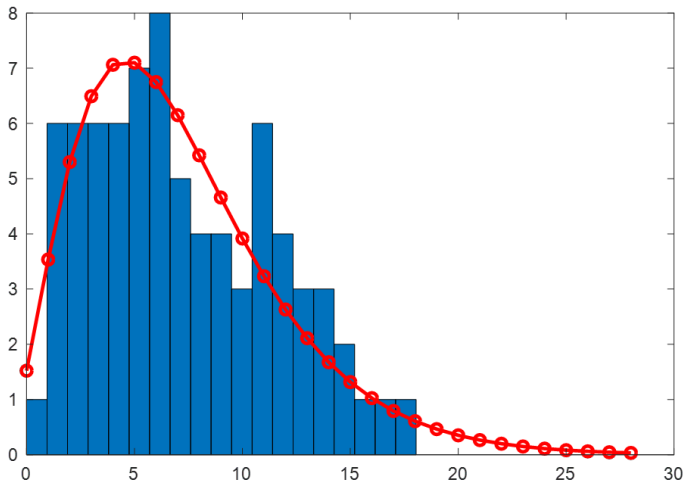

Figure 6.3: Negative binomial fit for the hop distances for Novena

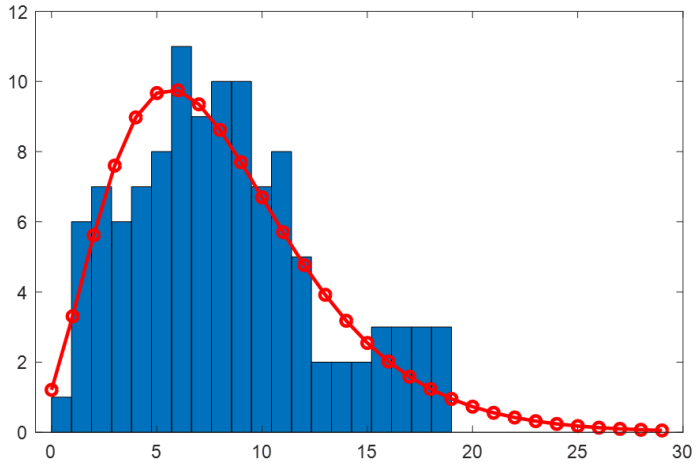

Figure 6.4: Negative binomial fit for the hop distances for Bukit Panjang

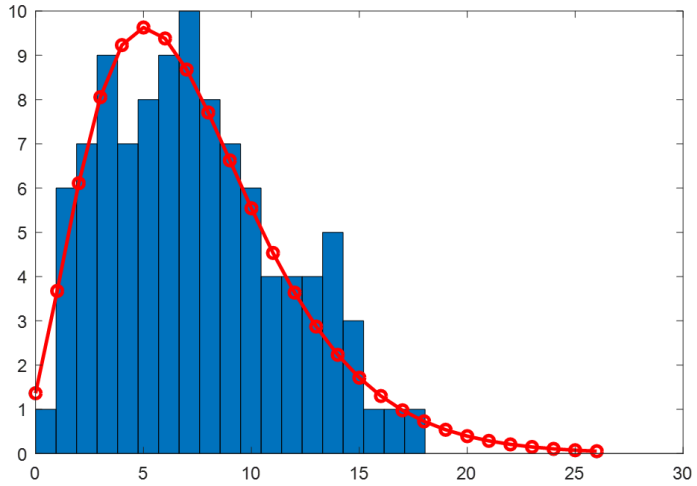

Figure 6.5: Negative binomial fit for the hop distances for Toa Payoh

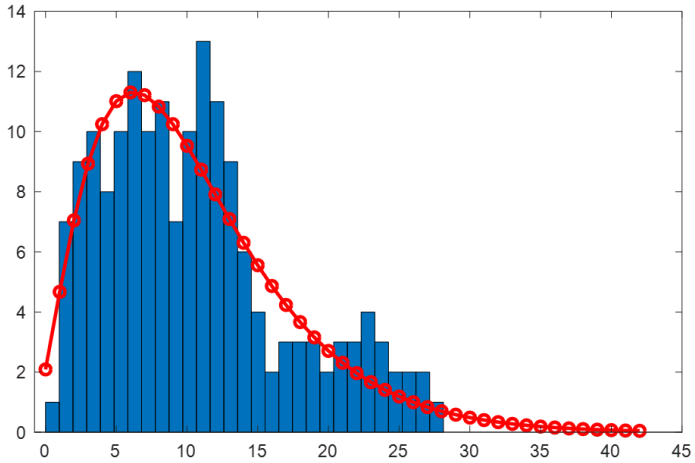

Figure 6.6: Negative binomial fit for the hop distances for Sengkang

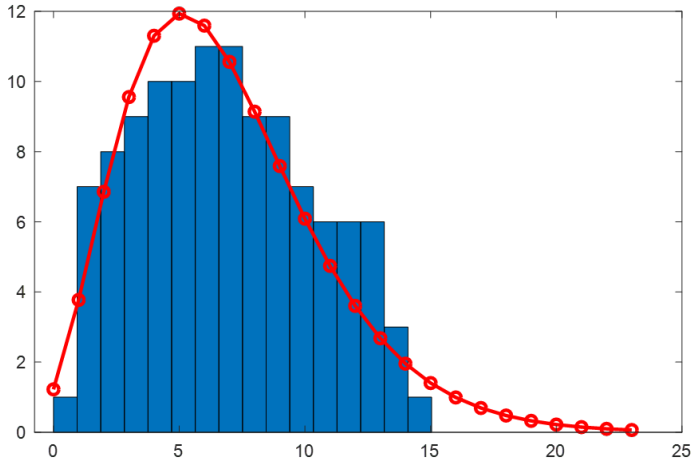

Figure 6.7: Negative binomial fit for the hop distances for Seletar

6.2 The 66 kV Sub-Transmission and 230 - 400 kV Transmission System

Following the generation of the synthetic distribution grid, the loads have been assigned to the sub-transmission substations and can be used as demand for the transmission system planning. Considering the segmentation of the system in a sub-transmission and a transmission voltage level, the transmission planning can be carried out as a separate optimization approach for each segment. However, an integrated transmission planning considering 66, 230 and 400 kV voltage levels will also provide a solution for the synthetic grid.

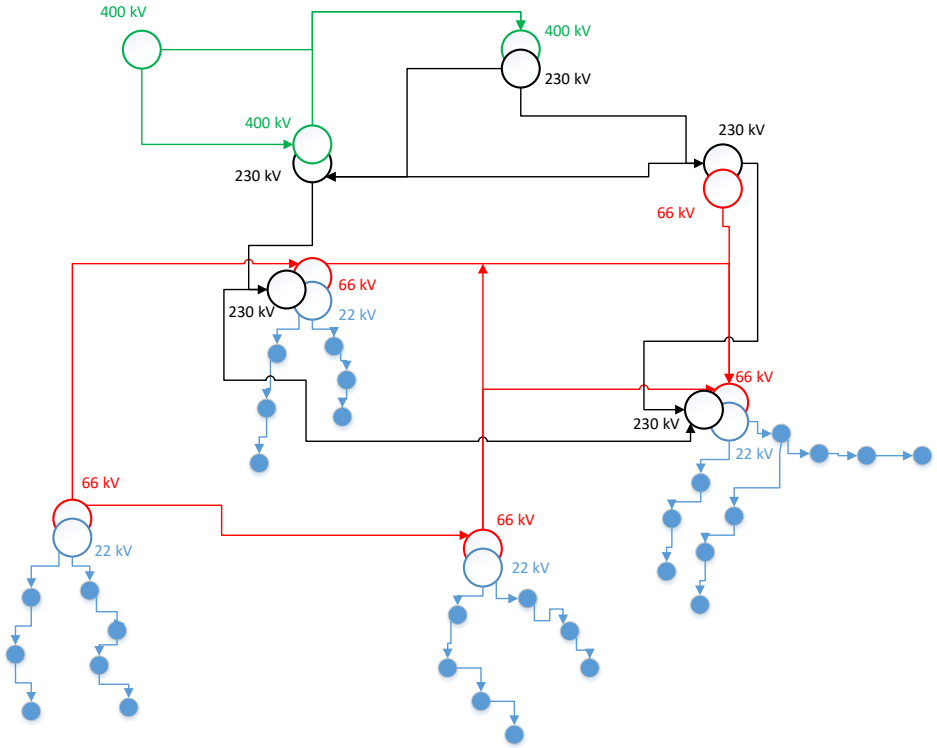

Figure 6.8: The structure of the Singaporean synthetic grid considering different voltage levels

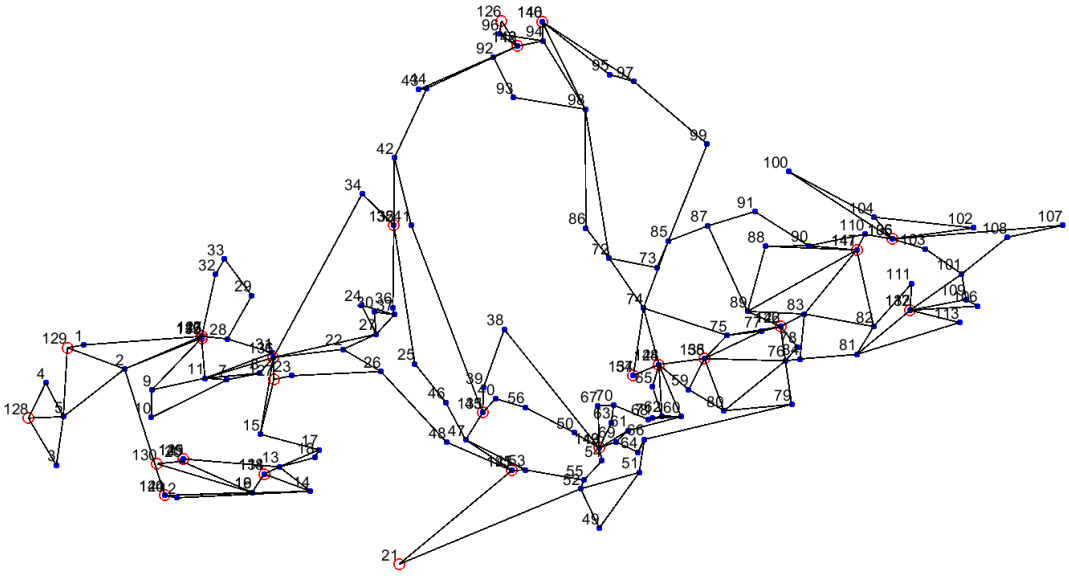

Figure 6.9: A plot of the 66 kV Singaporean synthetic sub-transmission grid

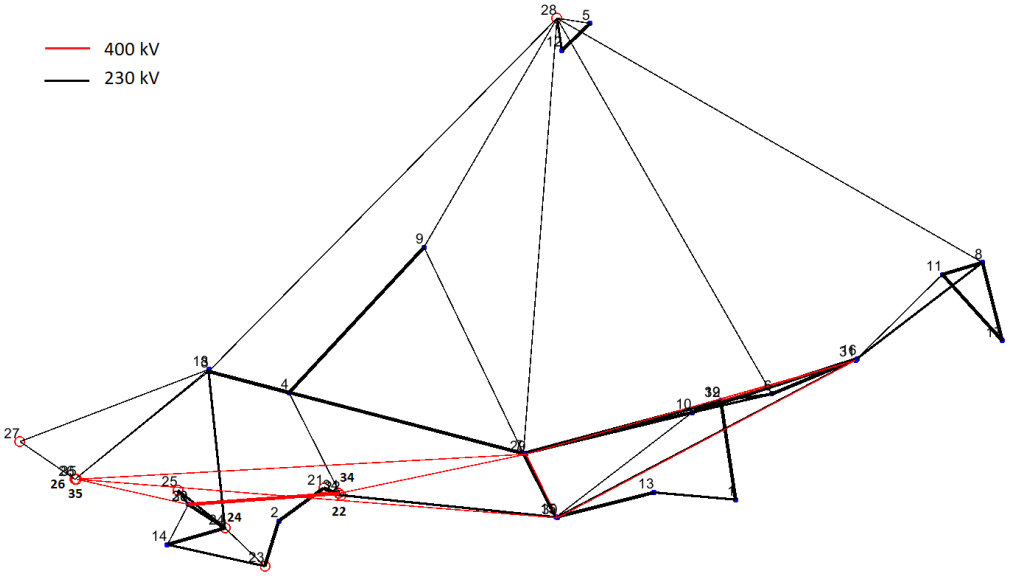

Figure 6.10: A plot of the 230 and 400 kV Singaporean synthetic transmission grid

The transmission planning approach will determine a mesh transmission network topology, the load allocation and generation levels of each generation, as well as the number of transformers installed at each substation respectively. The results of all the distribution, sub-transmission and the transmission system level combined together represent a synthetic grid of the Singaporean power system and can be used as an integrated system or segmented in the relevant voltage levels.

A representation of the structure of the Singaporean synthetic grid is given in Figure 6.8. Figure 6.9 details the 66kV sub-transmission system configuration, which is supplied by the 230 and 400 kV transmission system level shown in Figure 6.10. The 66 kV sub-transmission system is modeled to consider one line per corridor, while the 230 and 400 kV transmission system considers multiple lines per corridor. Therefore, it can be noticed that the thickness of the lines in 6.10 varies depending on the number of lines selected in the given corridor. Furthermore, the lines found and confirmed in the Singaporean system shown in 5.10 are included in the results with their respective sizing and technical parameters.

Although there are some small generating units assigned to the 66kV voltage level, the more relevant and bigger generators are found connected to the 230 and 400 kV voltage level.The complete data of the demand, the generators, the transformers, the shunt reactors and the system topology is detailed in the Appendix.

6.2.1 MATPOWER Power Flow analysis

To assess the technical viability of the developed sub-transmission and transmission synthetic grid, a power flow analysis is used. The power flow feasibility is analyzed on the integrated 66, 230 and 400 kV transmission system level using MATPOWER.

In addition to the loads, generation, voltage and line flows, what is evident about the Singaporean power system is the reactive branch charging injection due to the capacitive nature of a completely underground high voltage power system. To offset this phenomenon and obtain a feasible and operational power system, shunt reactors are placed at various locations around the system. This can be also observed in the power flow analysis as the total negative injection of the shunt.

The MATPOWER power flow analysis results are as follows

```
MATPOWER Version 6.0, AC Power Flow (Newton)

Converged in 0.02 seconds
================================================================================
|     System Summary                                                          |
================================================================================

How many?                How much?              P (MW)            Q (MVAr)
---------------------    -------------------  -------------  -----------------
Buses            165     Total Gen Capacity   13259.5        1145.5 to 2979.2
Generators        43     On-line Capacity      8236.3        1145.5 to 2979.2
Committed Gens    28     Generation (actual)   6886.2            1491.8
Loads            114     Load                  6820.0            2286.2
  Fixed          114       Fixed               6820.0            2286.2
  Dispatchable     0       Dispatchable          -0.0 of -0.0      -0.0
Shunts            23     Shunt (inj)           -0.0             -3901.4
Branches         367     Losses (I^2 * Z)       66.19             732.61
Transformers      51     Branch Charging (inj)     -             5428.4
Inter-ties        51     Total Inter-tie Flow  7364.4            2703.7
Areas              3

                         Minimum                      Maximum
                  -------------------------  -------------------------------
Voltage Magnitude   0.954 p.u. @ bus 73         1.003 p.u. @ bus 163
Voltage Angle      -6.83 deg   @ bus 87         0.48 deg   @ bus 164
P Losses (I^2*R)             -                 1.97 MW    @ line 158-136
Q Losses (I^2*X)             -                16.86 MVAr  @ line 146-122

================================================================================
|     Bus Data                                                                 |
================================================================================
 Bus      Voltage          Generation             Load
  #   Mag(pu) Ang(deg)   P (MW)   Q (MVAr)   P (MW)   Q (MVAr)
----- ------- --------  --------  --------  --------  --------
    1  0.981   -4.643       -         -      116.36     38.75
    2  0.983   -4.401       -         -      135.60     45.08
```

3	0.982	-4.884	-	-	69.58	23.33
4	0.983	-4.795	-	-	48.53	16.11
5	0.983	-4.745	-	-	58.11	19.46
6	0.982	-4.282	-	-	12.10	3.98
7	0.981	-4.401	-	-	13.22	4.35
8	0.981	-4.341	-	-	12.39	4.08
9	0.980	-4.457	-	-	59.26	19.79
10	0.979	-4.556	-	-	51.86	17.42
11	0.981	-4.368	-	-	57.70	19.32
12	0.994	-3.256	-	-	60.00	21.28
13	0.990	-3.654	-	-	60.00	21.64
14	0.991	-3.540	-	-	60.00	21.21
15	0.983	-4.280	-	-	60.00	21.63
16	0.996	-3.091	-	-	60.00	21.62
17	0.986	-4.000	-	-	60.00	21.60
18	0.986	-3.989	-	-	60.00	21.63
19	0.996	-3.091	-	-	60.00	20.01
20	1.000	-2.727	-	-	60.00	20.14
21	0.986	-3.984	122.69	56.44	15.10	5.17
22	0.975	-4.905	-	-	51.38	17.24
23	0.981	-4.418	-	-	35.97	11.99
24	0.971	-5.153	-	-	18.97	6.29
25	0.967	-5.228	-	-	74.24	24.80
26	0.975	-4.901	-	-	74.22	24.53
27	0.972	-5.067	-	-	22.60	7.47
28	0.984	-4.092	-	-	29.33	9.69
29	0.984	-4.206	-	-	20.38	6.72
30	0.969	-5.262	-	-	50.09	17.14
31	0.982	-4.307	-	-	46.71	15.64
32	0.984	-4.208	-	-	39.62	13.23
33	0.983	-4.224	-	-	13.12	4.34
34	0.969	-4.724	-	-	66.73	22.20
35	0.970	-4.475	-	-	57.46	19.18
36	0.969	-5.136	-	-	48.76	16.39
37	0.969	-5.177	-	-	36.55	12.21
38	0.969	-5.315	-	-	60.84	20.58
39	0.970	-5.051	-	-	28.23	9.40
40	0.971	-4.934	-	-	14.98	5.09
41	0.962	-5.423	-	-	52.22	17.29
42	0.962	-5.299	-	-	126.60	42.34
43	0.961	-5.073	-	-	78.87	26.52
44	0.961	-5.072	-	-	53.66	18.11
45	0.971	-4.852	-	-	46.19	15.47
46	0.969	-5.109	-	-	24.88	8.29

47	0.973	-4.840	-	-	37.39	12.50
48	0.975	-4.756	-	-	17.16	5.67
49	0.974	-5.074	-	-	12.79	4.65
50	0.974	-4.984	-	-	38.99	13.00
51	0.973	-5.140	-	-	11.84	4.27
52	0.975	-4.932	-	-	23.40	8.10
53	0.975	-4.730	-	-	40.25	13.42
54	0.975	-4.932	-	-	41.91	13.95
55	0.975	-4.908	-	-	12.65	4.20
56	0.972	-5.089	-	-	46.93	16.05
57	0.972	-5.106	-	-	77.85	25.99
58	0.969	-5.366	-	-	129.77	43.05
59	0.967	-5.566	-	-	71.49	23.74
60	0.969	-5.446	-	-	137.34	45.89
61	0.974	-5.057	-	-	33.72	11.31
62	0.969	-5.389	-	-	63.18	21.07
63	0.973	-5.154	-	-	37.60	12.44
64	0.971	-5.303	-	-	15.38	5.56
65	0.970	-5.262	-	-	70.40	23.34
66	0.969	-5.516	-	-	25.50	8.61
67	0.972	-5.200	-	-	54.07	18.26
68	0.969	-5.421	-	-	35.47	11.85
69	0.974	-5.026	-	-	11.42	3.78
70	0.971	-5.285	-	-	43.41	14.46
71	0.969	-5.456	-	-	35.51	11.92
72	0.956	-6.480	-	-	71.00	23.68
73	0.954	-6.748	-	-	60.48	20.07
74	0.961	-6.120	-	-	50.60	16.76
75	0.958	-6.378	-	-	262.17	87.80
76	0.957	-6.538	-	-	142.25	47.15
77	0.959	-6.216	-	-	129.86	43.11
78	0.957	-6.523	-	-	70.78	23.48
79	0.956	-6.783	-	-	202.80	67.43
80	0.960	-6.259	-	-	67.04	22.52
81	0.962	-6.410	-	-	64.07	21.35
82	0.963	-6.247	-	-	43.74	14.55
83	0.960	-6.356	-	-	134.73	44.58
84	0.957	-6.644	-	-	202.24	67.26
85	0.955	-6.752	-	-	70.03	23.35
86	0.955	-6.393	-	-	73.67	24.51
87	0.955	-6.831	-	-	59.72	20.10
88	0.959	-6.643	-	-	185.86	61.91
89	0.958	-6.529	-	-	184.62	61.31
90	0.964	-6.210	-	-	28.75	9.61

91	0.956	-6.827	-	-	69.66	23.18
92	0.966	-4.459	-	-	61.36	20.48
93	0.964	-4.820	-	-	37.28	12.35
94	0.966	-4.562	-	-	112.91	37.42
95	0.963	-5.327	-	-	49.84	16.73
96	0.966	-4.450	-	-	134.97	44.74
97	0.962	-5.441	-	-	63.62	21.15
98	0.962	-5.309	-	-	65.24	21.92
99	0.954	-6.549	-	-	83.79	28.33
100	0.970	-5.970	-	-	58.19	19.30
101	0.971	-5.864	-	-	29.56	9.81
102	0.970	-5.890	-	-	61.03	20.19
103	0.972	-5.713	-	-	29.55	9.78
104	0.971	-5.797	-	-	27.30	9.01
105	0.974	-5.473	-	-	12.63	4.16
106	0.969	-6.055	-	-	63.78	21.08
107	0.970	-6.016	-	-	11.66	3.86
108	0.969	-6.099	-	-	37.54	12.77
109	0.970	-5.874	-	-	14.72	4.90
110	0.970	-5.692	-	-	54.63	18.12
111	0.967	-6.064	-	-	40.21	13.36
112	0.972	-5.681	-	-	54.63	18.19
113	0.965	-6.203	-	-	44.84	14.82
114	0.995	-3.074	-	-	-	-
115	0.984	-4.014	-	-	-	-
116	0.972	-4.341	-	-	-	-
117	0.971	-5.514	-	-	-	-
118	0.967	-4.230	-	-	-	-
119	0.976	-4.822	-	-	-	-
120	0.995	-3.144	-	-	-	-
121	0.976	-4.560	-	-	-	-
122	0.960	-6.056	-	-	-	-
123	0.986	-3.889	-	-	-	-
124	0.971	-5.064	-	-	-	-
125	1.000	-2.704	-	-	-	-
126	0.967	-4.337	52.80	24.29	-	-
127	0.983	-4.188	172.80	79.49	-	-
128	0.985	-4.613	126.72	58.29	-	-
129	0.983	-4.539	45.89	21.11	-	-
130	1.001	-2.607	128.16	58.95	-	-
150	0.991	-1.122	-	-	8.79	3.17
138	0.999	0.253	-	-	-	-
139	0.995	-0.230	-	-	-	-
131	0.996	-0.259	-	-	-	-

140	0.996	-0.143	-	-	-	-
135	0.990	-1.240	-	-	-	-
133	0.993	-0.809	-	-	-	-
136	0.987	-1.645	-	-	-	-
132	0.995	-0.474	-	-	-	-
134	0.991	-1.182	-	-	-	-
141	0.986	-1.678	-	-	-	-
142	0.997	-0.139	-	-	-	-
143	0.991	-1.020	-	-	-	-
144	1.000	0.309	-	-	-	-
145	0.992	-0.862	-	-	-	-
146	0.989	-1.386	-	-	-	-
137	0.986	-1.749	-	-	-	-
147	0.994	-0.080	-	-	-	-
148	0.991	-1.167	-	-	-	-
149	1.000	0.343	-	-	-	-
151	0.999	0.198	258.48	34.46	-	-
152	0.998	0.132	633.47	72.48	-	-
153	0.999	0.299	290.51	40.84	-	-
154	1.000	0.323	220.00	34.69	-	-
155	1.000	0.370	696.15	102.73	-	-
156	0.996	0.424	571.65	102.33	-	-
157	0.996	0.407	293.27	78.22	-	-
158	0.998	0.000*	2103.96	512.90	-	-
159	0.999	0.060	-	-	-	-
160	0.999	0.017	-	-	-	-
161	0.996	-0.251	-	-	-	-
162	0.994	-0.336	-	-	-	-
163	1.003	0.471	-	-	-	-
164	1.002	0.479	522.29	100.16	-	-
165	1.002	0.474	647.34	114.41	-	-
			--------	--------	--------	--------
		Total:	6886.18	1491.80	6819.99	2286.19

The complete power flow results including the branch flow data are given in the Appendix with the complete transmission synthetic model.

6.2.2 Validation of the synthetic transmission grid

Similarly to the validation approach of the distribution grid, the transmission grid is validated using the complex network theory statistical parameters discussed in [39]. To validate the higher voltage system levels with mesh network configuration, Delaunay triangulation is used. An example of delaunay triangulation with set of five points is shown on Figure 6.11, detailed in [39].

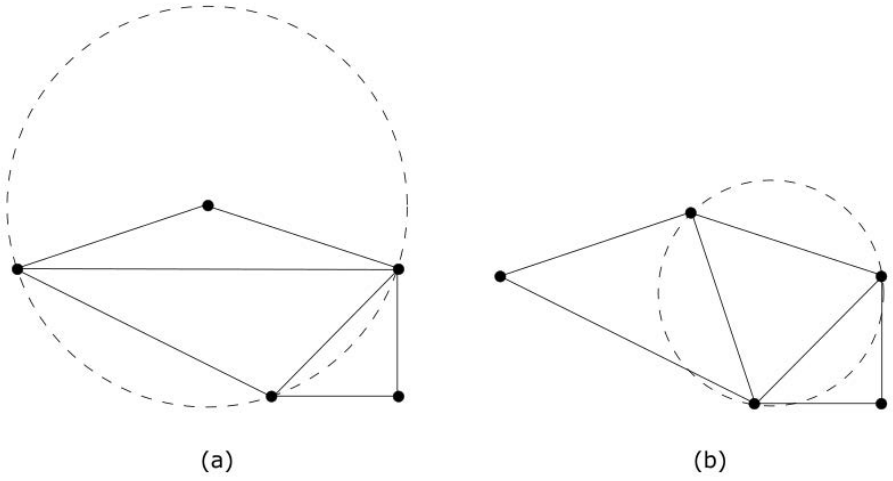

Figure 6.11: Triangulation of a set of 5 points. (a) is not the Delaunay triangulation, because at least one triangle's circumcircle contains another point. (b) is the Delaunay triangulation of these points.

The set of line candidates includes 1^{st}, 2^{nd} and 3^{rd} delaunay triangulation neighbors. Following the analysis of real power system, the targets in percentages are introduced as relaxed constraints in the model definition in Section 4.2.3. The constraints are limiting the selection of the number of each delaunay set of neighbors to meet the percentage target of the total number of lines in the system. The percentage targets for each delaunay set out of the total number of selected lines are defined as follows

$$\begin{aligned} Delaunay\, 1^{st} \quad & 74 \sim 80\% \\ Delaunay\, 2^{nd} \quad & 18 \sim 22\% \\ Delaunay\, 3^{rd} \quad & 2 \sim 4\% \end{aligned}$$

To illustrate the application of this approach for validation of the synthetic grid, the sub-transmission network shown in Figure 6.9 consists of

$$\begin{aligned} 77.2\% \quad & Delaunay\, 1^{st}\ neighbors \\ 18.5\% \quad & Delaunay\, 2^{nd}\ neighbors \\ 3.9\% \quad & Delaunay\, 3^{rd}\ neighbors. \end{aligned}$$

The use of delaunay triangulation neighboring targets for the network topology together with the feasible power flow analysis results conclude the validation process of the synthetic transmission system.

The complete sub-transmission and transmission system topology, including the generating units and the power flow results are given in the Annex.

7 Application for Distribution Network Expansion Planning with Li-ion BESS

To demonstrate the importance and usefulness of having realistic synthetic grid models for developing, testing and analyzing the potential benefits of new concepts for the ongoing grid modernization, this chapter defines a case study of a novel DSEP method. A hybrid optimization approach of a GA with a deterministic sub-optimization to account for both line and BESS expansion planning is proposed. The test case is defined using the framework proposed in this thesis, and the results are presented and analyzed to evaluate the DSEP method.

In this chapter, a slightly modified content of 'A Hybrid Optimization Method for Distribution System Expansion Planning with Lithium-ion Battery Energy Storage Systems' published in the proceedings of 2020 IEEE Sustainable Power and Energy Conference (iSPEC) is reproduced [6].

7.1 Introduction

The technological advancements in mobility electrification, driven by a strong holistic policy support, are significantly expanding the EV deployment. The industry and governments have committed to electrifying the public transportation and incentivizing the private and commercial vehicles electrification [124]. Such widespread adoption of EVs will change the traditional load curve and pose a challenge for the existing grid infrastructure.

For instance, Singapore has a goal of a 100% cleaner energy public bus fleet by 2040 [23]. While the annual energy demand can be considered trivial with less than 1.5% of the total electricity consumption, certain locations and time periods of high charging demand require a substantial increase in the distribution grid capacity [22]. The spare power capacity at bus depots and bus interchanges is often insufficient, particularly when 450 kW fast chargers are considered. To ensure the grid's capability to handle the demand and maintain the reliability and continuity of supply without causing excessive electricity tariffs, it is a necessity for the planning engineers to use economically viable expansion planning strategies.

Traditionally, distribution system planning is accomplished by determining the most economical solution for the placement and sizing of the distribution assets such as feeders and/or substations. The economic objectives are often the sum of fixed investment costs and variable costs, as detailed in Chapter 3. The investment costs of adding, reinforcing or replacing lines, transformers, switchgear and substations are considered as fixed costs,

whereas the variable costs are dependent on parameters such as the power losses, reliability, operation and maintenance [45]. However, due to the widespread deployment and availability of distributed energy resources (DERs) and the deregulation of electricity markets, the traditional passive distribution systems are subjected to become active. Therefore, the use of traditional planning methods is no longer conclusive and some of the drawbacks include unnecessary and costly distribution grid reinforcements, increasing network losses, and unattainable development and environmental targets [125].

Numerous of the recent DSP methods consider the allocation and sizing of DG and ESS. Furthermore, ESS are seen as an enabling technology that can save consumers money, improve reliability and resilience, help reduce environmental impacts and integrate highly variable and intermittent renewable DG such as solar and wind. Some of the benefits offered by the ESS are load leveling, curtailing operations by storing surplus energy, storing low-cost energy to be used during peak periods at higher rates, voltage support, emergency black start, frequency regulation and spinning reserve services.

Due to the cost competitiveness of some ESS technologies, distribution system expansion can also be deferred and investments reduced. In particular, the price of LIB fell 87% since 2010, making BESS a viable tool for the modern distribution system. To take the full advantage of installing BESS, it is essential to ensure optimal placement and capacity. Oversizing the BESS may lead to higher costs, which may disadvantage the commercial deployment. Similarly, an inadequate number and location of BESS may cause an additional burden to the utilities due to the high initial investment cost [126].

The implementation of ESS in the power system network has been studied widely in the literature considering a plethora of applications. In [127], optimal asset expansion in distribution systems with nonlinear battery characteristics is explored. The work considers the effect of cycling due to the charging-discharging operation of the LIB storage and minimizes the net asset expansion cost comprising of generation costs and BESS installation costs. In [128], a MIP optimization is used to solve the DSEP problem with distributed ESS on an IEEE 33-bus system. The ESS helps in shaving the peak load demand, resulting in savings from the peak load curtailment and the deferred installation of new lines.

The cost of assets such as feeders, transformers and BESS with their replacements, operation and maintenance as well as customer interruption costs are studied in a more holistic approach in [129]. The optimization problem is solved using interior point method in MATLAB's OPTI Toolbox. The solution provides the installation plan of new lines and/or BESS depending on the amount of energy arbitrage for the storage.

The optimal deployment of BESS with the intent to defer expansion is explored in [130]. The work proffers that in addition to the the optimal sizing of BESS, economic benefits can be maximized using a deferral period subject to conditions such as annual rate of load increase and cost per unit length of feeders. The authors in [131] propose a two stage methodology to optimally place and size BESS for grid-supporting activities such as voltage support and minimizing total network losses. A GA is used to prepare the BESS optimal sizing and placement. In the second stage, the placement and sizing of the BESS are evaluated using an AC OPF via DIgSILENT PowerFactory program-

ming, solving the grid management for the integration of renewables, peak shaving and emergency backup challenges.

The study in [132] proposed a hybrid method to optimally integrate ESS devices in the smart grid. GA is used to allocate the BESS and capacitors to adequate nodes, before a sub-optimization estimates the optimal daily charge/discharge cycle, along with the DG and BESS reactive power supply. The sub-optimization is defined using an OPF for all time intervals of the day. With conditions such as price incentives on using BESS, the installation of ESS has proven beneficial and economically viable in terms of both system operation and expansion planning deferral.

In this chapter, a DSEP model for placement and sizing of BESS combined with new line installation or existing line reinforcement is introduced. The proposed model is characterized by a hybrid approach using a GA with a deterministic MIQCP sub-optimization. A relaxed AC second order conic power flow discussed in 3.1.3.1 is used to assure that the electrical constraints such as voltage and current limits are satisfied.

7.2 Model Definition and Implementation

The objective of the proposed model is to provide a cost effective solution for the modern grid expansion problem considering both lines and BESS placement and sizing. The problem definition is of highly complex nature, including a non-linear, mixed integer, constrained optimization problem with a high number of binary decision variables and a cost minimization function subjected to numerous equality and inequality constraints, such as an AC power flow, voltage and current limits and BESS operating and capacity limits.

To efficiently solve the expansion planning definition, a hybrid optimization approach using a GA and a MIQCP is used. The primary optimization of the hybrid model is defined as a GA to determine the selection of new lines and/or the reinforcement of existing lines combined with the placement of the BESS. The new line configuration and the BESS node allocation are then assigned to the MIQCP sub-optimization to obtain an optimal BESS sizing considering the AC power flow feasibility of the solution. The results obtained from the MIQCP sub-optimization are then evaluated within the GA using the fitness function, and the solution of the new/reinforced line configuration and the BESS placement and sizing is improved until a convergence is reached.

The combination of a GA and a MIQCP is preferred as a way to employ their capabilities and compensate for the deficiencies. Studies for power system planning and optimal ESS allocation demonstrated that GA is a suitable tool capable of solving complex systems [125, 126]. However, GA has shown some inadequacy in solving planning problems for a longer time horizon due to a substantial computational burden. Therefore, a MIQCP has been employed to solve the BESS sizing problem to optimality as a sub-optimization problem. Furthermore, selecting the line configuration and allocating the BESS within the GA significantly reduces the complexity of the MICQP optimization.

7.2.1 Expansion Planning Model Definition

To define the DSEP model, the following squared variables are introduced as follows

$$v_{i,t} = V_{i,t}^2 \qquad \text{and} \qquad \ell_{ij,t} = I_{ij,t}^2$$

The cost minimization objective function of the total investment cost of the grid expansion, including new lines and BESS is defined as follows

$$\text{minimize} \qquad \lambda = \lambda_1 + \lambda_2 \tag{7.1}$$

subject to

$$\omega_1 = AF^{lines} \cdot \sum_{i,j \in \Omega_l} L_{ij} \cdot 2 \cdot \Psi_{ij}^{line} \cdot \alpha_{ij} \tag{7.2}$$

$$AF^{lines} = \frac{u \cdot (1+u)^{t^{line}}}{(1+u)^{t^{line}} - 1} \tag{7.3}$$

$$\omega_2 = AF^{BESS} \cdot \sum_{i \in \Omega_n} \{\Psi^P \cdot P_i + \Psi^E \cdot E_i\} \cdot \beta_i \tag{7.4}$$

$$AF^{BESS} = \frac{u \cdot (1+u)^{t^{BESS}}}{(1+u)^{t^{line}} - 1} \tag{7.5}$$

The investment cost for installation of new lines or cables given in (7.2) is similarly defined as in section 3.1. It is calculated as the product of the length of the line, the unit cost of the selected cable and a binary decision variable which determines if a line is selected. Since the installation costs of a line with underground cables can amount to 50% of the total cost of the line, the cost of the cable is multiplied by a factor of two [79]. Equation (7.4) determines the investment cost for the installation of BESS. Since the BESS has a power converter unit and an energy storage unit, the total cost is decomposed into a product of the power cost coefficient and the power rating of the BESS. The product of the energy cost coefficient and the energy rating of the BESS are summed based on the installation status defined by the binary decision variable β_i.

Due to the very different lifetime expectancy of a line when compared to a BESS, the cost objectives λ_1 and λ_2 are equally weighted by using the annual equivalent-worth criterion, described in section 3.1 and detailed in [80]. Therefore, λ_1 and λ_2 are calculated as the equivalent uniform annual worth investment costs of lines and BESS by using the capital recovery factors defined with (7.3) and (7.5) respectively.

To satisfy the electrical grid constraints, a relaxed conic AC power flow detailed in section 3.1.3.1 is used. The objective function is subjected to

$$\sum_{(j,i) \in \Omega_l} P_{ji,t} - \sum_{(i,j) \in \Omega_l} P_{ij,t} - \sum_{(i,j) \in \Omega_l} R_{ij} \cdot \ell_{ij,t} + P_{i,t}^g + P_{i,t}^{dis} = P_{i,t}^d + P_{i,t}^{ch} \qquad \forall i \in \Omega_n, \forall t \in \Omega_T \tag{7.6}$$

$$\sum_{(j,i)\in\Omega_l} Q_{ji,t} - \sum_{(i,j)\in\Omega_l} Q_{ij,t} - \sum_{(i,j)\in\Omega_l} X_{ij,t}\cdot \ell_{ij,t} + Q^g_{i,t} = Q^d_{i,t} \qquad \forall i \in \Omega_n, \forall t \in \Omega_T \; (7.7)$$

$$\upsilon_{i,t} - \upsilon_{j,t} = \rho_{ij,t} + 2R_{ij}P_{ij,t} + 2X_{ij}Q_{ij,t} + Z^2_{i,j}\cdot \ell_{ij,t} \qquad \forall (i,j) \in \Omega_l, \forall t \in \Omega_T \; (7.8)$$

$$|\rho_{ij,t}| \leq \left((V^{max})^2 - (V^{min})^2\right)\cdot(1-\alpha_{ij}) \qquad \forall (i,j) \in \Omega_l, \forall t \in \Omega_T \; (7.9)$$

$$\upsilon_{j,t}\cdot \ell_{ij,t} \geq P^2_{ij,t} + Q^2_{ij,t}, \quad P_{ij,t} \geq 0 \qquad \forall (i,j) \in \Omega_l, \forall t \in \Omega_T \; (7.10)$$

$$|P_{ij,t}| \leq P^{max}_{ij}\cdot \alpha_{ij} \qquad \forall (i,j) \in \Omega_l, \forall t \in \Omega_T \; (7.11)$$

$$|Q_{ij,t}| \leq Q^{max}_{ij}\cdot \alpha_{ij} \qquad \forall (i,j) \in \Omega_l, \forall t \in \Omega_T \; (7.12)$$

$$0 \leq \ell_{ij,t} \leq (I^{max}_{ij})^2\cdot \alpha_{ij} \qquad \forall (i,j) \in \Omega_l, \forall t \in \Omega_T \; (7.13)$$

$$(V^{min})^2 \leq \upsilon_{i,t} \leq (V^{max})^2 \qquad \forall i \in \Omega_n, \forall t \in \Omega_T \; (7.14)$$

$$P^{gmin} \leq P_{i,t} \leq P^{gmax} \qquad \forall i \in \Omega_n, \forall t \in \Omega_T \; (7.15)$$

$$Q^{gmin} \leq Q_{i,t} \leq Q^{gmax} \qquad \forall i \in \Omega_n, \forall t \in \Omega_T \; (7.16)$$

Equations (7.6) and (7.7) define the active and the reactive power balance equalities to ensure that the generation and the BESS capacity corresponds to the consumer demand. The charging and discharging cycles of the BESS are expressed only in terms of active power for the purpose of simplification, as denoted in (7.6). The voltage drop is calculated with (7.7), while the auxiliary variable $\rho_{ij,t}$ constrained in (7.8) ensures that the voltage drop between two nodes is considered only if a line exist. Equation (7.10) calculates the power flow using a relaxed AC second order conic power flow model, the problem can be solved in polynomial time by interior point methods such that an optimally convergent solutions is obtained [133]. Equations (7.11) - (7.13) are used to set the operating power flow limits of a line. The node voltage limits are found in (7.14), while the generation limits are defined with (7.15) and (7.16).

The BESS model definition for optimal battery sizing and operation is defined as follows

$$SOC_{i,t} = SOC_{i,(t-1)} - \frac{P^{dis}_{i,t}}{\eta_D} + P^{ch}_{i,t}\cdot \eta_C \qquad \forall i \in \Omega_S, \forall t \in \Omega_T \; (7.17)$$

$$E^{min}_{Storage} \leq SOC_{i,t} \leq E_i \leq E^{max}_{Storage} \qquad \forall i \in \Omega_S, \forall t \in \Omega_T \; (7.18)$$

$$0 \leq P_{i,t}^{ch} \cdot \eta_C \leq P_i \cdot \omega_{i,t}^{ch} \qquad \forall i \in \Omega_S, \forall t \in \Omega_T \quad (7.19)$$

$$0 \leq \frac{P_{i,t}^{dis}}{\eta_D} \leq P_i \cdot (1 - \omega_{i,t}^{ch}) \qquad \forall i \in \Omega_S, \forall t \in \Omega_T \quad (7.20)$$

$$P_{Storage}^{min} \leq P_i \leq P_{Storage}^{max} \qquad \forall i \in \Omega_S \quad (7.21)$$

Equation (7.17) is an equality constraint that measures the energy State of Charge (SOC) of the storage unit at time t of the system at node i. The SOC directly correlates to the charge stored in the previous state at time $(t-1)$ and the net power added during a charging cycle or released through a discharging cycle. Equation (7.18) defines the bounds for the SOC of the BESS such that it does not drop below the minimum SOC required to maintain the battery, or the maximum SOC which is limited by the space constraints for the BESS location. Furthermore, (7.18) constrains the decision variable E_i which characterizes the energy capacity of the BESS and determines the BESS cost as part of the objective function. The power flow from the converter during charging and discharging cycles is detailed with (7.19) and (7.20). The binary variable $\omega_{i,t}^{ch}$ takes the value of 1 to control the power flow during the charging cycle and is assigned a value of zero during the discharging cycle. Equation 7.21 restricts the power flow from the converters within the defined limits.

$$0 \leq P_{i,t}^{ch} \cdot \eta_C \leq \gamma_{i,t} \qquad \forall i \in \Omega_S, \forall t \in \Omega_T \, (7.22)$$

$$0 \leq \frac{P_{i,t}^{dis}}{\eta_D} \leq P_i - \gamma_{i,t} \qquad \forall i \in \Omega_S, \forall t \in \Omega_T (7.23)$$

$$0 \leq \gamma_{i,t} \leq P_{Storage}^{max} \cdot \omega_{i,t}^{ch} \qquad \forall i \in \Omega_S, \forall t \in \Omega_T (7.24)$$

$$0 \leq P_i - \gamma_{i,t} \leq P_{Storage}^{max} \cdot (1 - \omega_{i,t}^{ch}) \qquad \forall i \in \Omega_S, \forall t \in \Omega_T (7.25)$$

However, the BESS model defined in (7.17) - (7.21) represents a nonlinear model difficult to optimally solve. Therefore, an auxiliary variable $\gamma_{i,t}$ is used in (7.22) - (7.25) to linearize the power flow model of the converter detailed in (7.19) and (7.20). Consequently, a MIQCP formulation that provides an optimal configuration of new lines and BESS placement and sizing with AC power flow feasibility can be defined with (7.1) - (7.18), and (7.22) - (7.25). The proposed model is a very complex model, difficult to solve with the current computational capabilities. Hence, a hybrid optimization approach of a genetic algorithm and a MIQCP is proposed.

7.2.2 Solution Method

The investment cost evaluation of the grid expansion plan solution within the genetic algorithm is defined using a fitness function detailed in (7.1)-(7.5). The GA initiates by creating a set of individuals representing the lines and the BESS candidates to form a population. The line and BESS individuals are characterized by genes joined into a string to define the chromosomes which act as potential solutions. Each gene within the chromosome represents a binary decision variable defined with α_{ij} and β_i, where a new line or a BESS unit is selected as shown in Fig. 7.1. However, a chromosome with a new line configuration and BESS allocation is not sufficient to evaluate the fitness function (7.1) since the BESS energy and power capacity required in (7.4) are unknown.

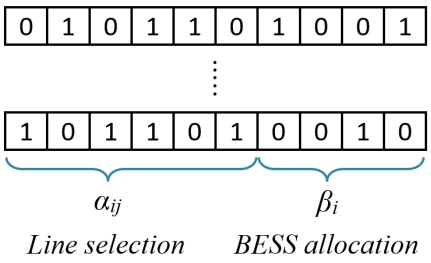

Figure 7.1: An example of GA chromosomes in a population

To obtain the required BESS capital costs and sizing, a MIQCP sub-optimization is defined. The MIQCP formulation provides an optimal BESS sizing and operation by considering the power flow feasibility constraints of the system. The line configuration is fixed to include the newly selected lines assigned as a candidate solution in the GA, while the BESS allocation taken as an input from the GA is specified as a set of nodes with BESS Ω_S. Equation (7.4) is used as an objective function to consider a cost minimization of the BESS installation based on the power and energy capacity decision variables and is subjected to the constraints defined with (7.6) - (7.18), and (7.22) - (7.25).

The power flow feasibility of the candidate solution is tested and the BESS power and energy capacity are optimally sized at each selected node based on an hourly charge-discharge cycle. Once the MIQCP sub-optimization provides a solution, the GA proceeds with the fitness function evaluation only if the power flow constraints are proven feasible and a solution exists. On the contrary, the fitness function of the particular candidate solution is penalized by being assigned a very high value.

Subsequently, the GA calculates the fitness value for all candidate solutions in the population using an iterative process. The fitness score of each individual is evaluated and the fittest individuals are selected for the reproduction process. A crossover point is chosen at random from within the genes and certain new offspring added to the population are subjected to a mutation with a low random probability. As the algorithm progresses, the GA keeps improving the solution by changing the individuals and creating new line configurations and BESS allocation and sizing. Once the offspring are not significantly different from the previous generation and it is realized that the solution

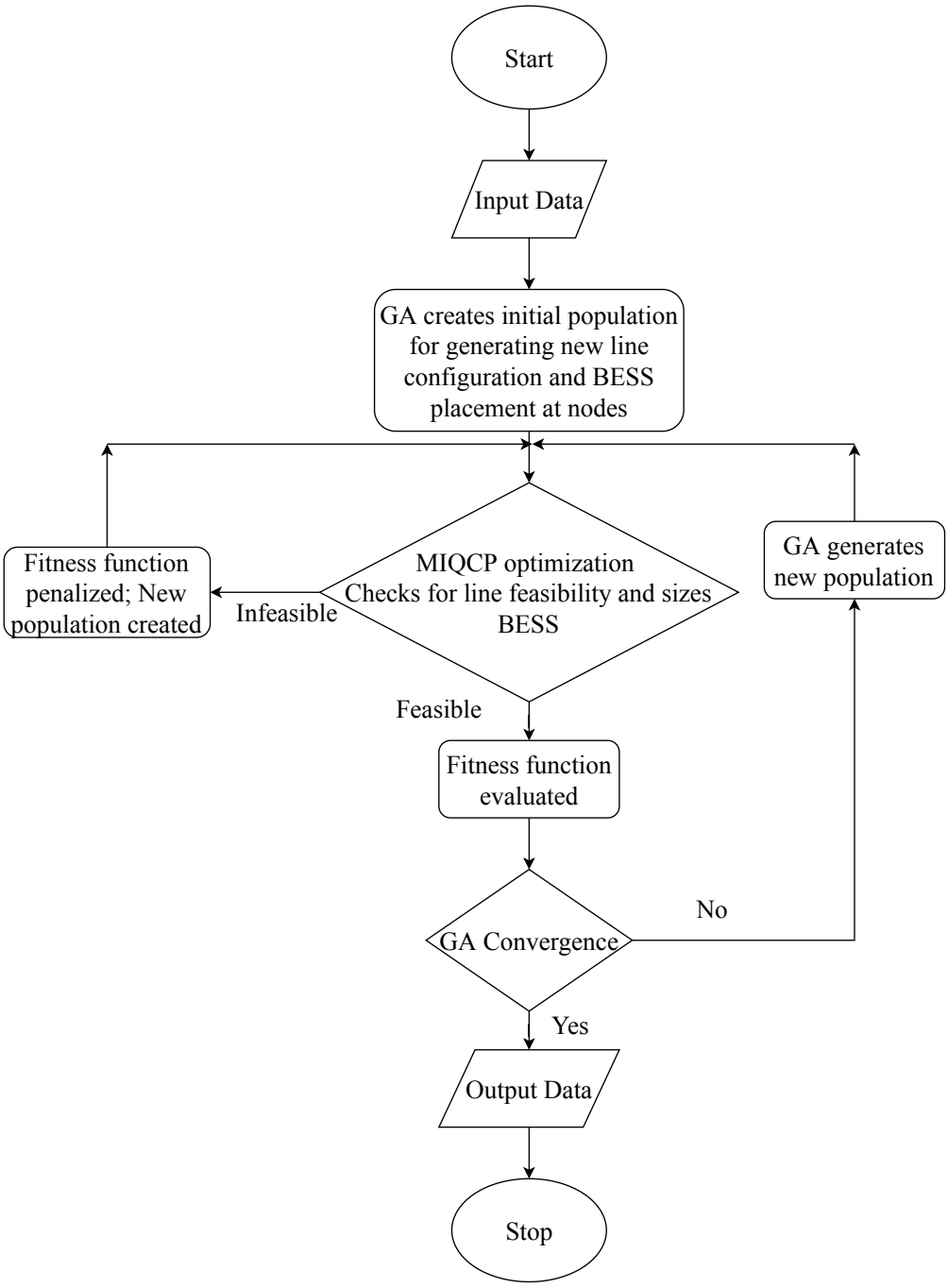

Figure 7.2: Flowchart of the BESS hybrid DSEP model formulation

does not improve further, the algorithm converges and a solution is obtained [99]. A flowchart of the hybrid model implementation is shown in Figure 7.2.

The solution output from the algorithm is detailed as follows

- New line configuration
- BESS allocation and optimal sizing
- Charging and discharging characteristics of the BESS
- Distribution system voltage and power losses profile
- Total cost for the proposed distribution system expansion

Parameters necessary for the BESS allocation and sizing formulation are as follows

- cost coefficients for BESS and lines
- lifetime for BESS and lines
- discount rates for BESS and lines
- electrical parameters and grid information
  - set of new line options
  - length of new and existing lines
  - line resistance, reactance and impedance parameters
  - voltage, current and capacity limits
  - maximum and minimum BESS power and energy ratings of a single unit

The constraints for the GA are limited to

- the number of new line options
- the number of nodes at which BESS can be allocated
- the algorithm also enforces a line set feasibility constraint. This allows the GA to proceed with the fitness function evaluation only if the solution line set, is proven feasible in the MIQCP. For an infeasible new line set, the objective function is penalized.

Cross section of XLPE cable	300 mm^2
Cost of cable (C^L in S$/km)	79,800
Lifetime in years	40
Discount Rate	5%

Table 7.1: Line considerations for expansion planning

Energy Storage System (ESS) type	Lithium-Ion Batteries
Cost of power coefficient (C^P in S$/MW)	205,200
Cost of energy coefficient (C^E in S$/MWh)	513,000
Lifetime in years	15
Discount rate	5%
Charging efficiency η_C	0.9
Discharging efficiency η_D	0.9
Maximum ESS rating at node	0.8 MWh/0.8 MW
Minimum ESS rating at node	0.08 MWh/0.08 MW
Analyzed operating period	72 hours

Table 7.2: BESS considerations for expansion planning

7.3 Case Study

As the initial purpose of this chapter to demonstrate the importance of the utilization of realistic synthetic grids, the proposed DSEP model is tested on a 22 kV case study from a Singaporean synthetic grid model, obtained by the framework for synthetic grid generation proposed in this thesis. The case study represents a single planning area of a 45 bus radially operated system with a single 66/22 kV substation, as shown in Fig. 7.3. The voltage tolerance is set to ±6%. The expansion planning is carried out as a single stage without considering uncertainties and further considerations of the future growth in demand at different points of time. In addition, the cost of relay protection upgrades are not considered in this study, having an assumption for an existing active distribution system.

The 45 bus case study includes three radial feeders which connect the consumers by the use of underground cables. The considerations taken into account for the calculation of the cost of the lines are detailed in Table 7.1, while a detailed specification of the underground cable is given in Table 7.3.

The initial grid model has been modified to consider significant growth in demand in the form of new EV fast chargers added to some of the existing nodes. The active load per charger is set to 450 KW. There are total of fourteen fast chargers added in the system, with two chargers installed at each of the nodes 17, 21, 25, 30, 34, 35 and 41. This is assumed to create a scenario with high EV integration which makes the existing network infeasible and unable to supply the new peak demand.

The BESS allocation is considered as an option at any of the 44 available nodes, excluding the substation. The assumptions made for the BESS within the optimization

are detailed in Table 7.2. To compute the charging and discharging cycles and the behavior of the allocated BESS, a 72 hour operating period is considered with the demand curve discretized in per unit hour.

Table 7.3: XLPE Cable Data Specification

Cross Section	Resistance R	Reactance X	Current limit I^{max}
mm^2	Ω/km	Ω/km	A
300	0.130	0.108	360

7.4 Results and Analysis

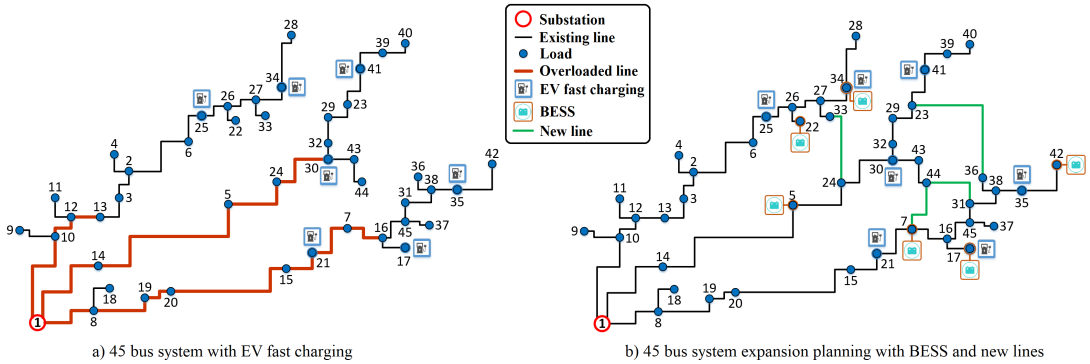

Figure 7.3: Case study grid model and BESS expansion planning results

The introduction of EV charging into the grid may cause a significant overloading of the existing infrastructure, as shown in Fig. 7.3 a). To increase the line carrying capacity, the existing cable should either be replaced with a new cable of bigger cross section or be reinforced with another cable in parallel to the existing one. Even though the latter may be preferred in terms of significantly increased reliability, the principles of power flow in parallel circuits impose the condition to have matching electrical properties of both cables in a line. Consequently, the reinforcement of a line doubles the line carrying capacity, which often results in an excessive spare capacity and cost inefficiency. This makes both options similarly priced and a very costly investment. The investment cost for reinforcing the overloaded lines in the 45 bus test system is estimated to an annualized cost of S$ 171,200.

The proposed optimization model provides an alternative solution that includes BESS and new lines with a total annualized cost of SGD$ 84,088, as show in Fig. 7.3 b). There are four new line options with an annualized cost of S$ 50,890, including 24−33, 23−36, 7−44 and 31−44. Furthermore, the BESS units are installed at six locations with an

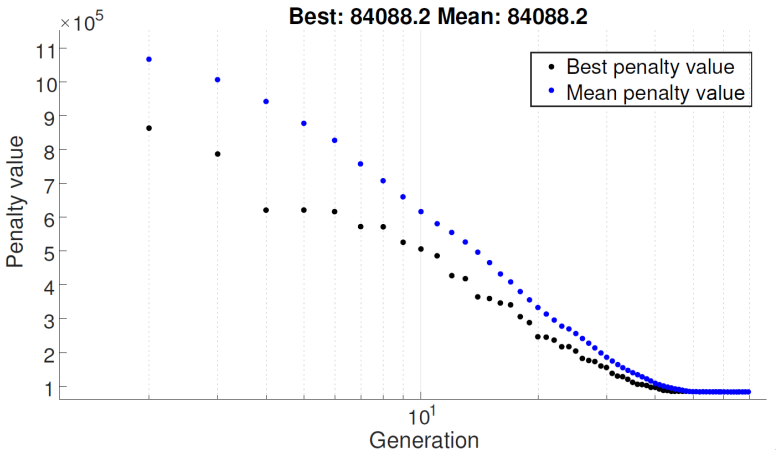

Figure 7.4: GA Convergence

annualized cost of S$ 33,198. The BESS are allocated at nodes 5, 7, 17, 22, 34 and 42, and they are equally sized at their minimum size requirement. It can be observed that all the BESS units are allocated either at nodes with EV chargers or at their close proximity at some of the neighboring nodes. Similarly, the new lines are also found in proximity to the new EV charging demand, such that the new loads are more equally distributed among the three feeders. Therefore, the results show that the proposed approach makes the best use of combining BESS and new lines to provide a feasible cost effective solution for the distribution system expansion planning problem.

The hybrid model is programmed using the global optimization toolbox in Matlab for the GA, and GAMS with CPLEX as a solver for the MIQCP optimization. The solution convergence criteria for the GA is set at a relative difference of 0.001%, while the relative optimality gap in the MIQCP is set to 1%. The GA convergence of the presented case study is given in Fig. 7.4, which shows the change in the relative difference between the fitness function values and the change in the number of generations.

7.5 Summary

The accelerating trend of DERs and EV integration is changing the landscape of the modern power system. Recent improvements in BESS give way to explore and consider their benefits in the distribution system planning problem. To maintain the continuity of supply under the new demand growth, a line expansion planning model with BESS is proposed.

A hybrid optimization approach using a GA and a MIQCP is defined. The combination of a GA and a MIQCP is preferred as a way to employ their capabilities and compensate for the deficiencies. The GA determines the selection of new lines combined with the placement of the BESS, which are then used in the MIQCP sub-optimization to provide the optimal BESS sizing and test the power flow feasibility. The GA uses the results

obtained from the MIQCP sub-optimization to evaluate the fitness function and improve the solution until a convergence is reached.

To demonstrate the key benefits of the proposed synthetic grid generation framework, the proposed model is tested on a 45 bus case study representing a planning area of the Singaporean synthetic grid model. The results are shown and analyzed to conclude the benefits of combining new lines and BESS as an approach for a feasible cost effective distribution system expansion planning solution.

Further research on larger test cases and longer operating periods is required to assess the scalability of the model. Improvements on the effectiveness of the model can be further explored with the use of preconditioning algorithms. The cycling effects of BESS and degradation due to aging can also add a greater accuracy to the current model.

8 Conclusion & Outlook

Given the recent technological advancements and rapid developments in the power sector, it has been identified a need for more advanced near-real world research, development and demonstration (RD&D) capabilities. The evolutionary path toward a modernized grid has to be supported by a seamless integration of new technologies and concepts without putting strain on the critical energy supply services they currently provide.

In this work, a holistic approach to generating realistic synthetic grid is proposed. The framework has focused to cover the process from the initial stage of research and data gathering, utilizing and working with the obtained data, identifying the missing components and using the appropriate methodology to generating the synthetic power system, which is then to be validated with a confirmed power flow feasibility.

For this purpose, various novel mathematical optimization models on distribution and transmission system planning are introduced. Having covered different types of distribution network configurations together with a security constrained transmission expansion planning to the highest voltage level, the different characteristics of both grids are taken into account for the design, planning and operation of a complete realistic power system.

The approach follows the power system planning concept typically used by planning engineers to plan and engineer the grid in a cost-effective manner with respect to the overall investment and operational costs. Consequently, the contribution of this work is two-fold as the proposed optimization methodology can also be used for the expansion planning of existing real-world distribution and transmission grids.

Once the synthetic grid is completed, a validation approach is elaborated for both the distribution and the transmission networks to verify the resemblance of a realistic grid and ensure a feasible and convergent operation of the system.

A case study of the Singaporean power system is used to demonstrate the application of the proposed framework. Consequently, this work shares the findings and the resultant Singaporean synthetic grid. To show the practicality of such system, the viability of a novel approach for distribution network expansion planning with Li-ion BESS is tested and presented.

The proposed framework can be used for the purpose of many different power system studies. However, depending on the requirements and the nature of the study, more data might be required when modeling the power system. Therefore, future work should focus to further detail and identify the different types of studies. The framework should then be extended to cover such cases accordingly. This might require extension of the proposed methodology, as well as a different validation criteria depending on the typical study.

In addition, the synthetic grid can be used as a starting point to define different scenarios with their own specific datasets. The synthetic grid can be used to examine an existing state of a system, past events, or future developments with different mix of technologies. For the purpose of such studies, different components and infrastructure may be added to the system for further examination.

This work proposes a holistic approach as a framework for the generation of synthetic grids that can be used to enable new technologies and concepts for the grid modernization. Further developments of the proposed framework will enable to strengthen the applicability and practicality of this approach for the future grid.

Bibliography

[1] A. Trpovski, D. F. R. Melo, T. Hamacher, and T. Massier. Stochastic optimization for distribution grid reconfiguration with high photovoltaic penetration. In *2017 IEEE International Conference on Smart Energy Grid Engineering (SEGE)*, pages 67–73, 2017. doi:10.1109/SEGE.2017.8052778.

[2] A. Trpovski, D. Recalde, and T. Hamacher. Synthetic distribution grid generation using power system planning: Case study of singapore. In *2018 53rd International Universities Power Engineering Conference (UPEC)*, pages 1–6, 2018. doi:10.1109/UPEC.2018.8542054.

[3] A. Trpovski and T. Hamacher. Scenario based n-1 transmission expansion planning using dc mixed integer programming. In *2019 IEEE Power & Energy Society General Meeting (PESGM)*, pages 1–5, 2019. doi:10.1109/PESGM40551.2019.8973506.

[4] A. Trpovski and T. Hamacher. A comparative analysis of transmission system planning for overhead and underground power systems using ac and dc power flow. In *2019 IEEE PES Innovative Smart Grid Technologies Europe (ISGT-Europe)*, pages 1–5, 2019. doi:10.1109/ISGTEurope.2019.8905510.

[5] A. Trpovski and T. Hamacher. Ring distribution system expansion planning using scenario based mixed integer programming. In *2020 IEEE/PES Transmission and Distribution Conference and Exposition (T D)*, pages 1–5, 2020. doi:10.1109/TD39804.2020.9299971.

[6] A. Trpovski, P. Banerjee, Y. Xu, and T. Hamacher. A hybrid optimization method for distribution system expansion planning with lithium-ion battery energy storage systems. In *2020 IEEE Sustainable Power and Energy Conference (iSPEC)*, pages 2015–2021, 2020. doi:10.1109/iSPEC50848.2020.9351208.

[7] D. Recalde, A. Trpovski, S. Troitzsch, K. Zhang, S. Hanif, and T. Hamacher. A review of operation methods and simulation requirements for future smart distribution grids. In *2018 IEEE Innovative Smart Grid Technologies - Asia (ISGT Asia)*, pages 475–480, 2018. doi:10.1109/ISGT-Asia.2018.8467850.

[8] S. Troitzsch, S. Hanif, K. Zhang, A. Trpovski, and T. Hamacher. Flexible distribution grid demonstrator (fledge): Requirements and software architecture. In *2019 IEEE Power Energy Society General Meeting (PESGM)*, pages 1–5, 2019. doi:10.1109/PESGM40551.2019.8973567.

[9] J. Romero Aguero, A. Khodaei, and R. Masiello. The utility and grid of the future: Challenges, needs, and trends. *IEEE Power and Energy Magazine*, 14(5):29–37, 2016. doi:10.1109/MPE.2016.2577899.

[10] J. Romero Agüero, E. Takayesu, D. Novosel, and R. Masiello. Grid modernization: challenges and opportunities. *The Electricity Journal*, 30(4):1–6, 2017. Special Issue: Contemporary Strategies for Microgrid Operation & Control. URL: https://www.sciencedirect.com/science/article/pii/S1040619017300660, doi:https://doi.org/10.1016/j.tej.2017.03.008.

[11] International Energy Agency (IEA), Paris. Global Energy Review 2020. Technical report.

[12] International Renewable Energy Agency (IRENA). Renewable Energy Statistics 2020. Technical report.

[13] UPDATE of the Solar Photovoltaic (PV) Roadmap for Singapore. Renewable Energy Statistics 2020. Technical report.

[14] I. J. PÉREZ-ARRIAGA and C. BATLLE. Impacts of intermittent renewables on electricity generation system operation. *Economics of Energy & Environmental Policy*, 1(2):3–18, 2012. URL: http://www.jstor.org/stable/26189488.

[15] P. Denholm, E. Ela, B. Kirby, and M. Milligan. Role of energy storage with renewable electricity generation. URL: https://www.osti.gov/biblio/972169, doi:10.2172/972169.

[16] J. P. Barton and D. G. Infield. Energy storage and its use with intermittent renewable energy. *IEEE Transactions on Energy Conversion*, 19(2):441–448, 2004. doi:10.1109/TEC.2003.822305.

[17] K. Divya and J. Østergaard. Battery energy storage technology for power systems—an overview. *Electric Power Systems Research*, 79(4):511–520, 2009. URL: https://www.sciencedirect.com/science/article/pii/S0378779608002642, doi:https://doi.org/10.1016/j.epsr.2008.09.017.

[18] U.S. Department of Energy. Energy Storage Grand Challenge: Energy Storage Market Report. Technical report.

[19] International Energy Agency (IEA), Paris. Energy Storage. Technical report.

[20] International Renewable Energy Agency (IRENA). Innovation landscape brief: Utility-scale batteries. Technical report.

[21] International Energy Agency (IEA), Paris. Global EV Outlook 2020. Technical report.

[22] National Research Foundation (NRF), National Climate Change Secretariat (NCCS), Land Transport Authority (LTA), Singapore. E-MOBILITY Technology Roadmap. Technical report.

[23] Land Transport Authority (LTA), Singapore. Land Transport Master Plan 2040.

[24] J. A. P. Lopes, F. J. Soares, and P. M. R. Almeida. Integration of electric vehicles in the electric power system. *Proceedings of the IEEE*, 99(1):168–183, 2011. doi:10.1109/JPROC.2010.2066250.

[25] V. C. Gungor, D. Sahin, T. Kocak, S. Ergut, C. Buccella, C. Cecati, and G. P. Hancke. Smart grid technologies: Communication technologies and standards. *IEEE Transactions on Industrial Informatics*, 7(4):529–539, 2011. doi:10.1109/TII.2011.2166794.

[26] A. P. S. Meliopoulos, E. Polymeneas, Z. Tan, R. Huang, and D. Zhao. Advanced distribution management system. *IEEE Transactions on Smart Grid*, 4(4):2109–2117, 2013. doi:10.1109/TSG.2013.2261564.

[27] P. Siano. Demand response and smart grids—a survey. *Renewable and Sustainable Energy Reviews*, 30:461–478, 2014. URL: https://www.sciencedirect.com/science/article/pii/S1364032113007211, doi:https://doi.org/10.1016/j.rser.2013.10.022.

[28] R. Zafar, A. Mahmood, S. Razzaq, W. Ali, U. Naeem, and K. Shehzad. Prosumer based energy management and sharing in smart grid. *Renewable and Sustainable Energy Reviews*, 82:1675–1684, 2018. URL: https://www.sciencedirect.com/science/article/pii/S1364032117310894, doi:https://doi.org/10.1016/j.rser.2017.07.018.

[29] H. Farhangi. The path of the smart grid. *IEEE Power and Energy Magazine*, 8(1):18–28, 2010. doi:10.1109/MPE.2009.934876.

[30] S. Peyghami, P. Davari, M. Fotuhi-Firuzabad, and F. Blaabjerg. Standard test systems for modern power system analysis: An overview. *IEEE Industrial Electronics Magazine*, 13(4):86–105, 2019. doi:10.1109/MIE.2019.2942376.

[31] R. L. Sullivan. Power system planning. URL: https://www.osti.gov/biblio/5024455.

[32] 23 - distribution planning. In C. Bayliss and B. Hardy, editors, *Transmission and Distribution Electrical Engineering (Third Edition)*, pages 867–906. Newnes, Oxford, third edition edition, 2007. URL: https://www.sciencedirect.com/science/article/pii/B9780750666732500276, doi:https://doi.org/10.1016/B978-075066673-2/50027-6.

[33] E. Schweitzer, A. Scaglione, A. Monti, and G. A. Pagani. Automated generation algorithm for synthetic medium voltage radial distribution systems. *IEEE Journal*

on Emerging and Selected Topics in Circuits and Systems, 7(2):271–284, 2017. doi:10.1109/JETCAS.2017.2682934.

[34] Z. Wang, A. Scaglione, and R. J. Thomas. Generating statistically correct random topologies for testing smart grid communication and control networks. *IEEE Transactions on Smart Grid*, 1(1):28–39, 2010. doi:10.1109/TSG.2010.2044814.

[35] H. Rui, M. Arnold, and W. H. Wellssow. Synthetic medium voltage grids for the assessment of smart grid techniques. In *2012 3rd IEEE PES Innovative Smart Grid Technologies Europe (ISGT Europe)*, pages 1–8, 2012. doi:10.1109/ISGTEurope.2012.6465639.

[36] M. Sarstedt, S. Garske, C. Blaufuß, and L. Hofmann. Modelling of integrated transmission and distribution grids based on synthetic distribution grid models. In *2019 IEEE Milan PowerTech*, pages 1–6, 2019. doi:10.1109/PTC.2019.8810823.

[37] S. H. Elyas and Z. Wang. Improved synthetic power grid modeling with correlated bus type assignments. *IEEE Transactions on Power Systems*, 32(5):3391–3402, 2017. doi:10.1109/TPWRS.2016.2634318.

[38] K. M. Gegner, A. B. Birchfield, Ti Xu, K. S. Shetye, and T. J. Overbye. A methodology for the creation of geographically realistic synthetic power flow models. In *2016 IEEE Power and Energy Conference at Illinois (PECI)*, pages 1–6, 2016. doi:10.1109/PECI.2016.7459256.

[39] A. B. Birchfield, T. Xu, K. M. Gegner, K. S. Shetye, and T. J. Overbye. Grid structural characteristics as validation criteria for synthetic networks. *IEEE Transactions on Power Systems*, 32(4):3258–3265, 2017. doi:10.1109/TPWRS.2016.2616385.

[40] A. B. Birchfield, T. Xu, and T. J. Overbye. Power flow convergence and reactive power planning in the creation of large synthetic grids. *IEEE Transactions on Power Systems*, 33(6):6667–6674, 2018. doi:10.1109/TPWRS.2018.2813525.

[41] A. B. Birchfield, E. Schweitzer, M. H. Athari, T. Xu, T. J. Overbye, A. Scaglione, and Z. Wang. A metric-based validation process to assess the realism of synthetic power grids. *Energies*, 10(8), 2017. URL: https://www.mdpi.com/1996-1073/10/8/1233, doi:10.3390/en10081233.

[42] A. B. Birchfield, K. M. Gegner, T. Xu, K. S. Shetye, and T. J. Overbye. Statistical considerations in the creation of realistic synthetic power grids for geomagnetic disturbance studies. *IEEE Transactions on Power Systems*, 32(2):1502–1510, 2017. doi:10.1109/TPWRS.2016.2586460.

[43] S. Soltan and G. Zussman. Generation of synthetic spatially embedded power grid networks. In *2016 IEEE Power and Energy Society General Meeting (PESGM)*, pages 1–5, 2016. doi:10.1109/PESGM.2016.7741383.

[44] M. H. Athari and Z. Wang. Introducing voltage-level dependent parameters to synthetic grid electrical topology. *IEEE Transactions on Smart Grid*, 10(4):4048–4056, 2019. doi:10.1109/TSG.2018.2848933.

[45] P. S. Georgilakis and N. D. Hatziargyriou. A review of power distribution planning in the modern power systems era : Models , methods and future research. *Electric Power Systems Research*, 121:89–100, 2015. URL: http://dx.doi.org/10.1016/j.epsr.2014.12.010, doi:10.1016/j.epsr.2014.12.010.

[46] S. Ganguly, N. C. Sahoo, and D. Das. Recent advances on power distribution system planning: a state-of-the-art survey. *Energy Systems*, 4(2):165–193, Jun 2013. URL: https://doi.org/10.1007/s12667-012-0073-x, doi:10.1007/s12667-012-0073-x.

[47] E. Naderi, H. Seifi, and M. S. Sepasian. A dynamic approach for distribution system planning considering distributed generation. *IEEE Trans. on Power Deliver.*, 27(3):1313–1322, July 2012. doi:10.1109/TPWRD.2012.2194744.

[48] W. El-Khattam, Y. G. Hegazy, and M. M. A. Salama. An integrated distributed generation optimization model for distribution system planning. *IEEE Trans. on Power Syst.*, 20:1158–1165, May 2005. doi:10.1109/TPWRS.2005.846114.

[49] T. Gönen and B. L. Foote. Distribution-system planning using mixed-integer programming. *IEE Proc. C - Gen., Trans. and Dist.*, 128(2):70–79, March 1981. doi:10.1049/ip-c:19810010.

[50] K. Zou, A. P. Agalgaonkar, K. M. Muttaqi, and S. Perera. Distribution system planning with incorporating DG reactive capability and system uncertainties. *IEEE Trans. on Sus. Energ.*, 3(1):112–123, Jan 2012. doi:10.1109/TSTE.2011.2166281.

[51] R. C. Lotero and J. Contreras. Distribution system planning with reliability. *IEEE Trans. on Power Deliver.*, 26(4):2552–2562, Oct 2011. doi:10.1109/TPWRD.2011.2167990.

[52] B. Zeng, J. Zhang, X. Yang, J. Wang, J. Dong, and Y. Zhang. Integrated planning for transition to low-carbon distribution system with renewable energy generation and demand response. *IEEE Transactions on Power Systems*, 29(3):1153–1165, May 2014. doi:10.1109/TPWRS.2013.2291553.

[53] G. Muñoz-Delgado, J. Contreras, and J. M. Arroyo. Distribution system expansion planning considering non-utility-owned DG and an independent distribution system operator. *IEEE Trans. on Power Syst.*, 34(4):2588–2597, July 2019. doi:10.1109/TPWRS.2019.2897869.

[54] N. Alguacil, A. L. Motto, and A. J. Conejo. Transmission expansion planning: a mixed-integer lp approach. *IEEE Trans. Power Syst.*, 18(3):1070–1077, Aug 2003. doi:10.1109/TPWRS.2003.814891.

[55] H. Zhang, G. T. Heydt, V. Vittal, and J. Quintero. An improved network model for transmission expansion planning considering reactive power and network losses. *IEEE Transactions on Power Systems*, 28(3):3471–3479, Aug 2013. doi:10.1109/TPWRS.2013.2250318.

[56] S. P. Torres and C. A. Castro. Expansion planning for smart transmission grids using ac model and shunt compensation. *IET Generation, Transmission Distribution*, 8(5):966–975, May 2014. doi:10.1049/iet-gtd.2013.0231.

[57] H. Yu, C. Y. Chung, K. P. Wong, and J. H. Zhang. A chance constrained transmission network expansion planning method with consideration of load and wind farm uncertainties. *IEEE Trans. Power Syst.*, 24(3):1568–1576, Aug 2009. doi:10.1109/TPWRS.2009.2021202.

[58] R. A. Gallego, A. Monticelli, and R. Romero. Transmission system expansion planning by an extended genetic algorithm. *IEE Proc. - Gener., Transm. Distrib.*, 145(3):329–335, May 1998. doi:10.1049/ip-gtd:19981895.

[59] R. Romero, C. Rocha, M. Mantovani, and J. R. S. Mantovani. Analysis of heuristic algorithms for the transportation model in static and multistage planning in network expansion systems. *IEE Proceedings - Generation, Transmission and Distribution*, 150(5):521–526, Sep. 2003. doi:10.1049/ip-gtd:20030725.

[60] H. Zhang, V. Vittal, G. T. Heydt, and J. Quintero. A mixed-integer linear programming approach for multi-stage security-constrained transmission expansion planning. *IEEE Transactions on Power Systems*, 27(2):1125–1133, May 2012. doi:10.1109/TPWRS.2011.2178000.

[61] L. H. Macedo, C. V. Montes, J. F. Franco, M. J. Rider, and R. Romero. Milp branch flow model for concurrent ac multistage transmission expansion and reactive power planning with security constraints. *IET Generation, Transmission Distribution*, 10(12):3023–3032, 2016. doi:10.1049/iet-gtd.2016.0081.

[62] L. P. Garces, A. J. Conejo, R. Garcia-Bertrand, and R. Romero. A bilevel approach to transmission expansion planning within a market environment. *IEEE Transactions on Power Systems*, 24(3):1513–1522, Aug 2009. doi:10.1109/TPWRS.2009.2021230.

[63] D. Pozo, E. E. Sauma, and J. Contreras. A three-level static milp model for generation and transmission expansion planning. *IEEE Transactions on Power Systems*, 28(1):202–210, Feb 2013. doi:10.1109/TPWRS.2012.2204073.

[64] J. H. Roh, M. Shahidehpour, and L. Wu. Market-based generation and transmission planning with uncertainties. *IEEE Transactions on Power Systems*, 24(3):1587–1598, Aug 2009. doi:10.1109/TPWRS.2009.2022982.

[65] S. Majumder, R. M. Shereef, and S. A. Khaparde. Two-stage algorithm for efficient transmission expansion planning with renewable energy resources. *IET Renewable Power Generation*, 11(3):320–329, 2017. doi:10.1049/iet-rpg.2016.0085.

[66] F. Zhang, Z. Hu, and Y. Song. Mixed-integer linear model for transmission expansion planning with line losses and energy storage systems. 7(November 2012):919–928, 2013. doi:10.1049/iet-gtd.2012.0666.

[67] S. Teimourzadeh and F. Aminifar. Milp formulation for transmission expansion planning with short-circuit level constraints. *IEEE Transactions on Power Systems*, 31(4):3109–3118, July 2016. doi:10.1109/TPWRS.2015.2473663.

[68] F. L. Alvarado and S. S. Oren. Transmission system operation and interconnection. Technical report, 05/2002 2002.

[69] M. Majidi-Qadikolai and R. Baldick. Stochastic transmission capacity expansion planning with special scenario selection for integrating$n-1$contingency analysis. *IEEE Transactions on Power Systems*, 31(6):4901–4912, Nov 2016. doi:10.1109/TPWRS.2016.2523998.

[70] H. Li, A. L. Bornsheuer, T. Xu, A. B. Birchfield, and T. J. Overbye. Load modeling in synthetic electric grids. In *2018 IEEE Texas Power and Energy Conference (TPEC)*, pages 1–6, 2018. doi:10.1109/TPEC.2018.8312059.

[71] A. A. Chowdhury and D. O. Koval. *Power Distribution System Reliability: Practical Methods and Applications*. Wiley, 2011.

[72] D. Ciechanowicz, D. Pelzer, B. Bartenschlager, and A. Knoll. A modular power system planning and power flow simulation framework for generating and evaluating power network models. *IEEE Transactions on Power Systems*, 32(3):2214–2224, May 2017. doi:10.1109/TPWRS.2016.2602479.

[73] K. Prakash, A. Lallu, F. Islam, and K. Mamun. Review of power system distribution network architecture. In *2016 3rd Asia-Pacific World Congress on Computer Science and Engineering (APWC on CSE)*, pages 124–130, 2016. doi:10.1109/APWC-on-CSE.2016.030.

[74] G. A. Pagani and M. Aiello. Towards decentralization: A topological investigation of the medium and low voltage grids. *IEEE Transactions on Smart Grid*, 2(3):538–547, Sept 2011. doi:10.1109/TSG.2011.2147810.

[75] R. G. Cespedes. New method for the analysis of distribution networks. *IEEE Trans. on Power Deliv.*, 5(1):391–396, Jan 1990. doi:10.1109/61.107303.

[76] M. C. O. Borges, J. F. Franco, and M. J. Rider. Optimal reconfiguration of electrical distribution systems using mathematical programming. *J. of Cont., Autom. and Elect. Syst.*, 25(1):103–111, 2014. doi:10.1007/s40313-013-0070-x.

[77] J. C. López, M. Lavorato, and M. J. Rider. Optimal reconfiguration of electrical distribution systems considering reliability indices improvement. *Int. J. of Elect. Power and Energy Syst.*, 78, 2016. doi:10.1016/j.ijepes.2015.12.023.

[78] C. R. Bayliss and B. J. Hardy. *Transmission and Distribution Electrical Engineering*. Newnes, Elsevier, 4th edition edition, 2012.

[79] K. Hall and H. E. Consulting. Out of Sight, Out of Mind. Technical Report January, Edison Electric Institute (EEI), 2013.

[80] Chan S. Park. *Contemporary Engineering Economics*. Prentice Hal, 5th edition edition, 2010.

[81] M. Lavorato, S. Member, J. F. Franco, S. Member, and M. J. Rider. Imposing Radiality Constraints in Distribution System Optimization Problems. *IEEE Trans. on Power Syst.*, 27(1), 2012.

[82] R. E. Rosenthal. *GAMS — A User 's Guide*. Number January. 2016.

[83] I. I. Cplex. V12. 1: User's manual for cplex. *International Business Machines Corporation*, 46(53):157, 2009.

[84] M. ApS. *MOSEK Optimization Suite Release 9.2.46*, 2021. URL: https://docs.mosek.com/9.2/intro.pdf.

[85] S. Boyd and L. Vandenberghe. *Convex Optimization*. Cambridge University Press, 2004. doi:10.1017/CBO9780511804441.

[86] M. Farivar and S. H. Low. Branch flow model: Relaxations and convexification—part i. *IEEE Transactions on Power Systems*, 28(3):2554–2564, 2013. doi:10.1109/TPWRS.2013.2255317.

[87] M. Farivar and S. H. Low. Branch flow model: Relaxations and convexification—part ii. *IEEE Transactions on Power Systems*, 28(3):2565–2572, 2013. doi:10.1109/TPWRS.2013.2255318.

[88] T. Ding, S. Liu, W. Yuan, Z. Bie, and B. Zeng. A two-stage robust reactive power optimization considering uncertain wind power integration in active distribution networks. *IEEE Transactions on Sustainable Energy*, 7(1):301–311, 2016. doi:10.1109/TSTE.2015.2494587.

[89] R. A. Jabr and S. Member. Polyhedral Formulations and Loop Elimination Constraints for Distribution Network Expansion Planning. 28(2):1888–1897, 2013.

[90] M. Lavorato, S. Member, M. J. Rider, and A. V. Garcia. A Constructive Heuristic Algorithm for Distribution System Planning Marina. 25(3):1734–1742, 2010.

[91] J. F. Gomez, H. M. Khodr, P. M. De Oliveira, L. Ocque, J. M. Yusta, R. Villasana, and A. J. Urdaneta. Ant colony system algorithm for the planning of primary distribution circuits. *IEEE Trans. on Power Syst.*, 19(2):996–1004, May 2004. doi:10.1109/TPWRS.2004.825867.

[92] A. K. Marvasti, Y. Fu, S. DorMohammadi, and M. Rais-Rohani. Optimal operation of active distribution grids: A system of systems framework. *IEEE Transactions on Smart Grid*, 5(3):1228–1237, 2014. doi:10.1109/TSG.2013.2282867.

[93] J.-C. Kim, S.-M. Cho, and H.-S. Shin. Advanced power distribution system configuration for smart grid. *IEEE Transactions on Smart Grid*, 4(1):353–358, 2013. doi:10.1109/TSG.2012.2233771.

[94] V. Murty and A. Kumar. Mesh distribution system analysis in presence of distributed generation with time varying load model. *International Journal of Electrical Power & Energy Systems*, 62:836–854, 2014. doi:https://doi.org/10.1016/j.ijepes.2014.05.034.

[95] R. Billinton and R. N. Allan. *Reliability Evaluation of Power Systems*. Plenum Press, 2 edition, 1996.

[96] R. Brown. *Electric Power Distribution Reliability*, volume 20020625 of *Power Engineering (Willis)*. CRC Press, mar 2002. doi:10.1201/9780824744281.

[97] T. Kong, H. Cheng, Z. Hu, and L. Yao. Multiobjective planning of open-loop mv distribution networks using comgis network analysis and moga. *Electric Power Systems Research*, 79(2):390–398, 2009. URL: https://www.sciencedirect.com/science/article/pii/S0378779608002204, doi:https://doi.org/10.1016/j.epsr.2008.08.004.

[98] A. J. Wood, B. F. Wollenberg, and G. B. Sheblé. *Power generation, operation, and control*. Wiley-Interscience, Hoboken, New Jersey, 3 edition, 2013.

[99] D. E. Goldberg. *Genetic Algorithms in Search, Optimization, and Machine Learning*. Addison-Wesley, 1989.

[100] M. Mitchell. *An introduction to genetic algorithms*. MIT Press, 1996.

[101] D. Whitley. A genetic algorithm tutorial. *Statistics and Computing*, 4:65–85, 1994.

[102] R. D. Zimmerman, C. E. Murillo-Sánchez, and R. J. Thomas. Matpower: Steady-state operations, planning, and analysis tools for power systems research and education. *IEEE Transactions on Power Systems*, 26(1):12–19, 2011. doi:10.1109/TPWRS.2010.2051168.

[103] S. Hong and J. Lu. Composite Generation and Transmission Expansion Planning With Seeond Order Conie Relaxation of AC Power Flow. (51337005):1688–1693, 2016.

[104] R. A. Jabr. Optimization of ac transmission system planning. *IEEE Transactions on Power Systems*, 28(3):2779–2787, 2013. doi:10.1109/TPWRS.2012.2228507.

[105] S. Sojoudi and J. Lavaei. Physics of power networks makes hard optimization problems easy to solve. In *2012 IEEE Power and Energy Society General Meeting*, pages 1–8, 2012. doi:10.1109/PESGM.2012.6345272.

[106] A. Seifu, S. Salon, and G. List. Optimization of transmission line planning including security constraints. *IEEE Trans. Power Syst.*, 4(4):1507–1513, Nov 1989. doi:10.1109/59.41703.

[107] R. P. O'Neill, E. A. Krall, K. W. Hedman, and S. S. Oren. A model and approach for optimal power systems planning and investment. 2012.

[108] I. de J Silva, M. J. Rider, R. Romero, A. V. Garcia, and C. A. Murari. Transmission network expansion planning with security constraints. *IEE Proc. - Gene. Transm. and Distrib.*, 152(6):828–836, Nov 2005. doi:10.1049/ip-gtd:20045217.

[109] Energy Market Authority. Transmission Code. 2014.

[110] E. M. A. (EMA). Singapore energy statistics. https://www.ema.gov.sg/singapore-energy-statistics/, 2020.

[111] D. Ciechanowicz . A Power System Planning and Power Flow Simulation Framework for Generating and Evaluating Power Network Models - Investigating the Impact of Large-Scale Road Transportation Electrification on Urban Power Systems. PhD Thesis. Technical report, 2017.

[112] S. Chang, K. Chua, C. Slew, and T. Tan. Power quality initiatives in singapore. In *16th International Conference and Exhibition on Electricity Distribution, 2001. Part 1: Contributions. CIRED. (IEE Conf. Publ No. 482)*, volume 2, pages 4 pp. vol.2–, 2001. doi:10.1049/cp:20010747.

[113] Havells. LT/HT Power & Control Cables, 2014. URL: http://www.havells.com/content/dam/havells/brouchers/IndustrialCable/IndustrialCablepricelist.pdf.

[114] POLYCAB. HIGH TENSION XLPE CABLES. URL: http://www.prabhatcables.com/download/pdf-HT-XLPE.pdf.

[115] LGCE FTTX & Cable. LS EHV Cable System. URL: http://www.lgce.net/uploads/lgce{_}ehv.pdf.

[116] BICC Cables Ltd. *Electric Cables Handbook*. Third edit edition, 1997.

[117] IEC. IEC 60287, 2015. URL: https://webstore.iec.ch/publication/22097.

[118] ABERDARE Cables. Cables Facts and Figures. Technical report, 2008. URL: http://www.aberdare.co.za/download/map?map=sites/default/aberdare{_}cables/files/brochures/653/brochures{_}653.pdf.

[119] J. J. Graigner and W. D. Stevenson. *Power System Analysis*. 1994.

[120] ABB. XLPE Land Cable Systems User's Guide. Technical report.

[121] Energy Market Authority. Singapore Energy Statistics 2016. page 64, 2016. URL: http://www.ema.gov.sg/reports/id:72/{%}5Cninternal-pdf://989/id72.html, doi:2251-2624.

[122] Singapore Power Group. Annual Report 2008. Technical report, 2008. URL: https://www.spgroup.com.sg/wcm/connect/spgrp/d9618047-830b-450c-aa50-af3853b7af64/SP+Group+Annual+Report+FY0809.pdf?MOD=AJPERES{&}CONVERT{_}TO=url{&}CACHEID=ROOTWORKSPACE.Z18{_}M1IEHBK0MOUJ20ABQK7Q593U32-d9618047-830b-450c-aa50-af3853b7af64-lINZ2KR.

[123] California ISO. California ISO. URL: http://www.caiso.com/informed/Pages/StakeholderProcesses/ParticipatingTransmissionOwnerPerUnitCosts.aspx.

[124] International Energy Agency (IEA), Paris. Global EV Outlook 2020. Technical report.

[125] R. Li, W. Wang, Z. Chen, J. Jiang, and W. Zhang. A review of optimal planning active distribution system: Models, methods, and future researches. *Energies*, 10:1715, 10 2017. doi:10.3390/en10111715.

[126] W. Ling Ai, V. K. Ramachandaramurthy, P. Taylor, J. Ekanayake, S. Walker, and P. Sanjeevikumar. Review on the optimal placement, sizing and control of an energy storage system in the distribution network. *The Journal of Energy Storage*, 21, 02 2019. doi:10.1016/j.est.2018.12.015.

[127] N. Hajia, B. Venkatesh, and M. A. Awadallah. Optimal asset expansion in distribution networks considering battery nonlinear characteristics expansion. *Canadian Journal of Electrical and Computer Engineering*, 41(4):191–199, 2018.

[128] I. Alsaidan, W. Gao, and A. Khodaei. Distribution network expansion through optimally sized and placed distributed energy storage. In *2018 IEEE/PES Transmission and Distribution Conference and Exposition (T D)*, pages 1–5, 2018.

[129] K. Masteri, B. Venkatesh, and W. Freitas. A feeder investment model for distribution system planning including battery energy storage. *Canadian Journal of Electrical and Computer Engineering*, 41(4):162–171, 2018.

[130] T. Zhang, A. E. Emanuel, and J. A. Orr. Distribution feeder upgrade deferral through use of energy storage systems. In *2016 IEEE Power and Energy Society General Meeting (PESGM)*, pages 1–5, 2016.

[131] S. Salee and P. Wirasanti. Optimal siting and sizing of battery energy storage systems for grid-supporting in electrical distribution network. In *2018 International ECTI Northern Section Conference on Electrical, Electronics, Computer and Telecommunications Engineering (ECTI-NCON)*, pages 100–105, 2018.

[132] G. Carpinelli, F. Mottola, D. Proto, and A. Russo. Optimal allocation of dispersed generators, capacitors and distributed energy storage systems in distribution networks. In *2010 Modern Electric Power Systems*, pages 1–6, 2010.

[133] F. Alizadeh and D. Goldfarb. Second-order cone programming. *Mathematical Programming*, 95, 12 2001. doi:10.1007/s10107-002-0339-5.

A Appendix

A.1 SG Synthetic Distribution System

The synthetic distribution system data of the Singapore case study can be accessed at the following link https://bit.ly/3LZskPJ.

A.2 SG Synthetic Transmission System

The synthetic sub-transmission and transmission system data of the Singapore case study can be accessed at the following link https://bit.ly/3LZskPJ.

A.2.1 Sub-transmission & Transmission System Power Flow Results

```
MATPOWER Version 6.0, AC Power Flow (Newton)

Converged in 0.02 seconds
================================================================================
|     System Summary                                                          |
================================================================================

How many?                How much?              P (MW)            Q (MVAr)
---------------------    -------------------  -------------  -----------------
Buses             165    Total Gen Capacity   13259.5        1145.5 to 2979.2
Generators         43    On-line Capacity      8236.3        1145.5 to 2979.2
Committed Gens     28    Generation (actual)   6886.2            1491.8
Loads             114    Load                  6820.0            2286.2
  Fixed           114      Fixed               6820.0            2286.2
  Dispatchable      0      Dispatchable          -0.0 of -0.0      -0.0
Shunts             23    Shunt (inj)             -0.0           -3901.4
Branches          367    Losses (I^2 * Z)        66.19            732.61
Transformers       51    Branch Charging (inj)     -             5428.4
Inter-ties         51    Total Inter-tie Flow  7364.4            2703.7
Areas               3

                          Minimum                      Maximum
                  -------------------------  --------------------------------
Voltage Magnitude   0.954 p.u. @ bus 73         1.003 p.u. @ bus 163
Voltage Angle      -6.83 deg   @ bus 87         0.48 deg   @ bus 164
```

```
P Losses (I^2*R)            -                 1.97 MW    @ line 158-136
Q Losses (I^2*X)            -                16.86 MVAr  @ line 146-122

================================================================================
|     Bus Data                                                                 |
================================================================================
 Bus      Voltage          Generation             Load
  #   Mag(pu) Ang(deg)   P (MW)   Q (MVAr)   P (MW)   Q (MVAr)
----- ------- --------  --------  --------  --------  --------
    1  0.981   -4.643       -         -      116.36     38.75
    2  0.983   -4.401       -         -      135.60     45.08
    3  0.982   -4.884       -         -       69.58     23.33
    4  0.983   -4.795       -         -       48.53     16.11
    5  0.983   -4.745       -         -       58.11     19.46
    6  0.982   -4.282       -         -       12.10      3.98
    7  0.981   -4.401       -         -       13.22      4.35
    8  0.981   -4.341       -         -       12.39      4.08
    9  0.980   -4.457       -         -       59.26     19.79
   10  0.979   -4.556       -         -       51.86     17.42
   11  0.981   -4.368       -         -       57.70     19.32
   12  0.994   -3.256       -         -       60.00     21.28
   13  0.990   -3.654       -         -       60.00     21.64
   14  0.991   -3.540       -         -       60.00     21.21
   15  0.983   -4.280       -         -       60.00     21.63
   16  0.996   -3.091       -         -       60.00     21.62
   17  0.986   -4.000       -         -       60.00     21.60
   18  0.986   -3.989       -         -       60.00     21.63
   19  0.996   -3.091       -         -       60.00     20.01
   20  1.000   -2.727       -         -       60.00     20.14
   21  0.986   -3.984    122.69     56.44      15.10      5.17
   22  0.975   -4.905       -         -       51.38     17.24
   23  0.981   -4.418       -         -       35.97     11.99
   24  0.971   -5.153       -         -       18.97      6.29
   25  0.967   -5.228       -         -       74.24     24.80
   26  0.975   -4.901       -         -       74.22     24.53
   27  0.972   -5.067       -         -       22.60      7.47
   28  0.984   -4.092       -         -       29.33      9.69
   29  0.984   -4.206       -         -       20.38      6.72
   30  0.969   -5.262       -         -       50.09     17.14
   31  0.982   -4.307       -         -       46.71     15.64
   32  0.984   -4.208       -         -       39.62     13.23
   33  0.983   -4.224       -         -       13.12      4.34
   34  0.969   -4.724       -         -       66.73     22.20
   35  0.970   -4.475       -         -       57.46     19.18
```

36	0.969	-5.136	-	-	48.76	16.39
37	0.969	-5.177	-	-	36.55	12.21
38	0.969	-5.315	-	-	60.84	20.58
39	0.970	-5.051	-	-	28.23	9.40
40	0.971	-4.934	-	-	14.98	5.09
41	0.962	-5.423	-	-	52.22	17.29
42	0.962	-5.299	-	-	126.60	42.34
43	0.961	-5.073	-	-	78.87	26.52
44	0.961	-5.072	-	-	53.66	18.11
45	0.971	-4.852	-	-	46.19	15.47
46	0.969	-5.109	-	-	24.88	8.29
47	0.973	-4.840	-	-	37.39	12.50
48	0.975	-4.756	-	-	17.16	5.67
49	0.974	-5.074	-	-	12.79	4.65
50	0.974	-4.984	-	-	38.99	13.00
51	0.973	-5.140	-	-	11.84	4.27
52	0.975	-4.932	-	-	23.40	8.10
53	0.975	-4.730	-	-	40.25	13.42
54	0.975	-4.932	-	-	41.91	13.95
55	0.975	-4.908	-	-	12.65	4.20
56	0.972	-5.089	-	-	46.93	16.05
57	0.972	-5.106	-	-	77.85	25.99
58	0.969	-5.366	-	-	129.77	43.05
59	0.967	-5.566	-	-	71.49	23.74
60	0.969	-5.446	-	-	137.34	45.89
61	0.974	-5.057	-	-	33.72	11.31
62	0.969	-5.389	-	-	63.18	21.07
63	0.973	-5.154	-	-	37.60	12.44
64	0.971	-5.303	-	-	15.38	5.56
65	0.970	-5.262	-	-	70.40	23.34
66	0.969	-5.516	-	-	25.50	8.61
67	0.972	-5.200	-	-	54.07	18.26
68	0.969	-5.421	-	-	35.47	11.85
69	0.974	-5.026	-	-	11.42	3.78
70	0.971	-5.285	-	-	43.41	14.46
71	0.969	-5.456	-	-	35.51	11.92
72	0.956	-6.480	-	-	71.00	23.68
73	0.954	-6.748	-	-	60.48	20.07
74	0.961	-6.120	-	-	50.60	16.76
75	0.958	-6.378	-	-	262.17	87.80
76	0.957	-6.538	-	-	142.25	47.15
77	0.959	-6.216	-	-	129.86	43.11
78	0.957	-6.523	-	-	70.78	23.48
79	0.956	-6.783	-	-	202.80	67.43

80	0.960	-6.259	-	-	67.04	22.52
81	0.962	-6.410	-	-	64.07	21.35
82	0.963	-6.247	-	-	43.74	14.55
83	0.960	-6.356	-	-	134.73	44.58
84	0.957	-6.644	-	-	202.24	67.26
85	0.955	-6.752	-	-	70.03	23.35
86	0.955	-6.393	-	-	73.67	24.51
87	0.955	-6.831	-	-	59.72	20.10
88	0.959	-6.643	-	-	185.86	61.91
89	0.958	-6.529	-	-	184.62	61.31
90	0.964	-6.210	-	-	28.75	9.61
91	0.956	-6.827	-	-	69.66	23.18
92	0.966	-4.459	-	-	61.36	20.48
93	0.964	-4.820	-	-	37.28	12.35
94	0.966	-4.562	-	-	112.91	37.42
95	0.963	-5.327	-	-	49.84	16.73
96	0.966	-4.450	-	-	134.97	44.74
97	0.962	-5.441	-	-	63.62	21.15
98	0.962	-5.309	-	-	65.24	21.92
99	0.954	-6.549	-	-	83.79	28.33
100	0.970	-5.970	-	-	58.19	19.30
101	0.971	-5.864	-	-	29.56	9.81
102	0.970	-5.890	-	-	61.03	20.19
103	0.972	-5.713	-	-	29.55	9.78
104	0.971	-5.797	-	-	27.30	9.01
105	0.974	-5.473	-	-	12.63	4.16
106	0.969	-6.055	-	-	63.78	21.08
107	0.970	-6.016	-	-	11.66	3.86
108	0.969	-6.099	-	-	37.54	12.77
109	0.970	-5.874	-	-	14.72	4.90
110	0.970	-5.692	-	-	54.63	18.12
111	0.967	-6.064	-	-	40.21	13.36
112	0.972	-5.681	-	-	54.63	18.19
113	0.965	-6.203	-	-	44.84	14.82
114	0.995	-3.074	-	-	-	-
115	0.984	-4.014	-	-	-	-
116	0.972	-4.341	-	-	-	-
117	0.971	-5.514	-	-	-	-
118	0.967	-4.230	-	-	-	-
119	0.976	-4.822	-	-	-	-
120	0.995	-3.144	-	-	-	-
121	0.976	-4.560	-	-	-	-
122	0.960	-6.056	-	-	-	-
123	0.986	-3.889	-	-	-	-

124	0.971	-5.064	-	-	-	-
125	1.000	-2.704	-	-	-	-
126	0.967	-4.337	52.80	24.29	-	-
127	0.983	-4.188	172.80	79.49	-	-
128	0.985	-4.613	126.72	58.29	-	-
129	0.983	-4.539	45.89	21.11	-	-
130	1.001	-2.607	128.16	58.95	-	-
150	0.991	-1.122	-	-	8.79	3.17
138	0.999	0.253	-	-	-	-
139	0.995	-0.230	-	-	-	-
131	0.996	-0.259	-	-	-	-
140	0.996	-0.143	-	-	-	-
135	0.990	-1.240	-	-	-	-
133	0.993	-0.809	-	-	-	-
136	0.987	-1.645	-	-	-	-
132	0.995	-0.474	-	-	-	-
134	0.991	-1.182	-	-	-	-
141	0.986	-1.678	-	-	-	-
142	0.997	-0.139	-	-	-	-
143	0.991	-1.020	-	-	-	-
144	1.000	0.309	-	-	-	-
145	0.992	-0.862	-	-	-	-
146	0.989	-1.386	-	-	-	-
137	0.986	-1.749	-	-	-	-
147	0.994	-0.080	-	-	-	-
148	0.991	-1.167	-	-	-	-
149	1.000	0.343	-	-	-	-
151	0.999	0.198	258.48	34.46	-	-
152	0.998	0.132	633.47	72.48	-	-
153	0.999	0.299	290.51	40.84	-	-
154	1.000	0.323	220.00	34.69	-	-
155	1.000	0.370	696.15	102.73	-	-
156	0.996	0.424	571.65	102.33	-	-
157	0.996	0.407	293.27	78.22	-	-
158	0.998	0.000*	2103.96	512.90	-	-
159	0.999	0.060	-	-	-	-
160	0.999	0.017	-	-	-	-
161	0.996	-0.251	-	-	-	-
162	0.994	-0.336	-	-	-	-
163	1.003	0.471	-	-	-	-
164	1.002	0.479	522.29	100.16	-	-
165	1.002	0.474	647.34	114.41	-	-
			---	---	---	---
		Total:	6886.18	1491.80	6819.99	2286.19

Branch Data							
Brnch #	From Bus	To Bus	From Bus Injection P (MW)	From Bus Injection Q (MVAr)	To Bus Injection P (MW)	To Bus Injection Q (MVAr)	Loss (I^2 * Z) P (MW)	Loss (I^2 * Z) Q (MVAr)
1	123	1	70.58	12.34	-70.39	-14.33	0.188	1.00
2	129	1	45.99	23.87	-45.96	-24.42	0.022	0.12
3	2	5	28.63	-6.30	-28.60	3.35	0.032	0.17
4	115	2	57.08	-2.49	-57.01	1.07	0.072	0.38
5	120	2	44.81	11.46	-44.59	-18.55	0.221	1.17
6	123	2	83.94	16.43	-83.79	-17.33	0.153	0.81
7	129	2	-21.14	2.31	21.15	-3.96	0.010	0.05
8	5	3	26.75	4.04	-26.73	-5.41	0.013	0.07
9	128	3	42.90	16.33	-42.85	-17.92	0.048	0.25
10	5	4	7.59	-2.72	-7.58	1.03	0.001	0.01
11	128	4	40.97	16.01	-40.94	-17.14	0.031	0.16
12	128	5	42.85	25.95	-42.82	-26.73	0.029	0.15
13	129	5	21.04	-5.07	-21.03	2.61	0.014	0.08
14	6	8	33.62	8.61	-33.61	-9.07	0.007	0.04
15	11	6	-15.74	-5.07	15.75	3.56	0.005	0.03
16	15	6	1.66	5.80	-1.66	-7.42	0.001	0.00
17	6	22	85.05	36.24	-84.82	-37.15	0.226	1.19
18	6	27	73.65	34.69	-73.39	-36.40	0.259	1.37
19	6	34	22.88	22.43	-22.78	-28.32	0.094	0.50
20	127	6	62.72	38.31	-62.69	-38.60	0.030	0.16
21	131	6	179.63	78.42	-178.70	-63.50	0.933	14.92
22	8	7	13.96	3.33	-13.96	-4.52	0.003	0.02
23	7	10	18.35	5.13	-18.34	-7.47	0.011	0.06
24	11	7	17.61	4.44	-17.61	-4.96	0.002	0.01
25	11	8	-7.26	-2.69	7.26	1.65	0.001	0.00
26	9	10	33.54	9.18	-33.52	-9.94	0.013	0.07
27	9	11	-24.31	-9.72	24.32	8.72	0.009	0.05
28	115	9	68.61	18.03	-68.49	-19.25	0.114	0.60
29	11	31	-9.12	-7.74	9.13	5.69	0.003	0.02
30	115	11	67.59	15.98	-67.51	-16.98	0.088	0.46
31	14	12	-24.90	-10.49	24.92	7.23	0.028	0.15
32	120	12	84.96	28.31	-84.92	-28.51	0.037	0.20
33	14	13	53.03	21.38	-53.01	-21.89	0.025	0.13
34	13	17	79.34	30.11	-79.22	-30.81	0.112	0.59
35	13	18	85.64	32.43	-85.52	-32.97	0.117	0.62
36	114	13	91.62	30.82	-91.41	-31.60	0.209	1.10
37	125	13	80.86	28.78	-80.55	-30.70	0.309	1.63

38	114	14	54.70	16.72	-54.60	-18.73	0.099	0.52
39	120	14	33.59	10.11	-33.54	-13.36	0.053	0.28
40	17	15	44.74	20.67	-44.69	-22.23	0.056	0.30
41	127	15	16.98	3.71	-16.97	-5.20	0.006	0.03
42	16	19	64.64	27.85	-64.64	-27.85	0.000	0.00
43	16	20	-61.91	-23.16	62.00	21.84	0.091	0.48
44	130	16	62.86	24.60	-62.73	-26.31	0.127	0.67
45	17	18	-25.52	-11.46	25.52	11.34	0.001	0.01
46	114	19	3.31	-5.63	-3.31	4.52	0.000	0.00
47	120	19	-7.94	-5.42	7.94	3.32	0.002	0.01
48	20	125	-56.73	-7.23	56.74	7.14	0.004	0.02
49	130	20	65.30	34.36	-65.26	-34.75	0.037	0.19
50	21	52	68.84	27.24	-68.56	-29.77	0.274	1.45
51	121	21	-38.63	-27.93	38.75	24.03	0.122	0.65
52	22	26	-1.44	-2.92	1.44	1.75	0.000	0.00
53	22	27	34.88	22.83	-34.85	-24.04	0.031	0.16
54	23	26	57.04	25.73	-56.92	-27.52	0.121	0.64
55	127	23	93.10	37.47	-93.01	-37.72	0.089	0.47
56	27	24	24.93	14.61	-24.92	-15.56	0.011	0.06
57	24	37	5.95	9.27	-5.95	-10.79	0.003	0.01
58	35	25	48.37	0.37	-48.24	-3.69	0.121	0.64
59	25	46	-25.99	-21.11	26.01	19.86	0.019	0.10
60	48	26	18.75	-3.17	-18.74	1.25	0.009	0.05
61	27	30	36.46	17.30	-36.43	-18.64	0.032	0.17
62	27	37	24.23	21.05	-24.22	-22.35	0.019	0.10
63	28	29	25.08	6.07	-25.07	-7.31	0.011	0.06
64	28	31	55.89	20.47	-55.84	-21.33	0.049	0.26
65	123	28	110.39	36.16	-110.30	-36.23	0.088	0.46
66	33	29	-4.69	-1.64	4.69	0.59	0.000	0.00
67	37	30	13.67	-3.00	-13.66	1.50	0.004	0.02
68	32	33	8.43	2.16	-8.43	-2.70	0.001	0.00
69	123	32	48.11	13.79	-48.05	-15.38	0.059	0.31
70	35	34	43.98	-7.32	-43.95	6.12	0.036	0.19
71	35	36	68.97	-9.53	-68.82	7.94	0.149	0.79
72	35	42	123.52	41.51	-123.12	-41.19	0.399	2.11
73	132	35	171.98	58.95	-171.15	-45.60	0.834	13.35
74	132	35	171.98	58.95	-171.15	-45.60	0.834	13.35
75	36	37	20.05	-24.33	-20.05	23.93	0.005	0.03
76	38	39	-35.63	-3.78	35.67	2.04	0.032	0.17
77	119	38	25.27	11.49	-25.21	-16.80	0.061	0.32
78	45	39	63.94	10.85	-63.90	-11.44	0.045	0.24
79	45	40	38.10	-2.61	-38.09	2.12	0.010	0.05
80	40	56	23.11	-7.20	-23.10	5.63	0.012	0.06
81	41	42	-19.00	6.69	19.01	-8.14	0.008	0.04

82	45	41	33.33	19.61	-33.23	-23.98	0.102	0.54
83	44	42	22.50	-9.22	-22.49	6.98	0.018	0.09
84	43	44	-3.20	-9.03	3.20	8.89	0.000	0.00
85	118	43	75.90	15.83	-75.67	-17.49	0.231	1.22
86	118	44	79.60	16.32	-79.36	-17.79	0.241	1.27
87	45	47	-3.23	-9.55	3.23	7.67	0.002	0.01
88	133	45	179.36	97.21	-178.34	-80.96	1.016	16.26
89	47	46	50.95	26.99	-50.89	-28.15	0.065	0.34
90	47	53	-24.10	-17.93	24.11	16.65	0.015	0.08
91	121	47	67.55	28.48	-67.47	-29.23	0.080	0.42
92	121	48	35.94	1.20	-35.91	-2.50	0.023	0.12
93	49	51	5.08	0.20	-5.08	-3.82	0.001	0.01
94	52	49	17.88	2.76	-17.87	-4.85	0.009	0.05
95	50	56	23.84	20.42	-23.82	-21.68	0.018	0.09
96	119	50	62.88	32.92	-62.83	-33.42	0.048	0.25
97	52	51	38.61	9.87	-38.58	-11.18	0.030	0.16
98	51	66	31.82	10.73	-31.77	-13.74	0.049	0.26
99	55	52	11.32	-9.53	-11.32	9.04	0.001	0.01
100	53	55	34.26	-8.27	-34.24	7.08	0.020	0.11
101	121	53	98.68	21.66	-98.62	-21.80	0.061	0.32
102	54	55	-10.27	1.16	10.27	-1.76	0.001	0.00
103	119	54	31.66	14.19	-31.64	-15.11	0.015	0.08
104	57	74	106.10	42.89	-105.65	-43.12	0.447	2.36
105	124	57	11.44	-7.18	-11.44	6.33	0.002	0.01
106	134	57	173.45	90.21	-172.51	-75.21	0.938	15.00
107	58	59	62.87	19.83	-62.82	-20.42	0.049	0.26
108	58	75	116.99	47.02	-116.50	-46.75	0.491	2.59
109	58	76	122.87	41.87	-122.31	-41.41	0.566	2.99
110	58	77	79.59	33.56	-79.30	-34.93	0.288	1.52
111	58	80	88.93	28.25	-88.62	-29.29	0.308	1.63
112	124	58	65.32	21.08	-65.24	-21.93	0.077	0.41
113	135	58	179.55	79.22	-178.59	-63.88	0.959	15.34
114	135	58	179.55	79.22	-178.59	-63.88	0.959	15.34
115	135	58	179.55	79.22	-178.59	-63.88	0.959	15.34
116	59	80	96.79	31.18	-96.53	-31.70	0.261	1.38
117	124	59	105.67	34.30	-105.47	-34.49	0.206	1.09
118	61	60	61.27	27.76	-61.16	-28.99	0.105	0.55
119	60	62	-18.32	-3.05	18.32	2.25	0.004	0.02
120	60	71	2.13	-1.33	-2.13	0.24	0.000	0.00
121	124	60	60.08	11.27	-59.99	-12.52	0.082	0.43
122	69	61	12.48	6.47	-12.48	-7.18	0.002	0.01
123	119	61	82.59	31.51	-82.51	-31.89	0.079	0.42
124	62	65	-35.01	-4.82	35.03	3.96	0.015	0.08
125	62	68	16.90	-4.85	-16.90	4.40	0.002	0.01

126	124	62	63.46	12.68	-63.39	-13.65	0.074	0.39
127	63	70	63.06	26.29	-63.02	-26.68	0.035	0.18
128	119	63	100.80	38.53	-100.66	-38.73	0.137	0.72
129	64	66	73.62	25.03	-73.56	-25.50	0.062	0.33
130	69	64	89.10	30.25	-89.00	-30.60	0.097	0.51
131	124	65	105.51	27.21	-105.43	-27.31	0.078	0.41
132	66	79	79.83	30.63	-79.41	-32.67	0.417	2.21
133	67	70	32.38	14.69	-32.37	-15.36	0.012	0.06
134	119	67	86.58	32.43	-86.45	-32.95	0.133	0.70
135	70	68	51.99	27.58	-51.95	-28.14	0.033	0.18
136	68	71	33.38	11.89	-33.38	-12.16	0.005	0.02
137	119	69	113.10	40.49	-113.01	-40.50	0.092	0.49
138	72	73	59.70	8.56	-59.64	-9.37	0.056	0.29
139	74	72	48.64	26.48	-48.55	-28.04	0.085	0.45
140	72	86	-14.29	6.50	14.30	-7.82	0.005	0.02
141	98	72	68.13	7.86	-67.85	-10.70	0.275	1.45
142	85	73	0.84	9.91	-0.84	-10.71	0.001	0.01
143	74	75	28.44	11.29	-28.41	-13.53	0.031	0.17
144	74	85	74.12	24.86	-73.93	-26.09	0.185	0.98
145	124	74	96.55	35.49	-96.13	-36.27	0.412	2.18
146	77	75	49.71	11.63	-49.68	-12.30	0.030	0.16
147	122	75	67.66	14.42	-67.58	-15.21	0.079	0.42
148	78	76	5.26	-10.39	-5.26	9.89	0.001	0.00
149	76	79	46.27	9.34	-46.23	-10.46	0.041	0.22
150	80	76	40.80	15.09	-40.75	-16.64	0.047	0.25
151	76	84	86.64	4.56	-86.61	-4.70	0.031	0.16
152	122	76	107.01	12.71	-106.84	-12.90	0.177	0.93
153	122	77	100.33	19.71	-100.27	-19.81	0.057	0.30
154	122	78	76.16	12.21	-76.04	-13.09	0.125	0.66
155	80	79	77.31	23.38	-77.16	-24.30	0.156	0.82
156	82	81	51.66	17.58	-51.62	-18.24	0.033	0.18
157	81	84	53.03	42.14	-52.95	-42.99	0.079	0.42
158	112	81	37.22	18.16	-37.09	-22.98	0.131	0.69
159	113	81	28.43	20.36	-28.39	-22.27	0.035	0.19
160	82	83	22.52	28.65	-22.49	-30.07	0.029	0.15
161	111	82	29.85	23.11	-29.81	-24.73	0.035	0.18
162	117	82	88.38	35.21	-88.11	-36.05	0.269	1.42
163	83	84	62.74	18.75	-62.68	-19.57	0.069	0.37
164	83	89	30.88	9.29	-30.86	-10.63	0.021	0.11
165	117	83	97.49	52.63	-97.10	-52.97	0.390	2.06
166	122	83	108.86	-10.52	-108.76	10.43	0.107	0.57
167	85	87	20.31	-9.90	-20.31	9.07	0.006	0.03
168	85	99	-17.25	2.74	17.26	-5.37	0.012	0.06
169	98	86	88.31	15.39	-87.97	-16.69	0.337	1.78

170	89	87	35.67	12.05	-35.62	-14.01	0.043	0.23
171	87	91	-3.79	-15.16	3.79	14.20	0.003	0.02
172	89	88	15.19	-12.31	-15.19	10.76	0.008	0.04
173	90	88	79.09	34.34	-78.94	-35.03	0.147	0.78
174	117	88	92.17	36.61	-91.74	-37.64	0.432	2.28
175	117	89	82.94	41.24	-82.56	-42.58	0.386	2.04
176	122	89	122.26	7.92	-122.07	-7.85	0.194	1.03
177	90	91	73.66	36.21	-73.45	-37.38	0.207	1.09
178	110	90	92.58	45.29	-92.37	-45.70	0.217	1.15
179	117	90	89.38	33.68	-89.13	-34.46	0.253	1.34
180	92	93	79.31	9.76	-79.21	-10.40	0.098	0.52
181	118	92	70.40	14.57	-70.34	-15.12	0.058	0.31
182	118	92	70.40	14.57	-70.34	-15.12	0.058	0.31
183	93	98	41.94	-1.96	-41.87	-0.56	0.068	0.36
184	96	94	22.32	-8.03	-22.32	6.90	0.009	0.05
185	94	98	82.88	9.30	-82.67	-10.47	0.212	1.12
186	116	94	54.68	53.62	-54.58	-54.37	0.097	0.51
187	118	94	119.02	-0.77	-118.89	0.75	0.130	0.69
188	95	97	49.47	11.29	-49.45	-11.78	0.020	0.11
189	116	95	99.67	27.34	-99.30	-28.03	0.368	1.95
190	118	96	86.76	12.47	-86.69	-12.77	0.066	0.35
191	126	96	70.63	23.68	-70.60	-23.94	0.031	0.17
192	97	99	101.46	22.33	-101.05	-22.96	0.406	2.15
193	116	97	116.11	31.71	-115.63	-31.71	0.477	2.52
194	116	98	97.51	33.43	-97.13	-34.13	0.373	1.97
195	100	104	-19.93	-7.10	19.94	4.82	0.013	0.07
196	105	100	38.33	9.06	-38.26	-12.20	0.071	0.38
197	103	101	26.67	6.88	-26.65	-8.33	0.015	0.08
198	108	101	-25.84	-6.45	25.86	4.16	0.022	0.11
199	101	109	1.68	0.56	-1.68	-2.39	0.000	0.00
200	112	101	30.47	4.71	-30.45	-6.20	0.020	0.10
201	104	102	9.12	1.78	-9.12	-4.54	0.003	0.02
202	105	102	51.99	13.90	-51.91	-15.65	0.082	0.43
203	105	103	56.27	15.77	-56.22	-16.66	0.051	0.27
204	105	104	56.43	14.42	-56.36	-15.62	0.068	0.36
205	105	107	23.41	2.25	-23.36	-8.23	0.046	0.24
206	105	110	95.36	61.48	-95.25	-61.56	0.111	0.59
207	136	105	168.05	73.85	-167.21	-60.52	0.833	13.33
208	136	105	168.05	73.85	-167.21	-60.52	0.833	13.33
209	109	106	19.77	5.45	-19.75	-7.87	0.014	0.07
210	112	106	44.09	11.25	-44.03	-13.21	0.062	0.33
211	107	108	11.70	4.37	-11.70	-6.32	0.004	0.02
212	112	109	32.83	6.51	-32.80	-7.97	0.023	0.12
213	117	110	51.99	1.13	-51.96	-1.85	0.031	0.16

214	112	111	70.18	35.58	-70.05	-36.47	0.124	0.66
215	112	113	73.44	34.10	-73.27	-35.18	0.170	0.90
216	137	112	172.32	78.45	-171.43	-64.26	0.887	14.20
217	137	112	172.32	78.45	-171.43	-64.26	0.887	14.20
218	138	114	150.23	51.65	-149.62	-41.91	0.609	9.75
219	123	115	24.95	19.32	-24.93	-20.82	0.020	0.11
220	139	115	169.17	72.24	-168.35	-59.08	0.822	13.15
221	140	116	185.02	89.66	-183.98	-73.05	1.038	16.61
222	140	116	185.02	89.66	-183.98	-73.05	1.038	16.61
223	141	117	168.32	80.62	-167.45	-66.83	0.862	13.79
224	141	117	168.32	80.62	-167.45	-66.83	0.862	13.79
225	141	117	168.32	80.62	-167.45	-66.83	0.862	13.79
226	118	126	17.84	-2.06	-17.83	0.61	0.006	0.03
227	142	118	174.15	52.74	-173.30	-39.23	0.844	13.50
228	142	118	174.15	52.74	-173.30	-39.23	0.844	13.50
229	142	118	174.15	52.74	-173.30	-39.23	0.844	13.50
230	143	119	168.48	80.88	-167.62	-67.19	0.856	13.69
231	143	119	168.48	80.88	-167.62	-67.19	0.856	13.69
232	143	119	168.48	80.88	-167.62	-67.19	0.856	13.69
233	144	120	156.08	55.03	-155.42	-44.47	0.660	10.56
234	145	121	164.37	84.38	-163.54	-71.02	0.835	13.35
235	146	122	195.15	51.04	-194.10	-34.18	1.054	16.86
236	146	122	195.15	51.04	-194.10	-34.18	1.054	16.86
237	146	122	195.15	51.04	-194.10	-34.18	1.054	16.86
238	147	123	169.78	61.74	-168.99	-49.02	0.795	12.73
239	147	123	169.78	61.74	-168.99	-49.02	0.795	12.73
240	148	124	170.20	74.39	-169.34	-60.68	0.857	13.72
241	148	124	170.20	74.39	-169.34	-60.68	0.857	13.72
242	148	124	170.20	74.39	-169.34	-60.68	0.857	13.72
243	149	125	138.11	44.01	-137.60	-35.91	0.506	8.09
244	143	150	99.12	-12.62	-99.09	-10.01	0.025	0.18
245	143	150	99.12	-12.62	-99.09	-10.01	0.025	0.18
246	150	148	63.13	5.62	-63.12	-30.35	0.008	0.06
247	150	148	63.13	5.62	-63.12	-30.35	0.008	0.06
248	150	148	63.13	5.62	-63.12	-30.35	0.008	0.06
249	138	151	76.45	-19.29	-76.44	-4.93	0.010	0.07
250	138	151	76.45	-19.29	-76.44	-4.93	0.010	0.07
251	138	151	76.45	-19.29	-76.44	-4.93	0.010	0.07
252	153	138	126.54	51.04	-126.52	-64.42	0.019	0.13
253	153	138	126.54	51.04	-126.52	-64.42	0.019	0.13
254	153	138	126.54	51.04	-126.52	-64.42	0.019	0.13
255	139	131	48.24	-56.02	-48.24	38.22	0.006	0.04
256	139	131	48.24	-56.02	-48.24	38.22	0.006	0.04
257	139	131	48.24	-56.02	-48.24	38.22	0.006	0.04

258	139	133	282.40	-7.10	-281.98	-59.94	0.419	2.91
259	139	133	282.40	-7.10	-281.98	-59.94	0.419	2.91
260	139	133	282.40	-7.10	-281.98	-59.94	0.419	2.91
261	147	139	249.90	-207.21	-249.76	196.03	0.140	0.97
262	154	139	288.78	60.71	-288.32	-103.10	0.453	3.14
263	154	139	288.78	60.71	-288.32	-103.10	0.453	3.14
264	156	139	274.70	-48.63	-274.25	-1.43	0.449	3.12
265	158	139	60.50	-21.83	-60.46	-69.43	0.043	0.30
266	131	132	116.16	-32.28	-116.10	-29.89	0.063	0.44
267	131	132	116.16	-32.28	-116.10	-29.89	0.063	0.44
268	131	132	116.16	-32.28	-116.10	-29.89	0.063	0.44
269	152	131	383.81	75.14	-383.40	-96.26	0.410	2.85
270	142	140	9.87	3.84	-9.87	-21.71	0.000	0.00
271	142	140	9.87	3.84	-9.87	-21.71	0.000	0.00
272	142	140	9.87	3.84	-9.87	-21.71	0.000	0.00
273	158	140	340.59	105.17	-340.45	-114.18	0.142	0.98
274	134	135	99.40	57.31	-99.38	-71.27	0.023	0.16
275	134	135	99.40	57.31	-99.38	-71.27	0.023	0.16
276	135	146	115.55	3.95	-115.50	-46.80	0.046	0.32
277	135	146	115.55	3.95	-115.50	-46.80	0.046	0.32
278	135	146	115.55	3.95	-115.50	-46.80	0.046	0.32
279	148	135	179.47	86.75	-179.43	-96.16	0.045	0.31
280	148	135	179.47	86.75	-179.43	-96.16	0.045	0.31
281	158	135	328.78	30.85	-327.68	-110.54	1.105	7.68
282	132	133	195.47	27.03	-195.29	-65.54	0.179	1.25
283	133	134	178.01	3.23	-177.82	-74.32	0.181	1.26
284	133	134	178.01	3.23	-177.82	-74.32	0.181	1.26
285	133	134	178.01	3.23	-177.82	-74.32	0.181	1.26
286	145	133	-81.07	-54.38	81.09	30.41	0.015	0.11
287	145	133	-81.07	-54.38	81.09	30.41	0.015	0.11
288	145	133	-81.07	-54.38	81.09	30.41	0.015	0.11
289	133	148	188.11	10.91	-187.93	-75.36	0.184	1.28
290	133	148	188.11	10.91	-187.93	-75.36	0.184	1.28
291	133	148	188.11	10.91	-187.93	-75.36	0.184	1.28
292	158	133	193.15	-12.09	-192.74	-82.09	0.416	2.89
293	159	133	95.75	35.20	-95.67	-33.54	0.083	1.67
294	159	133	95.75	35.20	-95.67	-33.54	0.083	1.67
295	159	133	95.75	35.20	-95.67	-33.54	0.083	1.67
296	136	141	112.28	10.18	-112.27	-19.82	0.010	0.07
297	136	141	112.28	10.18	-112.27	-19.82	0.010	0.07
298	136	141	112.28	10.18	-112.27	-19.82	0.010	0.07
299	146	136	226.26	60.08	-226.09	-85.14	0.170	1.18
300	146	136	226.26	60.08	-226.09	-85.14	0.170	1.18
301	136	137	71.52	-21.54	-71.51	-26.14	0.019	0.13

302	136	137	71.52	-21.54	-71.51	-26.14	0.019	0.13
303	136	137	71.52	-21.54	-71.51	-26.14	0.019	0.13
304	158	136	437.30	64.79	-435.33	-137.99	1.969	13.67
305	158	132	191.37	-0.47	-191.14	-55.27	0.238	1.65
306	145	134	113.56	-13.13	-113.47	-50.30	0.096	0.67
307	134	146	142.95	24.90	-142.86	-73.96	0.086	0.60
308	134	146	142.95	24.90	-142.86	-73.96	0.086	0.60
309	134	146	142.95	24.90	-142.86	-73.96	0.086	0.60
310	148	134	51.39	-7.84	-51.38	-2.10	0.002	0.01
311	148	134	51.39	-7.84	-51.38	-2.10	0.002	0.01
312	148	134	51.39	-7.84	-51.38	-2.10	0.002	0.01
313	146	141	298.52	79.38	-298.27	-99.98	0.249	1.73
314	137	141	-43.37	-26.16	43.38	-27.48	0.008	0.05
315	137	141	-43.37	-26.16	43.38	-27.48	0.008	0.05
316	137	141	-43.37	-26.16	43.38	-27.48	0.008	0.05
317	158	142	276.13	73.72	-276.02	-84.86	0.109	0.75
318	158	142	276.13	73.72	-276.02	-84.86	0.109	0.75
319	145	143	234.66	49.99	-234.56	-72.47	0.103	0.71
320	145	143	234.66	49.99	-234.56	-72.47	0.103	0.71
321	145	143	234.66	49.99	-234.56	-72.47	0.103	0.71
322	149	144	68.01	14.11	-68.01	-25.87	0.006	0.05
323	153	144	-16.48	-31.11	16.49	13.95	0.001	0.01
324	153	144	-16.48	-31.11	16.49	13.95	0.001	0.01
325	144	154	-40.35	-19.02	40.35	6.37	0.002	0.01
326	144	154	-40.35	-19.02	40.35	6.37	0.002	0.01
327	144	154	-40.35	-19.02	40.35	6.37	0.002	0.01
328	145	146	190.26	14.21	-189.98	-75.40	0.274	1.90
329	152	145	368.68	44.09	-367.70	-99.98	0.984	6.83
330	152	145	368.68	44.09	-367.70	-99.98	0.984	6.83
331	160	145	96.86	36.34	-96.78	-34.62	0.086	1.72
332	160	145	96.86	36.34	-96.78	-34.62	0.086	1.72
333	146	161	-123.81	-36.82	123.94	39.55	0.137	2.73
334	146	161	-123.81	-36.82	123.94	39.55	0.137	2.73
335	146	161	-123.81	-36.82	123.94	39.55	0.137	2.73
336	156	147	267.35	7.56	-267.00	-48.23	0.347	2.41
337	157	147	322.87	33.71	-322.46	-65.58	0.413	2.87
338	148	162	-90.19	-18.68	90.25	20.06	0.069	1.38
339	148	162	-90.19	-18.68	90.25	20.06	0.069	1.38
340	148	162	-90.19	-18.68	90.25	20.06	0.069	1.38
341	148	162	0.00	0.00	0.00	0.00	0.000	0.00
342	149	154	78.52	17.48	-78.52	-26.28	0.004	0.03
343	149	154	78.52	17.48	-78.52	-26.28	0.004	0.03
344	149	154	78.52	17.48	-78.52	-26.28	0.004	0.03
345	155	149	198.45	25.69	-198.44	-28.88	0.014	0.10

346	155	149	198.45	25.69	-198.44	-28.88	0.014	0.10
347	163	149	14.94	17.69	-14.93	-17.60	0.004	0.09
348	163	149	14.94	17.69	-14.93	-17.60	0.004	0.09
349	163	149	14.94	17.69	-14.93	-17.60	0.004	0.09
350	151	152	162.60	16.42	-162.57	-30.28	0.028	0.19
351	151	152	162.60	16.42	-162.57	-30.28	0.028	0.19
352	151	152	162.60	16.42	-162.57	-30.28	0.028	0.19
353	154	153	56.16	38.98	-56.15	-50.04	0.006	0.04
354	155	154	149.62	25.67	-149.60	-32.99	0.019	0.13
355	155	154	149.62	25.67	-149.60	-32.99	0.019	0.13
356	157	156	-29.61	44.52	29.61	-55.01	0.004	0.03
357	160	159	-185.29	-121.80	185.30	73.87	0.016	0.19
358	161	159	-324.58	-262.75	324.78	68.79	0.197	2.32
359	164	159	475.53	66.35	-475.20	-242.82	0.336	3.96
360	165	159	322.35	-52.93	-322.13	-205.14	0.213	2.51
361	161	160	-318.08	-246.84	318.24	76.51	0.166	1.95
362	165	160	326.92	-54.36	-326.68	-226.89	0.243	2.86
363	162	161	-270.76	-257.94	270.83	192.59	0.063	0.74
364	164	163	15.59	-122.68	-15.58	8.70	0.003	0.03
365	164	163	15.59	-122.68	-15.58	8.70	0.003	0.03
366	164	163	15.59	-122.68	-15.58	8.70	0.003	0.03
367	163	165	1.94	-79.16	-1.93	-179.58	0.005	0.06
							--------	--------
						Total:	66.188	732.61